CHAPTER 1

INTRODUCTION

1.1 Background of Study

The most critical issues in environmental analytical chemistry today are related to water quality control. Phenols can be easily found in our environment due to its release directly or indirectly (Feng et al., 2009), thus they appear to be one of the problematic groups globally. Owing to its stability, toxicity, and bioaccumulation, determining and removing phenols from our environment are crucial in order to treat and to purify the water system.

To date, a lot of new adsorbents based on natural and polymeric material have been developed to extract phenols from our environment. The growing interest in supramolecular chemistry has allowed us to prepare cyclodextrin-based polymer to extract pollutants, since it is eco-friendly and has high regeneration value. Cyclodextrins (CDs) are groups of structurally related natural products formed during bacterial digestion of cellulose. These cyclic oligosaccharides consist of (α-1,4)-linked α-D-glucopyranose units, and contain a somewhat lipophilic central cavity and a hydrophilic outer surface (Szejtli, 1998). Every D-glucose unit consists of three free hydroxyl unit groups, which differ in their reactivity and functions. The ability of β-CD to form solid inclusion compounds (host-guest complexes) with a wide range of solid, liquid, and gaseous compounds via molecular complexation (Mohamad et al., 2011; Sambasevam et al., 2013; Srinivasan et al., 2012), and through various kinds of interactions (Van der Waals force, hydrophobic interaction, electrostatic affinity, dipole-dipole interaction, and hydrogen bonding) (Zhang et al., 2011). Besides, CDs have been applied widely in various applications, such as chemical separations (Chin et al., 2010; Crini, 2008), adsorbents (Liu et al., 2011a; Mohamad et al., 2013), food processing (López-de-Dicastillo et al., 2010), and pharmaceutical excipients (Qian et al., 2008).

On the other hand, ionic liquid (IL) is a kind of salt, in which the ions are poorly coordinated. Consequently, these compounds are liquid below 100 °C or even at room temperature (RTILs) (Fontanals et al., 2009; Subramaniam et al., 2010). ILs have unique properties, such as non volatility, non flammability, low viscosity, and have chemical and electrochemical stability (McEwen et al., 1999), and also can remain in liquid state over a wide range of temperature range. Recently, the number of publications and reviews on ILs has increased due to the growing interests and applications of ILs in analytical chemistry (Aguilera-Herrador et al., 2010; Martinis, et al., 2010; Colin F Poole & Poole, 2010; Sun & Armstrong, 2010; Sun et al., 2010a). The applications of ILs in analytical chemistry have been mostly related to studies concerning extractions (Aguilera-Herrador et al., 2010), and separations (Berthod et al., 2008). Apart from that, the ILs are also considered as templating solvents in some syntheses due to their ability to self-assemble in different domains, which are polar and non-polar, and these properties of ILs have been transferred to the development of supramolecular polymers (Mecerreyes, 2011). Thus, novel classes of IL polymers have become famous among researchers since these materials exhibit the properties of ILs and the polymers (Qiu et al., 2010). Owing to the properties of β-CD polymers and ILs, the functionalization of β-CD with the ILs has sparked the interest to develop a new generation material, which demonstrated an interesting phenomenon in the extraction studies. The physical properties of CD can be altered by functionalising it with various precursors in order to make them suitable for a wide range of applications (Badruddoza et al., 2011; Chai & Ji, 2012).

To the best of our knowledge, CD functionalized IL materials have been applied as stationary phases in high performance liquid chromatography (HPLC) (Ong et al., 2008; Zhou et al., 2010), and as chiral selectors in capillary electrophoresis (Ong et al., 2005; Tang et al., 2007). So far, CD-IL polymer has been reported for preliminary sorption study for the removal of organic pollutants and heavy metals (Mahlambi et al., 2010). Previously, CD based materials have been applied in solid phase extraction (SPE) as an adsorbent for various analytes (Fan et al., 2003; Zhu et al., 2009), but the application of new macroporous Cyclodextrin functionalized ionic liquid polymer (βCD-BIMOTs-TDI) for extraction of phenol compounds has not been reported in any studies yet. Although the applications of these materials in the analytical chemistry are still at their early stages, the academic interest in the combination of ILs and CDs is increasing. Herein, in this study, β-CD was functionalized using IL and was further cross-linked with toluene 2,4-diisocyanate (TDI) to form an insoluble polymer for the extraction of phenols.

1.2 Objectives of the research

This study embarked on the following objectives:

1. To synthesis β-cyclodextrin functionalized ionic liquid polymer (βCD-BIMOTs-TDI).

2. To characterise and compare βCD-BIMOTs-TDI with native β-cyclodextrin polymer (βCD-TDI) by using different analytical instruments.

3. To optimize and compare the parameters from batch adsorption studies, such as the effects of pH, concentration, time, and temperature, using the newly synthesized βCD-BIMOTs-TDI for removal of 2,4-DCP, 2,4,6-TCP, and 2,4-DNP.

4. To develop and apply the newly synthesized βCD-BIMOTs-TDI as an adsorbent for solid phase extraction (SPE) and to optimize the SPE parameters, such as the effects of pH, sample volume, eluting solvent, eluting solvent volume, washing step, and the effects of modifier for the extraction of phenols.

1.3 Scope of study

This research involved the synthesis of βCD-BIMOTs-TDI. The synthesized polymer was characterized by Fourier Transform-Infrared (FTIR), X-ray Diffraction (XRD), Scanning Electron Microscopy (SEM), Brunauer–Emmett–Teller (BET), and Thermo gravimetric Analysis (TGA). The performance of βCD-BIMOTs-TDI was evaluated via preliminary batch adsorption study for the removal of phenols from aqueous solution and was compared with native β-CD polymer without modification (βCD-TDI). Based on preliminary batch adsorption study, 2,4-dichlorophenol (2,4-DCP), 2,4,6-trichlorophenol (2,4,6-TCP), and 2,4-dinitrophenol (2,4-DNP) were selected for optimization of batch adsorption study using newly synthesized macroporous βCD-BIMOTs-TDI. The interaction and mechanism of the modified CD (βCD-BIMOTs) with one selected phenol (2,4-dichlorophenol) were studied. Finally, this βCD-BIMOTs-TDI sorbent was applied as an adsorbent for SPE of phenols in water samples.

1.4 Outline of the thesis

The present thesis is organized into six chapters. Chapter 1 gives a brief introduction on research background, research objectives, and scope of study. A review of related literature is presented in Chapter 2. Chapter 3 presents the synthesis and characterization results of βCD-BIMOTs-TDI and the performance of this polymer compared to native polymer (βCD-TDI) through preliminary batch adsorption study to remove phenols. Chapter 4 reports the optimization and comparison of batch adsorption study using synthesized βCD-BIMOTs-TDI for removal of 2,4-DCP, 2,4,6-TCP and 2,4-DNP. Chapter 5 discusses the optimization of SPE method for the extraction of phenols using synthesized macroporous βCD-BIMOTs-TDI sorbent. Finally, the overall conclusion, together with recommendations, is provided in Chapter 6.

CHAPTER 2

LITERATURE REVIEW

2.1 Cyclodextrin (CD)

2.1.1 Introduction

Supramolecular chemistry studies are an important frontier area of research in analytical chemistry, especially CD chemistry, as one of the main branches in this study has been a hot topic among many researchers (Crini & Morcellet, 2002; Gaidamauskas et al., 2009; Wang et al., 2006). Supramolecular chemistry involves all intermolecular interactions, where covalent bonds are not established between the interacting species, for example, molecules, ions, or radicals (Szejtli, 1998). Most of these interactions are of the host-guest type. There are many potential hosts, but CDs seem to be the most important ones. CDs are semi natural products and are produced from a renewable natural material; starch, by a relatively simple enzymic conversion (Connors, 1997; Szejtli, 1998), and are produced in thousands of tons per year via environmentally friendly technologies. The high prices of CDs have dropped due to large scale production and many people have started to use it for industrial purposes. Besides, the ability to form inclusion complex has made the complex substances to modify significantly. Thus, “molecular encapsulation” is widely used in many industries, technologies, and analytical method as well.

CDs can be defined as cyclic torus-shaped oligosaccharides consisting of six (α-cyclodextrin), seven (β-cyclodextrin), eight (γ-cyclodextrin) or more glucopyranose units linked by α-(1,4) bonds (Chernykh & Brichkin, 2010; Khan et al., 1998; Szejtli, 1998), as shown in Figure 2.1. CDs (sometimes called cycloamyloses) are a family of compounds made up of sugar molecules bound together in a ring (cyclic oligosaccharides), which is produced from starch by enzymatic conversion (Chen et al., 2006). Connors (1997) stated that a cyclodextrin molecule, which consists of eight or more glucose residues, is very soluble, difficult to separate, and hardly studied to date. α- CD, β-CD, and γ-CD are commonly referred to as the native CDs, whereas less than six glucose residues are too strained to exist (Connors, 1997). Typical CDs contain a number of glucose monomers ranging from six to eight units in a ring, creating a cone shape.

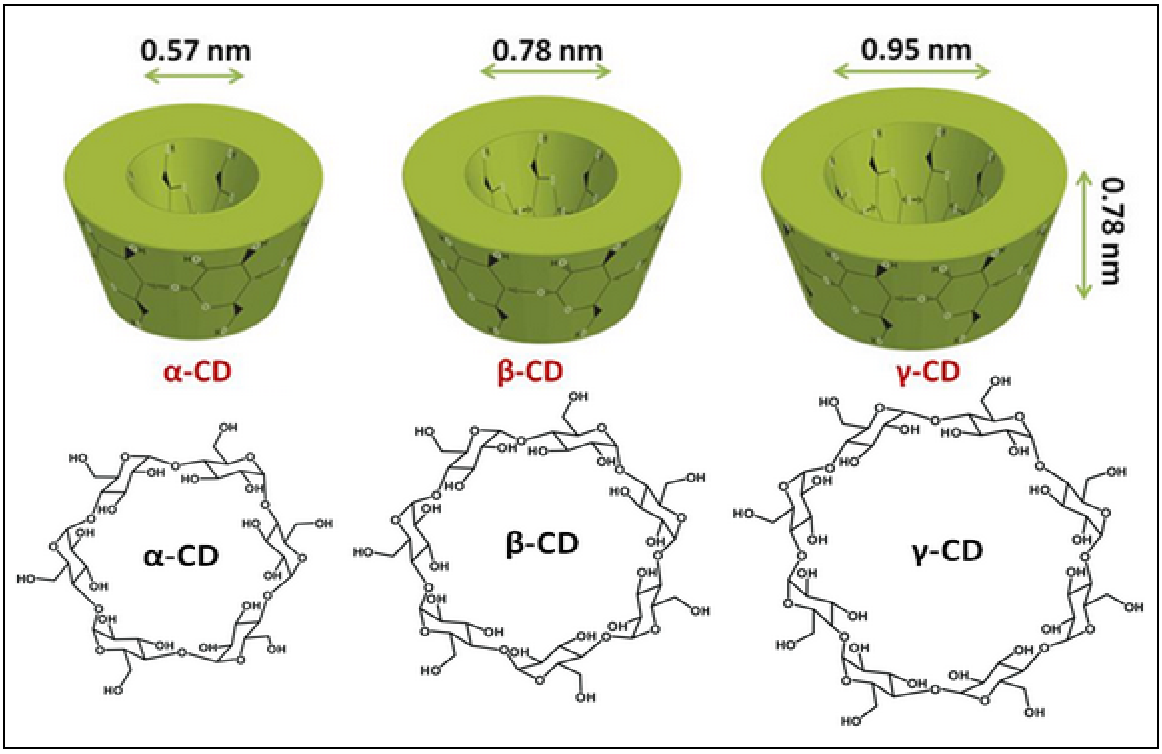

Figure 2.1: Types of CD molecules (Connors, 1997)

2.1.2 Basic properties of CD

CDs can be divided into three types; crystalline, homogeneous, and non hyroscopic substances, which are of torus-like macro ring shape, derive from glupyranose units. CDs are commonly classified as α (6), β (7), γ (8) - cyclodextrin based on the number of glucopyranose units. Among all the available CDs, β-CD is the most accessible with lowest-priced, and generally, the most useful. Moreover, CDs consist of relatively hydrophobic internal cavity, which allows many organic and inorganic molecules to form inclusion complexes (Szejtli, 1998). In addition, CDs exhibit regio- and stereoselectivity and consist of hydrophilic surface with primary and secondary hydroxyl groups. The properties of CDs are summarized in Table 2.1.

Table 2.1: Properties of α, β, γ-CD

Properties	α	β	γ
Number of glucose units	6	7	8
Molecular weight (g/mol)	972	1135	1297
Solubility in water at 25°C (g/100ml)	14.5	1.85	23.2
Volume of cavity (Å^3)	174	262	427
Cavity diameter (Å)	4.7-5.3	6-6.5	7.5-8.3
Outer diameter (Å)	14.6	15.4	17.5
Height of the torus (Å)	7.9	7.9	7.9

Apart from that, in CD molecules, glucose units are connected through glycosidic α-1,4 bonds, as illustrated in Figure 2.2. These molecules are often described as torus, but are more realistically as a shallow truncated cone, the primary hydroxyl rim of the cavity opening having a somewhat reduced diameter compared with the secondary hydroxyl rim. Even sometimes, the torus departs significantly from the perfect symmetry. In addition, the possession of the cavity that makes the molecules attractive subjects for this study (Figure 2.3).

Figure 2.4 shows the exterior of the molecule, bristling with hydroxyl groups, which are fairly polar, while the interior of the cavity is non-polar, relative to the exterior and relative to the usual external environments; water in particular. According to Szejtli (1998), these molecules are suitable to be studied as “hosts” for “guest” molecules are capable of entering either in whole or in part of the cavity, and form non covalent host-guest inclusion complexes. Summarizing the literature available, Szejtli in the year of 2004 concluded that CDs are very interesting, have promising molecules, and are worthy of further study, particularly due to their apparent industrial possibilities (Szejtli, 2004).

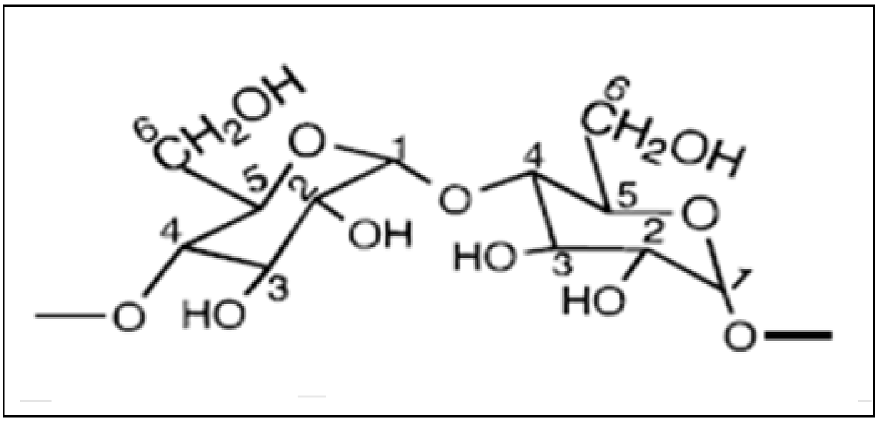

Figure 2.2: Glycosidic linkage of α-1,4 CD molecule (Connors, 1997).

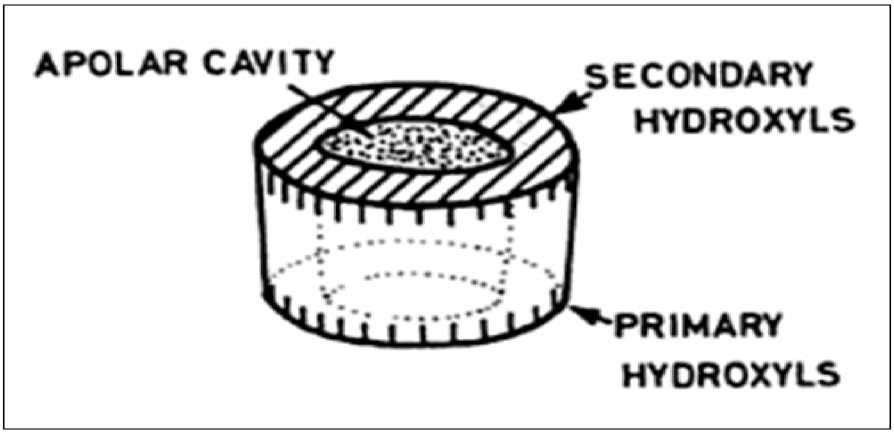

Figure 2.3: CD with empty ‘cylinders’ rings structure (Connors, 1997)

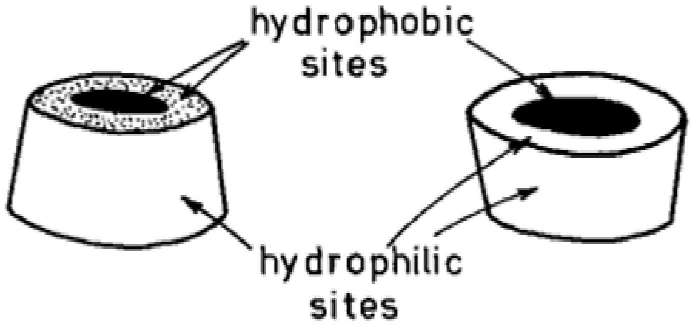

Figure 2.4: Schematic representations of the hydrophobic and hydrophilic regions of a CD cylinder (Szejtli, 1998)

2.1.3 CD derivatives

The physical and chemical properties of CDs can be altered by exploiting the hydroxyl groups at the outer cavity (Szejtli, 1998). Generally, functionalization on CDs is carried out in order to decrease their solubility, increase their stability in the presence of light, heat, and oxidizing agents, and to increase volatility (Harada, 1997). CDs consist of three different types of hydroxyl groups, which are primary (C-6, OHs) and secondary (C-2, C-3, OHs) as shown in Figure 2.5. Primary hydroxyl groups are more reactive compared to secondary hydroxyl groups. Thus, the modifications at primary C-6 hydroxyl group are easy to be carried out and are found to be more reactive during nucleophilic substitution. The primary hydroxyl groups at C-6 are basic, thus a base can be used in order to remove the H from the OH, as shown in equation below:

$$\text{R-OH} + \text{OH}^{-} \longrightarrow \text{R-O}^{-} + \text{H}_2\text{O} \qquad (2.1)$$

Meanwhile, C-2 hydroxyl groups are acidic, and C-3 hydroxyl groups are found to be less reactive due to steric hindrance, and therefore, not easily accessible.

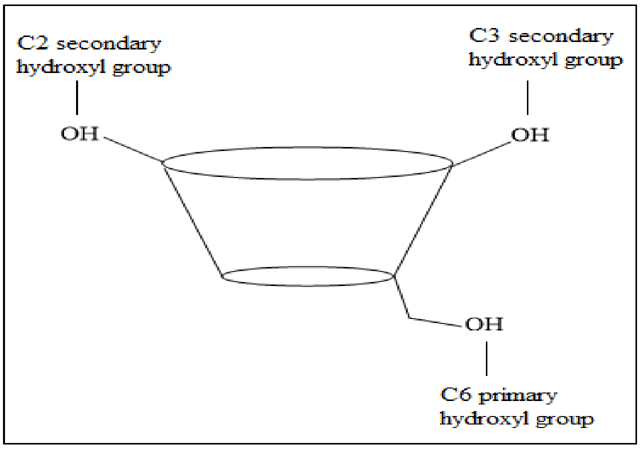

Figure 2.5: The structure of CD with three different hydroxyl groups

2.1.4 Monofunctionalization at the C-6-position of the β-CDs

Generally, there are two ways to modify the β-CDs, such as monofunctionalization, which involves functionalizing of only one out of seven hydroxyl groups in one β-CD unit and per-functionalization, which involves functionalizing of an entire set of hydroxyl group. Monofunctionalization of the β-CDs can be carried out by reacting the hydroxyls groups with an electrophile. Modification at single desired place is found to be complicated because of the presence of a large number of hydroxyl groups at three different positions of β-CDs (Bender & Komiyama, 1978). However, difference in the chemical properties and reactivity of these hydroxyls groups can yield a specific product. In addition, di- and tri-functionalizations exist, but they have not been well investigated since they are difficult to perform.

Apart from that, regioselective reactions should be the target in monofunctionalization. This reaction basically involves the protection of other OH groups in order to prevent them from participating in the reaction, meanwhile, the target OH group is exposed during the reactions. In the presence of base (NaOH), monofunctionalization at hydroxyl C-6 can be achieved by removing the proton to make O^-, which is nucleophilic, that can be easily substituted. The common procedure to form monofunctionalized β-CDs derivative (CDOTs), which is an important precursor for the β-CDs derivative, can be achieved by reacting β-CD with p-toluene sulfonic anhydride (TS_2O) in a basic medium. Figure 2.6 shows the example of nucleophilic substitution process between tosylate β-CD and benzylimidazolium. This is because, tosylate is a good leaving and can be easily substituted by other nucleophiles. The tosyl group on the β-CDs can be displaced by other nucleophiles to produce corresponding modified β-CDs. Some examples of nucleophiles are iodide, azide, thioacetate, hydroxylamine, aryl, and polyaklyalmine. These groups can displace the tosyl group in order to form monoiodo (Ueno et al., 1987), monoazido (Melton & Slessor, 1971; Tsujihara et al., 1977), and monoalkylamino CDs (Petter et al., 1990).

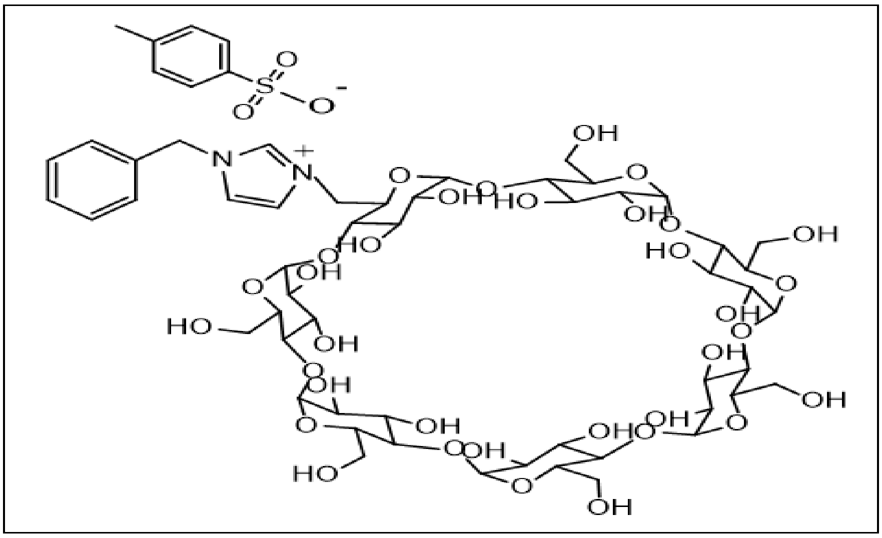

Figure 2.6: Nucleophilic substitution process between tosylate β-CD and benzylimidazolium

2.1.5 CD inclusion complexes

CDs play an important role in practical applications and scientific researches because of its ability to selectively form inclusion complexes with other molecules, ions, and radicals (Chernykh & Brichkin, 2010). Inclusion complexes can be defined as molecular compounds, as one compound (host molecule) spatially encloses another (guest). Inclusion complex is formed by Van der Waals (or hydrophobic) interactions between the hydrophobic "guest" molecules and the cavity of CD. In addition, the formation of hydrogen bonds between hydroxyl group of CD and polar functional groups of guest molecules also lead to the formation of inclusion complexes. During the formation of inclusion complexation, the high energy (high enthalpy) water molecules in the CD cavities is substituted by the guest compound. This is because, in aqueous solutions, hydrophobic CD cavities are occupied by water molecules, which are energetically unfavourable (polar and non polar interactions) and can be substituted by guest molecules, which have less polarity than water, as shown in Figure 2.7 (Chernykh & Brichkin, 2010; Liu & Guo, 2002).

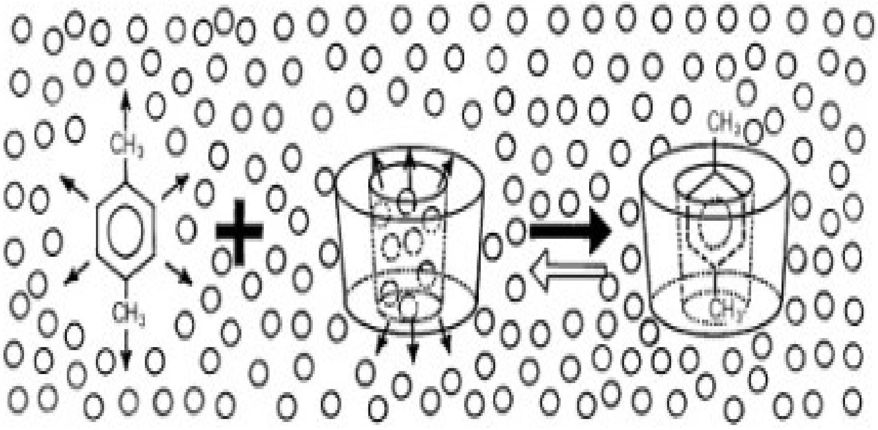

Figure 2.7: Schematic representation of CD inclusion complex formation: p-Xylene is the guest molecule, and the small circles represent water molecules

In a recent research, Ashnager and his co-workers demonstrated that in the production of pharmaceuticals, pesticides, foodstuffs, and toiletry articles, CD and modified CD can be used advantageously (Ashnagar et al., 2007). The (microencapsulated) active and aromatic substances enclosed within them are protected from the effects of light and atmosphere, can be easily handled, and are stored in powder form. Ashnager and his co-workers also stated that general interest in their physical and chemical properties among scientists has grown considerably over the past four decades, which can be seen from the increasing number of publications and patents dealing with inclusion compounds (Ashnagar et al., 2007). Besides, in order to form inclusion complex, the chemical properties of guest molecule are largely independent and have basic requirement for inclusion complex formation, whereby the size is compatible between host and guest molecules. Furthermore, guest molecules must fit, entirely or at least partially, into the CD cavity.

Furthermore, inclusion complex studies between β-CD with various types of compounds, such as drugs, pesticides, and so on, are widely investigated (Karathanos et al., 2007; Villaverde et al., 2004; Wen et al., 2004). However, limited work has been reported on inclusion complex studies with modified CDs. Since modified CDs exhibit better physical and chemical properties, thus the inclusion phenomena of modified CD with various guest compounds has been rapidly growing and the details are summarized clearly in Table 2.2. Among all the modified CDs, hydroxypropyl-β-CD has been found to be the most famous among our researchers.

Besides, there are various methods that can be used to confirm and characterize the formation of CD inclusion complex. However, NMR spectroscopy method was found to be the most important ones to evaluate the geometry of inclusion formation between hosts and guest. In addition, 2D NMR is a powerful tool to investigate the intermolecular interactions and to gain more information on the conformation of the inclusion complex (Li et al., 2003b).

Table 2.2: Types of modified β-CD studied to form inclusion complex with various guest compounds

Modified β-CD	**Guest**	**Reference**
Hydroxypropyl-β-CD	Cholesterol	(Williams III et al., 1998)
Hydroxypropyl-β-CD	Butyl-methoxydibenzoyl methane	(Scalia et al., 1998)
β-cyclodextrin 6-*O*-monobenzoate methylcyclohexane, cyclooctane, methylcyclooctane.	n-hexane, *n*-heptane, *n*-octane, cyclohexane	(Jiang et al., 2000)
Hydroxypropyl-β-CD	Cryptotanshinone	(Li et al., 2003a)
2,6-di-O-methyl-β-CD (DM-β-Cyd)	Celecoxib (CCB)	(Ventura et al., 2005)
Hydroxypropyl-β-CD	Azelaic acid	(Manosroi et al., 2005)
Hydroxypropyl-β-CD,sulfobutyl ether-β-CD, glucosyl-β-CD, maltosyl-β-CD, and sulfobutyl ether-γ-CD	Prednisolone and 6α-methyl prednisolone	(Larsen et al., 2005)
Sulfoalkyl Ether-Alkyl Ether CD Derivatives	6α-methylprednisolone	(Tongiani et al., 2005)
Hydroxypropyl-β-CD	Trazodone hydrochloride	(Misiuk & Zalewska, 2009)
Sulfobutylether-alkylether (SBE-AE-CD)	Steroid molecules	(Tongiani et al., 2009)
MAH-β-CD (modified β-CD carrying seven vinyl carboxylic acid groups)	APAP = 4-Acetamino phenol	(Ding et al., 2010)

Table 2.2 (Continued)

Hydroxypropyl-β-CD	Zerumbone	(Eid et al., 2011)
Dimethyl-β-CD (DIMEB)	Loratadine (LOR)	(Szabados-Nacsa et al., 2011)
3-hydroxypropyl-β-CD	Benzophenone	(Berbicz et al., 2011)
Hydroxypropyl-β-CD	Cilnidipine	(Hu et al., 2012)
Modified β-CD with amino groups	Polyaniline	(Mlika et al., 2012)
Hydroxypropyl-β-CD thiosemicarbazones	Hepatitis C virus (HCV) of 1-indanone	(Glisoni et al., 2012)
2-hydroxypropyl-β-CD (HP-β-CD)	Canthaxanthin (CTX)	(Gharibzahedi et al., 2014)
Methyl-β-CD (M-β-CD)	Valsartan(VAL)	(Chadha et al., 2014)
Amino acid-modified β-CD	Doxorubicin	(Zhao et al., 2014)

2.1.6 The application of CD in separation studies

The applications of CDs in separation science have increased over the past few decades due to its unique structure and properties (Del Valle, 2004; Loftsson, & Duchene, 2007). The ability of CD to form inclusion complexes with various analytes could be the main reasons for its application in separation studies. Some examples of applications include chemical separations (Chin et al., 2010), adsorbents (Liu et al., 2011; Sharifah Mohamad et al., 2013), as shown in Table 2.3, chiral selector (Ong et al., 2005; Tang et al., 2007), and stationary phases (Ong et al., 2008; Zhou et al., 2010).

Table 2.3: Summary on removal of various pollutants using CD based materials

CD-based material	Analyte	Reference
CD-based materials containing carboxylic groups	C.I. Basic Blue 9 (BB9)	(Crini & Peindy, 2006)
β-CD cross linked with hexamethylene diisocyanate (HMDI)	Azo dyes	(Ozmen et al., 2008)
CD(s) cross linked with epichlorohydrin polymer	Cationic dyes	(Grégorio Crini, 2008)
CD-modified HMS-type mesoporous silicas	Removal Red 3BS	(Asouhidou et al., 2009)
CD polyurethanes	Natural organic matter (NOM)	(Nkambule et al., 2009)
Fe_3O_4 nanoparticles (MNP) with carboxymethyl-β-CD (CM-β-CD)	Methylene blue (MB)	(Badruddoza et al., 2010)
β-CD,4-methylene-bisphenyl Diisocyanate (MDI), and β-CD-hexamethylenediisocyanate (HMDI) polymers	Azo dyes and aromatic amines	(Yilmaz et al., 2010)
β-CD grafted multiwalled carbon nanotubes	Polychlorinated biphenyls	(Shao et al., 2010)
β-CD modified Zeolites	Nitrophenols	(Li et al., 2011b)
β-CD/attapulgite composites	2,4-didichlorophenol, 2,6-didichlorophenol	(Pan et al., 2011)
Electrospun CD-functionalized mesoporous polyvinyl alcohol/SiO_2 nanofiber membrane	Indigo carmine dye	(Teng et al., 2011)
CD(s) cross linked with epichlorohydrin polymer (CDP)	Pesticides	(Liu et al., 2011a)
β-CD-based hydrogel (CAM)	Cd^{2+}, Pb^{2+} and Cu^{2+} ions	(Huang et al., 2013)
PAN hollow fibre membranes with triacetyl-β-CD	Pesticides	(Cassano et al., 2013)
β-CD cross-linked with 1,2,3,4-butanetetracarboxylic dianhydride (BTCA) polymers	Bisphenol A	(Kono & Nakamura, 2013)

Table 2.3 (Continued)

Carboxymethyl-β-CD (CM-β-CD) polymer modified Fe_2O_4 nanoparticles (CDpoly-MNPs)	Pb^{2+}, Cd^{2+}, Ni^{2+}	(Badruddoza et al., 2013)
6-Deoxy-6-ethylenediamino-β-CD (β-CDen) grafted thiodiglycolic acid (TDGA) modified magnetic nanoparticles (CDen-MNPs)	Naproxen, carbamazepine, bisphenol	(Ghosh et al., 2013)
β-CD-Modified Cellulose nanocrystals	Procaine hydrochloride and imipramine hydrochloride	(Chen et al., 2014)
β-CD functionalized cellulose acetate (CA) nanofibers	Phenanthrene	(Celebioglu et al., 2014)
β-CD coated on silica	17 β-estradiol, perfluorooctanoic acid (PFOA), and bisphenol-A (BPA)	(Bhattarai et al., 2014)

2.2 An Introduction to Ionic Liquids (ILs)

The term “ionic liquid” (IL) can be defined as a broad class of salts, which have appreciable liquid ranges and melt at or below 100 °C. Besides, room temperature ionic liquids (RTILs) can be classified as a subset of IL, which is found to be liquid at room temperature (25°C). ILs exhibit unique properties (as shown in Figure 2.8) due to the fact that they are composed entirely of ions, such as classical metallic molten salts (sodium chloride (NaCl)). Thus, ILs may behave quite differently when compared to other common molecular liquids when used as solvents (Sun & Armstrong, 2010).

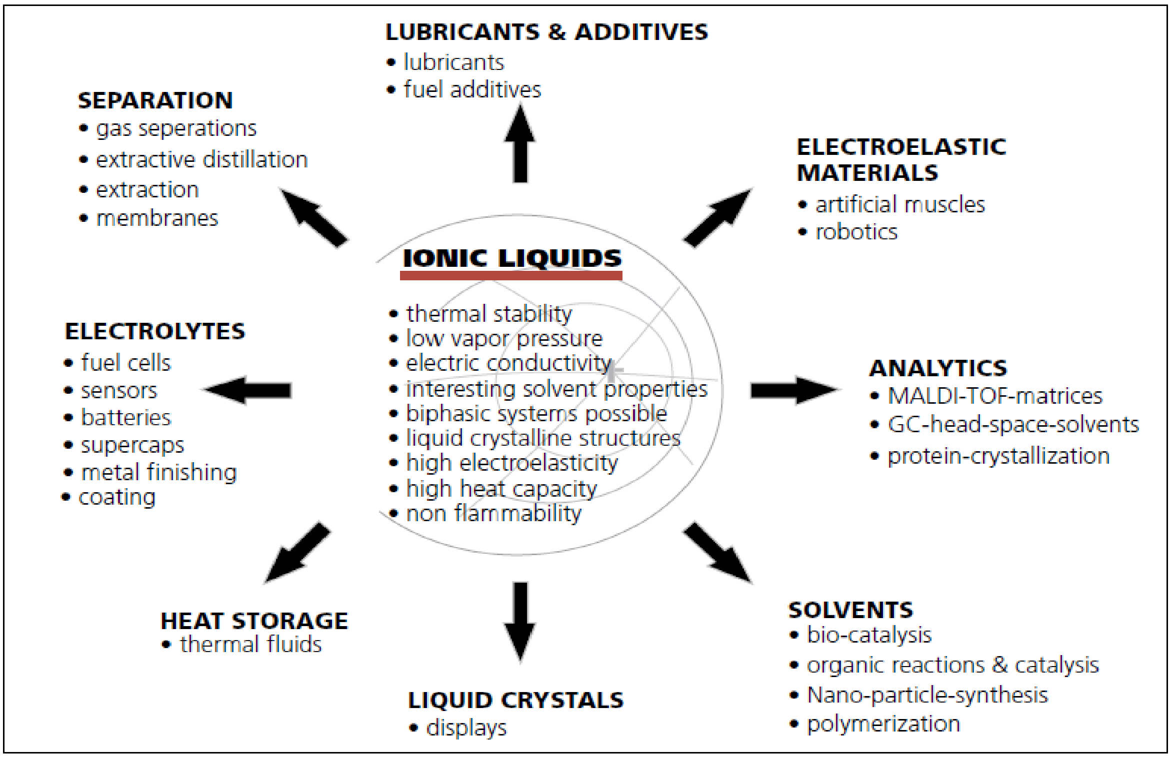

Figure 2.8: Properties of ILs and their potential and current applications

In addition, RTILs consist of organic cations, such as imidazolium, pyridinium, pyrrolidinium, phosphonium, ammonium, and inorganic anions, such as Cl^-, PF_6^-, and BF_4^-. Recently, more new RTILs that consist of organic anions have been discovered, such as trifluoromethylsulfonate $[CF_3SO_3]^-$, bis[(trifluoromethyl)sulfonyl]imide $[(CF_3SO_2)_2N]^-$ (i. e., NTf_2), and trifluoroethanoate $[CF_3CO_2]^-$. The common structures of cations and anions of ILs are shown in Figure 2.9. ILs exhibit lower melting points due to their relatively large size of one or both ions in ILs and low symmetry (Krossing et al., 2006). Therefore, ILs have many fascinating properties, such as low volatilities (negligible vapour pressure), wide liquid ranges, good thermal stabilities, electrolytic conductivity, wide range of viscosities, adjustable miscibility, reusability, and non-flammability (Sun & Armstrong, 2010). The physical and chemical properties may be significantly affected if varying cations or anions are involved. Thus, tremendous number of ILs can be produced by combinations of a variety of cations and anions, and make custom syntheses feasible. It is estimated that there could be 10^{18} different types of ILs available (Carmichael & Seddon, 2000). This provides a large pool for scientists to select the ILs for specific applications and these intrinsic features of ILs, combined with their easy way of preparation, have resulted in a remarkable increase in researches.

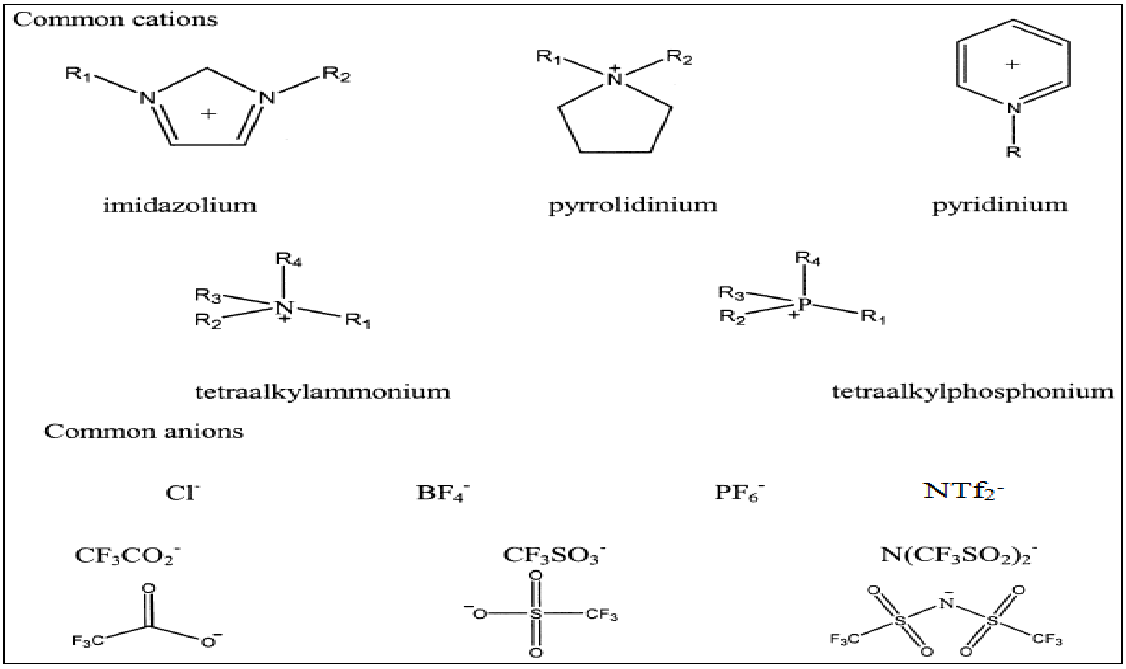

Figure 2.9: Common structure of cations and anions of ILs (Sun & Armstrong, 2010)

ILs can be considered as alternatives to classical organic solvents. This is because, it has been applied in various applications, such as organic synthesis, electrochemistry, liquid phase extraction, catalysis for clean technology, and polymerization processes (Duchet et al., 2010; Fontanals et al., 2009; Kubisa, 2009; Seddon, 1997; Zanoni et al., 2010). Accordingly, the application of ILs in separation technology has attached great attention (Table 2.4). Previously, alkylimidazolium-based ILs have been applied as a stable stationary phase for gas chromatography (Ragonese et al., 2009; Yao & Anderson, 2009). These could be due to an unusual selectivity behaviour of ILs with “dual nature”, where ILs can separate polar compounds as if they were polar stationary phases and non polar compounds, suggesting that ILs might be useful multimodal media for chromatographic separations. Furthermore, ILs can be used in reversed-phase chromatography as mobile phase additives because they can be mixed with other low viscosity solvents (He et al., 2003; Xiaohua et al., 2004). Previously, ILs have been applied as electrolyte additives, running buffer modifiers and supported coatings on the capillary walls in capillary electrophoresis (CE) (Borissova et al., 2008; Jiang et al., 2003).

Table 2.4: Applications of ILs in separation studies

Target compounds	Ionic liquids	Application	Ref.
Ephedrines	1-allyl-3-hexyl imidazolium tetrafluoroborate	IL-based silica sorbent as HPLC stationary phase	(Liu et al., 2004)
Inorganic anions	Imidazolium functionalized silica	IL-based silica sorbent as HPLC stationary phase	(Qiu et al., 006)
Esters	Bis[(trifluoromethyl) sulfonyl]imide	IL-based polymer sorbent for SPE	(Zhao et al., 2008)
Alcohols and aromatic compounds	1-butyl-3-methylimidazolium chloride and 1-butyl-3-methylimidazolium bis[(trifluoromethyl) sulfonyl]imide	GC stationary phases	(Baltazar et al., 2008)
Fatty acid methyl esters	1,9-di(3-vinyl-imidazolim) nonanebis(trifluoromethyl) sulfonylimidate	GC stationary phases	(Ragonese et al., 2009)
Acidic, basic, neutral compounds	1-octyl-3-propylimidazolim chloride	IL-based silica sorbent for SPE	(Chou et al., 2009)
Tanshinones	1-methylimidazole	IL-based silica sorbent for SPE	(Tian et al., 2009b)
Liquiritin, glycyrrhizic acid	2-ethyl-4-methylimidazole	IL-based silica sorbent for SPE	(Tian et al., 2009)
Caffeine, theophylline	1-methylimidazole	IL-based polymer sorbent for SPE	(Tian et al., 2009a)

Table 2.4 (Continued)

Caffeine, theophylline theobromine	Imidazole,1-methylimidazole,2-ethyl-4-methylimidazole	IL-based silica sorbent as HPLC stationary phase	(Bi & Row, 2010)
Peptides	Butyl-imidazol	IL-based silica sorbent as HPLC stationary phase	(Chitta et al., 2010)

2.3 CD functionalized IL material

Owing to the properties of β-CD and ILs, the functionalization of β-CD with IL has generated interest among researchers. The application of CDILs in separation science begins as a chiral selector in chiral capillary electrophoresis (CE). In addition, Ong and co-workers in the year of 2005 had successfully synthesized novel single isomers of positively charged β-CDs (Ong et al., 2005). It was found that, resolution and selectivity of these cationic CDs were dependent on certain parameters, such as concentration of chiral selectors, pH of running buffer, counter anions of the CDs, side chain length, temperature of the capillary column, and organic modifier as well.

The applications of CDILs were further extended as a chiral stationary phase. Wang, and co-workers have successfully synthesized cationic β-CD derivatives as a chiral stationary phase for high-performance liquid chromatography (HPLC) and supercritical fluid chromatography (SFC) (Wang et al., 2008). Based on their findings, they came to a conclusion that n-octyl group of imidazolium moiety group on CD ring exhibits strong interaction with analyte. In another work, Ong and co-workers have synthesized and applied mono-6-(3-methylimidazolium)-6-deoxyperphenylcarbamoyl-β-CD chloride as a chiral stationary phase for HPLC and SFC in the year of 2008 (Ong et al., 2008). Good enantioseparation was obtained for the aromatic alcohols investigated under SFC separation. In 2010, Zhou. and co-workers further explored the application of CDILs as a chiral stationary phase in HPLC (Zhou et al., 2010). They discovered that high resolutions depend on the properties of the cations and anions on the selectors in combination with the chiral recognition sites of the CD. Moreover, in 2012, Wang and co-workers also synthesized a new cationic CD with chemically bonded chiral stationary phases for HPLC, (Wang et al.,2012) and they found that imidazolium containing β-CD stationary phase afforded more favourable enantioseparations under normal phased HPLC.

In addition, the application of CDILs as a chiral stationary phase in gas chromatography (GC) had been explored by Huang, (Huang et al., 2010). They found that CDILs stationary phase exhibits several better properties as compared to commercial column, such as different enantioseparations, more symmetric peak shapes, and some complementary enantioseparations.

In 2010, an attempt was made by Mahlambi and co-workers had synthesized CDIL polymers as an adsorbent for removal of organic pollutants and heavy metals from water samples and they found that CDIL polymer exhibited enhanced absorption capacity towards organic and inorganic pollutants (Mahlambi et al., 2010). Recently, (Zhou et al., 2013; Zhou & Zhu, 2013) had successfully synthesized CDIL polymers as an adsorbent for SPE. The developed methods were successfully applied for the determination of Kaempferol in red wine and magnolol in drug samples.

Summarising the literature available, CDILs material have been found as a promising material to be study further. Therefore, in this work, new macroporous CDIL polymer had been successfully synthesized and applied as an adsorbent for the extraction of phenols.

2.4 Adsorption

An adsorption process would be the most efficient and economically feasible method for the removal of toxic organic pollutants (Raoov et al., 2013). Adsorption process seems to be the most important part of separation and is used widely in various fields, such as chemical, biological, analytical, and environmental fields. Hence, in order to ensure adequate surface area for adsorption process, adsorbents with diameters ranging from sub-micron to micron and large internal porosities are needed.

Adsorption isotherms are very important to study the interaction between the adsorbate and adsorbent, and in order to optimize the use of adsorbent. Thus, as for adsorption data prediction, the correlation of experiment equilibrium data, either a theoretical or an empirical equation, is essential (Ahmed & Dhedan, 2012). Apart from that, adsorption kinetics can be defined as the study of the rate at which pollutants are adsorbed onto adsorbent surface, which controls the residence time of the adsorbent uptake at the solid-solution interface (Altenor et al., 2009). Therefore, in order to understand the adsorption process more precisely, this study had investigated the adsorption equilibrium, kinetics, mechanism, and the parameters affecting the adsorption process.

2.4.1 Adsorption equilibrium

a) Langmuir’s Model

The Langmuir isotherm has been widely studied for the sorption of pollutants. It is based on the assumption concerning the monolayer adsorptions on a homogenous surface with uniform energies of adsorption for all the binding sites. Furthermore, no further adsorption process would occur if the site is occupied by a solute (Hall et al., 1966). The linear form of the Langmuir isotherm equation (Srivastava et al., 2006; Wang et al., 2011) can be represented by the following equation:

$$\frac{1}{q_e} = \frac{1}{bq_m} + \frac{C_e}{q_m} \tag{2.2}$$

where C_e (mg/L) is the equilibrium concentration of the adsorbate, C_o (mg/L) is the initial adsorbate concentration, qe (mg/g) is the adsorption capacity at equilibrium, q_m (mg/g) and b (L/mg) are Langmuir constant related to the adsorption capacity and the rate of adsorption respectively. Further dimensionless separation factor (R_L) is calculated in order to determine if the adsorption process is favourable or unfavourable using the following equation (Hall et al., 1966):

$$R_L = \frac{1}{1 + bC_o} \tag{2.3}$$

b) Freundlich's Model

The Freundlich isotherm assumes a heterogeneous system with different energies of active sites and reversible adsorption, which is not restricted to monolayer formations (McKay et al., 1982). The Freundlich constant can be obtained from a plot of log qe versus log Ce. The linear form of the Freundlich isotherm is as shown below:

$$\log q_e = \log K_F + \frac{1}{n} \log C_e \tag{2.4}$$

where K_F ((mg/g) (L/mg)$^{1/n}$) is the adsorption capacity, while n represents Freundlich constants, respectively. Larger value of K_f indicates greater adsorption capacity, while n values indicate the favourability of the adsorption process. If n is above unity, then the adsorption process is favourable.

c) Dubinin-Radusckich’s model

The D-R isotherm analysis has been widely used in order to ascertain the high degree of rectangularity (Dubinin & Radushkevich, 1947). The linear form of the D-R isotherm equation is as follows:

$$\ln q_e = \ln q_m - \beta\varepsilon^2 \qquad (2.5)$$

where β (mol^2/kJ^2) represents the adsorption energy constant obtained from the slope of the straight-line plot of ln qe versus ε^2 and ε, the Polanyi potential, can be calculated using the following equation:

$$\varepsilon = RT \ln [\ 1 + 1/C_e] \qquad (2.6)$$

where R is the universal gas constant in kJ/(molK), and T is the temperature in Kelvin (K). The mean free energy, E (kJ/mol) can be obtained by the following equation:

$$E\ (kJ/mol) = (2\beta^{-0.5}) \qquad (2.7)$$

d) Temkin’s Model

Another model for the analysis of indirect adsorbent/adsorbate interactions on adsorption isotherms is Temkin and Pyzhev (Temkin & Pyzhev, 1940). Apart from that, this isotherm assumes that the heat of adsorption of all the molecules in the layer would decrease linearly with coverage and the adsorption is characterized by a uniform distribution of binding energies, up to some maximum binding energy. The linear form of Temkin isotherm equation is as follows:

$$q_e = \beta \ln K_T + \beta \ln C_e \qquad (2.8)$$

where $\beta = RT/b_T$. A plot of q_e versus ln C_e, constant K_T and b_T can be found from the intercept and slope. K_T (L/mg) represents Temkin constant related to the equilibrium binding energy, while b_T(J/mol) is Temkin constant related to the heat of adsorption.

2.4.2 Adsorption kinetics

Several kinetic models were used to investigate the mechanisms of adsorption and kinetic parameters, such as the pseudo first order (Febrianto et al., 2009; Memon et al., 2011), pseudo second order (Ho et al., 2000; Bingjun Pan et al., 2008), Elovich, film diffusion, and intra particles diffusion (Weber & Morris, 1963) models. The characteristics and equations of these models are described in detail below:

a) Pseudo first order model

The pseudo first order equation is widely used for the adsorption of an adsorbate from an aqueous solution. Furthermore, this kinetic equation is based on the assumption that the rate of change of solute uptake with time is directly proportional with the difference of saturated concentration and the amount of solid adsorbed with time (Lagergren, 1898). The pseudo first order kinetic equation is presented as:

$$\frac{dq_t}{d_t} = k_1(q_e-q_t) \tag{2.9}$$

When q_t=0 at t=0, Eq. (2.9) can be integrated into the following equation:

$$\log (q_e-q_t) = \log q_e - \frac{k_1}{2.303} t \tag{2.10}$$

where q_e and q_t are the amount of analyte adsorbed (mg/g) at equilibrium and at time, t, is the contact time (min), and k_1 is the rate constant of this equation (min^{-1}). The values of k_1 and q_e were calculated from the plot of log (q_e-q_t) versus t.

b) Pseudo second order model

The behaviour over the whole range of adsorption predicted by the pseudo second order model, which is in agreement with an adsorption mechanism, is the rate controlling steps compared to the pseudo first order model (Hameed, 2007). The pseudo second order kinetic equation is presented by Ho, and Mckay (Ho & McKay, 1999) as:

$$\frac{dq_t}{d_t} = k_2 (q_e-q_t)^2 \tag{2.11}$$

Integrating Eq. (2.11) and noting that q_t=0 at t=0, the equation obtained can be re-arranged into a linear form:

$$\frac{t}{q_t} = \frac{1}{k_2q_e^2} + \frac{1}{q_e} t \quad \text{where, } h=k_2q_e^2 \text{ and } t_{1/2}=(k_2q_e^{-1}) \tag{2.12}$$

where h is the initial adsorption rate (mg/g) min, $t_{1/2}$ is half equilibrium time (min), and k_2 is the pseudo second order rate constant (g/mg min). The values of q_e, k_2, h, and $t_{1/2}$ can be obtained by a linear plot t/q_t vs. t.

c) Elovich’s model

To further prove that the sorption is based on chemisorptions, the Elovich’s model was employed. The Elovich model equation is as shown below (Castro López et al., 2012):

$$q_t = \frac{1}{\beta} \ln(\alpha\beta) + \frac{1}{\beta} \ln t \qquad (2.13)$$

where α is the initial sorption rate (mg/g min), β is related to the extended surface coverage, and activation energy for chemisorption (g/mg). The values of α and β can be obtained by a linear plot q_t vs. ln t.

2.4.3 Adsorption mechanism

To further investigate and understand the mechanism of adsorption process and to determine the rate of controlling step, which mainly depend on external diffusion/film, followed by intra particle or pore diffusion, and finally, sorption into the interior sites of the adsorbent. The final process is very rapid, hence the sorption of the adsorbate on the sorbent may be governed by external and/or intra particle diffusion (Bhatnagar & Minocha, 2009).

a) External diffusion

The external diffusion model or film diffusion is described as follows in Eq. (2.14):

$$\mathrm{Ln}\,\frac{C_t}{C_o} = -k_{ext}\,t \qquad (2.14)$$

where C_o and C_t represent the concentration of the solute in the initial solution and in the liquid phase at time t and k_{ext} (1/min) is a diffusion rate parameter. The plot of ln (C_t/C_o) against t should give a linear line with zero intercept if external diffusion is applicable (Castro López et al., 2012).

b) Weber and Moris' model

The intraparticle diffusion equation can be written as:

$$q_t = Kt^{0.5} + c \tag{2.15}$$

where, c represents the intercept (mg/g) and K is the intra particle diffusion rate constant (mg/g min). A plot of q_t versus $t^{0.5}$ (square root of time) should be linear if intraparticle diffusion is involved in the adsorption process, and when this line passes through the origin, the intraparticle diffusion is said to be the rate-controlling step. If the plot does not pass through the origin, this is indicative of some degree of boundary layer control, and this further shows that the intraparticle diffusion is not the only rate-limiting step, but other kinetic models may control the rate of adsorption, all which may operate simultaneously (Kilic et al., 2011).

2.4.4 Adsorption Thermodynamics

Gibb's free energy change ((ΔG^o) was evaluated using Eq. (2.16), while enthalpy change ($\Delta H°$) and entropy change ($\Delta S°$) were calculated from the slope and intercept of the Van't Hoff plot (ln k_d vs. 1/T) using Eq. (2.17) (Ning et al., 2009).

$$\Delta G^o = -RT \ln k_d \tag{2.16}$$

$$\ln k_d = \frac{\Delta S^o}{R} - \frac{\Delta H^o}{RT} \tag{2.17}$$

Where R represents universal gas constant in kJ/(mol K), T is the temperature (K), while k_d is the equilibrium constant (m^3/mol) (Rojas et al., 2005).

2.5 Extraction Methods for Chemical Analysis

Most of the analytical procedures involve a few steps, such as sampling, sample preparation, separation, quantitation, and statistical evaluation. Thus, in order to obtain accurate and reproducible results, each step should be conducted correctly. Among all the steps involved, sample preparation is found to be the most important steps in order to determine the success of overall analytical procedure. In order to make the analyte more suitable for separation and detection, sample preparation steps are very important for analyte pre-concentration and removal of interferences from complex matrices, such as environmental, biological, and foodstuff samples (Fontanals et al., 2012). Apart from the advances made in separation and detection techniques, sample preparation plays an important role in analytical process, and it is essential if reliable results are to be achieved and instrument performance maintained (Chen et al., 2008).

Generally, sample preparation can be categorised into a number of different classes of activities, which can be as simple as filtration, sedimentation, and centrifugation or more tedious procedures, such as solvent extraction, sorbent extraction, and compound isolation and membrane separations. Some examples of sample preparation techniques are solid phase extraction (SPE), solid phase microextraction (SPME), stir bar sportive extraction (SBSE), dispersive liquid-liquid microextraction (DLLME), liquid-liquid extraction (LLE), and liquid phase microextraction (LPME).

2.5.1 Solid phase extraction

Solid phase extraction (SPE) is the most widely used sample preparation technique for liquid samples among all the different extraction techniques (Fontanals et al., 2012). SPE has also been found to be famous among researchers to prepare liquid samples and to extract semi volatile analytes. In addition, SPE also can be used with solids that are pre-extracted into solvents. Basically, SPE carries three important principle goals: trace enrichment (concentration), matrix simplification (sample clean-up), and medium exchange (transfer from the sample matrix to a different solvent or to a gas phase) (Poole, 2003).

Initially, SPE is developed as a complement or replacement for liquid-liquid extraction (LLE) (Poole, 2003). This is because, with SPE, many problems caused by LLE, such as incomplete phase extraction, use of expensive and breakable specialty glassware, less-than-quantitative recoveries, and wastage of large quantities of organic solvents, can be prevented. Apart from that, SPE has been found to be more efficient than LLE, easy to perform, rapid, can be automated, less solvent use, and lab time is reduced (Poole, 2003). Thus, SPE has become a common sampling technique in many fields, such as chemistry, environmental chemistry, pharmaceutical, clinical, food, and industrial chemistry, for sample pre-treatment.

SPE also belongs to the groups of sorptive-based extraction techniques, where the samples are placed in contact with a suitable material, so that the availability of different materials to carry out the extraction is essential. Therefore, more researches into sample preparation techniques should focus on developing new materials in order to achieve higher selectivity and capacity of the technique (Fontanals et al., 2012). The common classic sorbents used in SPE are (Fritz, 1999):

1) Silica-based, modified with C18, C8, phenyl, CH, CN or NH_2 groups
2) carbon based sorbents, including graphitized carbon black (GCB), and porous graphitic carbon (PGC)
3) porous polymeric sorbents, such as macroporous polystyrene-divinyl-benzene (PS-DVB)

In recent decades, researches into SPE sorbents have focused on improving capacity, as well as selectivity, within a single material, and have led to the development of dual phase or mixed mode sorbents. Usually, these materials combine silica or polymeric (the most common for promoting non ionic interactions) skeleton with ionic groups with two different types of interactions, such as reversed phase (RP) (from the skeleton) and ionic-exchange (from the ionic group). These sorbents are classified as cationic or anionic, and the strength of sorbent also depends on the ion group that is attached to it. Therefore, these materials need careful choice of pH medium, and the solvent at each SPE step allows the matrix components to interfere to be eluted separately from the analytes of interest during the washing and elution steps, respectively (Fontanals et al., 2012).

In recent years, ILs have been immobilized or attached chemically or physically on various types of polymers for SPE applications, as summarized in Table 2.5, due to their unique characteristics, as discussed above. Apart from that, CD polymers are very famous for SPE applications (Table 2.6) among many researchers due to their good properties. Therefore, the combination of CD with ILs has allowed for the preparation of a new class of material for extraction and separation studies.

Table 2.5: IL-polymer sorbents used in SPE

Adsorbent	Analyte	Recoveries	Reference
Cross linked polymer supported on N-Methylimidazolium trifluoroacetate	Pharmaceutical products	90-100%	(Fontanals et al., 2009)
N-Methylimidazolium modified functional polymer	(a) Caffeine (b)Theophylline	Caffeine: 87-90% Theophylline: 89-91%	(Tian, et al., 2009a)
Amino-imidazolium polymer	(a) Oxymatrine (b) Matrine	Oxymatrine: 94% Matrine: 81%	(Bi et al., 2010b)
Methylimidazolium chloride onto PVC surface	Cr (VI)	92-100%	(Chen et al., 2010)
Alkyl-pyridinium polymer sorbent	(a) Liquiritin (b)Glycyrrhizin	80-90%	(Bi et al., 2010a)
IL modified porous polymer	Tashinone I, tanshinone IIA and cryotanshinone	Not available	(Tian et al., 2011)

Table 2.6: Summary on previous SPE based on CD based material

CD-based material	Analyte	Extraction method	References
β-CD bonded silica (CDS)	4-nitrophenol	SPE-HPLC	(Fan et al., 2003)
β-CD-polyurethane polymer	Aromatic amines	SPE-HPLC	(Bhaskar et al., 2004)
β-CD-bonded silica particles	Phenols	SPE-GC-MS	(Faraji, 2005b)

Table 2.6 (Continued)

βCD/epichlorohydrin Copolymer	Urinary cannabinoids	SPE-GC-MS	(Moon et al., 2008b)
βCD cross linked with epichlorohydrin	Steroids	SPE-GC-MS SPE-LC-MS	(Moon et al., 2008a)
β-CD epichlorohydrin polymer	Cu(II)	SPE-GFAAS	(Zhu et al., 2008)
β-CD cross linked with epichlorohydrin	Co(II)	SPE-ICP-MS	(Zhu et al., 2009)
β-CD epichlorohydrin polymer (β-CDP)	Brilliant Blue	SPE-UV	(Li et al., 2009)
β-CD epichlorohydrin polymer	Amaranth Colorant	SPE-UV-VIS	(Li et al., 2011a)
β-CD epichlorohydrin polymer	Cr(III), Cr (VI)	SPE-GFAAS	(Gu & Zhu, 2011)
Molecularly imprinted polymers of allyl-β-CD and methacrylic aci	Phthalate	MISPE-UV-VIS	(Yongfeng et al.,2012)
IL loaded β-CD-cross-linked polymer	Rhodamine B	SPE-HPLC	(Ping et al., 2013)
β-CD on Dowex resin as an insoluble polymeric matrix	Pb (II)	SPE-FAA	(Mirzajani et al., 2013)
mono-6-deoxy-6-imidazole-β-CD polymer (β-CDIMCP)	Kaempferol	SPE-UV-VIS	(Zhou et al., 2013a)
Carboxymethyl-hydroxy propyl-β-CD polymer modified magnetic particles Fe_3O_4 (CM-HP-β-CDCP-MNPs)	Rutin	SPE-UV-VIS	(Gong et al., 2014)
Magnetic nanoparticles grafted β-CD	5-hydroxy-3-indole acetic acid	SPE-SF	(Ahmed et al., 2014)

2.6 Phenols

2.6.1 Introduction

The most critical issues in environmental analytical chemistry today are related to water quality control. Phenols easily can be found in our environment due to its release directly or indirectly (Feng et al., 2009), thus they appear to be one of the problematic groups globally. Chlorophenols are usually released to the environment by the chlorination of municipal water, from pesticides production, dyes, pharmaceuticals, and degradation of chemicals (Hameed, 2007). Therefore, the Environmental Protection Agency (EPA) has listed chlorophenols as pollutants (Lin & Tseng, 1999) due to their carcinogenic effect to the environment, which can permeate human skin by in vitro and absorbed by gastro-intestinal tract.

Nitrophenols are other phenolic derivatives which belong to major organic pollutants that have been analyzed in the environment frequently. Nitrophenols are products from pesticides degradation, car exhaust, and industrial waters, and are listed as priority pollutants. Nitrophenols have great potential toxicities of carcinogenics, teratogenesis, and mutagenesis (Guo et al., 2004). Thus, nitrophenols and chlorophenols are very hazardous to our environment and have been the subject for numerous ecological surveys of fauna and flora in aquatic, terrestrial, and aerial environments (Abay et al., 2005). Chlorophenols are very toxic to animals and they depend on the degree of chlorination, the position of the chlorine atoms, and the purity of the sample (Boyd et al., 2001). Owing to its stability, toxicity, and bioaccumulation, monitoring of their levels in our environmental is critically important in order to protect the human health and the environment. This has increased the demand for the development of simple, economically feasible, reliable, sensitive, and rapid analytical methods.

2.6.2 Extraction of phenols

Phenols present in low levels in our environment, thus, they need to be accurately determined in environmental extracts that are often complex, and pre-treatment (extraction and purification) of the samples is always in demand. The popularity of sorbent-based techniques, such as SPE and solid-phase micro extraction (SPME), have increased, as illustrated in Table 2.7, especially dealing with extractions of phenols, followed by determination via high-performance liquid chromatography (HPLC) or gas chromatography (GC).

Table 2.7: Summary of the extraction method of phenols

Adsorbent	Phenols	Matrix	Extraction method	LOD	Reference
Polyaniline	2-Chlorophenol, 4-chlorophenol , 2,4-dichlorophenol, 2,4,6-trichlorophenol, Pentachlorophenol	Water samples	SPE-GC-ECD	3-110 ng/L	(Bagheri & Saraji, 2001)
Pyrrole-based conductive polymer	Phenol, 2-chlorophenol, 4-chlorophenol , 2,4-dichlorophenol, 2,4,6-trichlorophenol	Water samples	SPE-GC-FID, SPE-GC-MS	15-118 ng/L	(Bagheri & Mohammadi, 2003)
Conductive Polymers	Phenol, 2,4-dimethylphenol, 2-chlorophenol, 4-chlorophenol, 2,4-dichlorophenol, 2,4,6-trichlorophenol, Pentachlorophenol	Water sample	SPE-GC-FID SPE-GC-ECD	1 - 40 ng/L	(Bagheri & Saraji, 2003)
Pyrrole-based polymer	Phenol, 2-chlorophenol, 4-chlorophenol, 2,4-dichlorophenol, 2,4,6-trichlorophenol	Water sample	SPE-HPLC	15–100 ng/L, 35–150 ng/L	(Bagheri et al., 2004)
4-vinylpyridine–divinylbenzene (VP-DVB) resin	Phenol, 4-nitrophenol, 2,4-dinitrophenol	River water, waste water	SPE-LC-UV	0.1-0.2 µg/L	(Fontanals et al., 2004b)

Table 2.7 (Continued)

Hydrophilic copolymeric sorbent	Phenol, 4-nitrophenol, 2,4-dinitrophenol	Water sample	SPE-LC	0.1-0.2 µg/L	(Fontanals et al., 2004a)
β-CD- bonded silica particles	Phenol, 2,4-dimethylphenol, 4-nitrophenol , 3-chlorophenol, 4-methylphenol	Water samples	SPE-GC-FID SPE-GC-MS	10-100 ng/L	(Faraji, 2005)
Imprinted amino-functionalized silica gel	Pentachlorophenol, phenol, 2,4-dichlorophenol, phenol, 2,4-dichlorophenol	Lake water, river water, wastewater samples	SPE-HPLC	6 ng/L	(Han et al., 2005)
MIP with methylacrylic acid (MAA) monomer, and ethylene glycol dimethacrylate (EGDMA) cross linker	Phenol, 4-chlorophenol, 2,4-dichlorophenol, 2,4,6-trichlorophenol, pentachlorophenol	Tap water, river water, raw sewage	MISPE-HPLC	0.016-0.082 mg/L	(Feng et al., 2009)
Graphene	2-Chlorophenol, 3-chlorophenol, 2,4-dichlorophenol, 3,4-dichlorophenol , 2,4,6-trichlorophenol, 4-chlorophenol 2,3,5-trichlorophenol 2,3-dichlorophenol	Tap water, river water	SPE-HPLC	0.1–0.4 ng/mL	(Liu et al., 2011)

Table 2.7 (Continued)

Magnetic microsphere Confined IL sorbent	3-Chlorophenol, 2,4-dichlorophenol, pentachlorophenol	Water sample	MSPE- HPLC	0.20–0.35 mg/L	(Yang et al., 2011)
Hydrophilic C18 monolithic sorbent	Phenol, 2,4-dimethylphenol, 2,4-dichlorophenol, 2,4,6-trichlorophenol, 2,4,6-trimethylphenol	Water samples	PE-LC	1.6-4.7 ng/mL	(Li et al., 2011c)
Sol–gel technique	Phenol, 4-chlorophenol, o-cresol, m-cresol	Waste water,urine sample	HS-SPME-GC-FID	0.001 to 0.1 ng/mL	(Sarafraz-Yazdi et al., 2012)

Chapter 3

Results and Discussion

Part 1: Synthesis and Characterization of βCD-BIMOTs-TDI

3.1 Introduction

The application of βCD-BIMOTs-TDI in the adsorption of toxic pollutants is still in its early stages; thus, academic interest in combinations of ILs and CD is increasing. Therefore, in this study, β-CD was functionalized with IL and was further polymerized with an isocyanate linker to form an insoluble polymer (βCD-BIMOTs-TDI). The prepared βCD-BIMOTs-TDI was characterized by using various instruments, and the structure and properties of the βCD-BIMOTs-TDI were studied and compared with native β-CD polymer (βCD-TDI). Finally, the prepared polymers were applied for the removal of phenol compounds as a preliminary investigation.

3.2 Experimental

3.2.1 Chemicals, materials, and reagents

β-CD is commercially available and was purchased from Acros (Acros, Geel, Belgium) (99%). 1-Benzylimidazole (BIM) (99%) and toluene 2,4-diisocyanate (TDI) (95%) were supplied from Sigma Aldrich (Aldrich, Buches SG, Switzerland). Other reagents and chemicals were of the analytical reagent grade and were used and received without further purification. Double distilled water was used throughout the experiment.

All the reactions were performed under inert conditions. *N*,*N*-Dimethylformamide (DMF), p-Toluene sulfonic acid, and hexane anhydrous were purchased from Merck (Merck, New York, NY, USA). 2-chlorophenol (2-CP), 2-nitrophenol (2-NP), 2,4-dichlorophenol (2,4-DCP), 4-chlorophenol (4-CP), 4-chloro-3-methylphenol (4-CMP), 4-nitrophenol (4-NP), 2,4-dinitrophenol (2,4-DNP), 2,4,6-Trichlorophenol (2,4,6-TCP), and p-Toluene sulfonyl chloride were purchased from Sigma Aldrich (Steinheim, Germany), while β-CD was purchased from Acros (Hungary) (99%). The standard stock solutions of 2,4-DCP, 2,4,6-TCP and 2,4-DNP (1000 mg/L) were prepared separately in methanol and were stored in a dark amber glass at 4°C to prevent degradation. The working solution was freshly prepared by diluting the stock solutions with water. The progress of the reactions were monitored by thin layer chromatography (TLC) using Merck TLC cards (70643) (Merck, New York, NY, USA), and the spots were visualized by using UV GL-58 Handheld UV-Lamp (UVP, Upland, CA, USA). The structure of chemicals used and properties of phenols are shown in Tables 3.1 and 3.2.

Table 3.1: Materials used for synthesis of βCD-BIMOTs-TDI

Name	Function
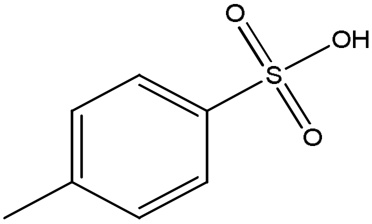 p-Toluene sulfonic acid	Precursor
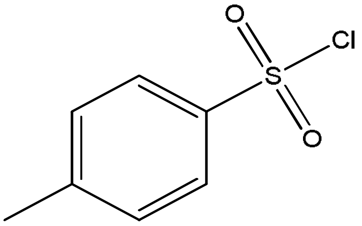 p-Toluene sulfonyl chloride	Precursor
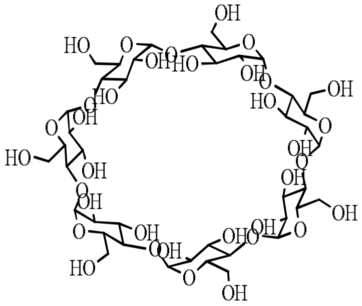 β-Cyclodextrin	Monomer
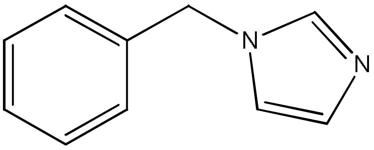 1-benzyl imidazole	Functionalization

Table 3.1 (Continued)

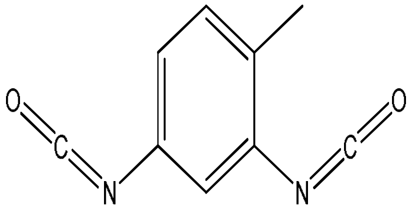 Toluene 2,4-diisocyanate	Cross linker
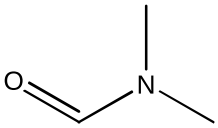 Dimethylformamide	Solvent

Table 3.2: Structure and properties of the studied phenols

Analytes	Boiling point	Chemical structure	$\log k_{ow}$	pK_a
2-CP	174.9°C	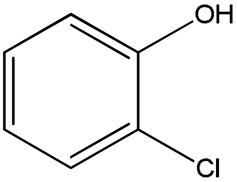	2.15	8.55
4-CMP	235°C	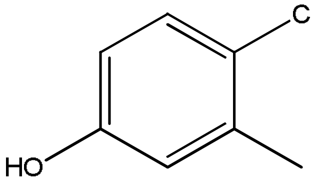	3.10	9.55
4-NP	279°C	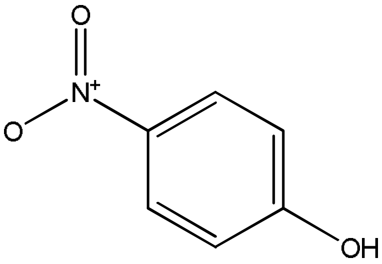	1.90	7.46
2, 4, 6-TCP	246°C	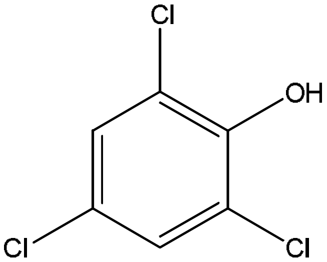	3.69	7.42
2-NP	214-216°C	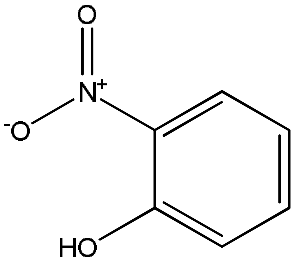	1.78	7.21

Table 3.2 (Continued)

4-CP	220°C	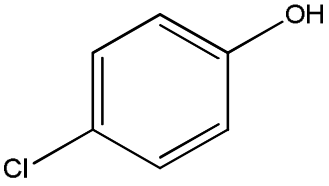	2.41	9.18
2, 4-DCP	209-210°C	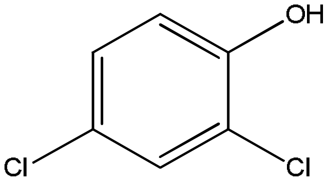	3.08	7.85
2, 4-DNP	113°C	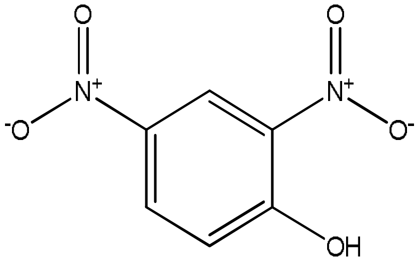	1.53	4.09

3.2.2 Characterization of the samples

Fourier transform infrared (FT-IR) spectra were recorded on a Perkin–Elmer RX1 FT-IR (Perkin Elmer, Waltham, MA, USA) between 4000 and 400 (1/cm) with a resolution of 2 (1/cm). The samples were adequately mixed with KBr powder and were pressed into disks. ^{1}H NMR, ^{13}C NMR, and NOESY spectra were recorded on AVN 600 MHz (Bruker, Fällanden, Switzerland), and Dimethyl Sulfoxide (DMSO-D_6) had been used as solvent. An elemental analysis of the sample was determined with a Perkin Elmer CHNS-2400 analyzer (Perkin Elmer, Waltham, MA, USA). The scanning electron microscope (SEM) analysis for the morphology of the samples was obtained with a Leica S440 (Leica, Wetzlar, Germany). The Brunauer-Emmett-Teller (BET) analysis was determined from low temperature nitrogen adsorption isotherms at 77.40 K using Quantachrome Autosorb Automated Gas Sorption System (Quantachrome, Boynton Beach, FL, USA). Typically, at least 1 g of sample was used each time during the analysis. The surface area was obtained by the BET method, while the average pore diameter and pore volume of βCD-BIMOTs-TDI in the dry state were measured from the adsorption branch of the isotherms by the Barret–Joyner–Halenda (BJH) model. X-ray diffraction (XRD) patterns were taken using Cu K_α irradiation with a Siemens D5000 X-ray diffractometer (voltage, 40 kV; current, 100 mA (Siemens, Frimley, UK). Powder samples were mounted on a sample holder and were scanned from 5° to 30° at a speed of 3° per min. Thermo gravimetric analyses (TGA) curves were examined using a TA Instruments Q500 (Perkin Elmer, Waltham, MA, USA). A linear heating rate was set at 20 °C per min within the temperature range from 50 °C to 900 °C in a stream of nitrogen atmosphere. Differential Scanning Calorimetry (DSC) analysis was done by heating the samples from 30 °C to 400 °C at 20 °C per min.

3.2.3 Synthesis of βCD-BIMOTs-TDI

The preparation of βCD-BIMOTs-TDI involved 4 steps, such as preparation of p-Toluene sulfonic anhydride (Ts_2O) as the first step, preparation of 6-O-Monotosyl-6-deoxy-β-CD monomer (β-CDOTs) as the second step, synthesis of Mono-6-deoxy-6-(3-benzylimidazolium)-β-CD (βCD-BIMOTs) as the third step, and the final step was the synthesis of βCD-BIMOTs-TDI. The preparation of each step is clearly explained as in below (Raoov et al., 2014a):

(i) Preparation of p-toluene sulfonic anhydride (Ts_2O)

p-Toluene sulfonic anhydride was prepared according to a literature procedure (Zhong et al., 1998), and was used without further purification, as shown in Scheme 1. The preparation of Ts_2O was carried by dissolving *p*-Toluene sulfonyl chloride (2.00 g, 10.4 mmol) in dichloromethane (12.5 mL), and *p*-toluene sulfonic acid (0.52 g, 2.63 mmol) was added gradually with vigorous stirring under nitrogen atmosphere. The resulting mixture was stirred overnight at room temperature. The mixture was then filtered to remove the unreacted *p*-toluene sulfonic acid. Hexane (50 mL) was added to the filtrate and a precipitate was obtained after drying overnight under reduced pressure. Figure 3.1 shows ^1H NMR and ^{13}C NMR spectrums of *p*-toluene sulfonic anhydride (Ts_2O).

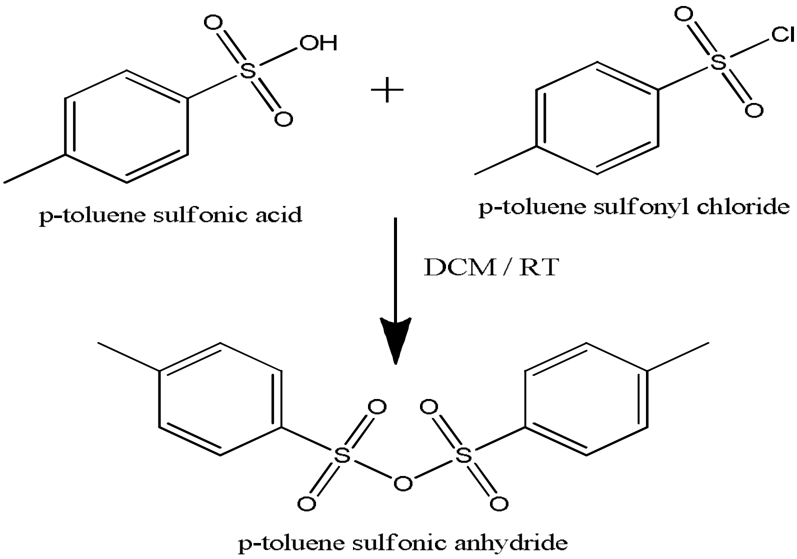

Scheme 1: Synthesis of p-toluene sulfonic anhydride (Ts_2O)

The obtained product was successfully characterized using several analytical techniques; FT-IR/KBr, cm^{-1} 3062 (CH, Ar), 2925 (C–H), 1928, 1652, 1591, 1488 (SO_2), 1370, 1304, 1178 (SO_2) .^{1}H NMR, DMSO-D_6: 7.45 (H2, d), 7.10 (H3, d), 2.25 (H5, s). CHNS (%) C (43.1912), H (3.0598), S (16.7992). ^{13}C NMR/PPM, DMSO-D_6 C1 (144.4), C2 (139.8), C3 (129.3), C4 (126.28), C5 (21.58). TLC: Eluent: 2:1 hexane/ethylacetate, R_f = 0.75. Percentage yield (90%). Melting point (155.88 °C).

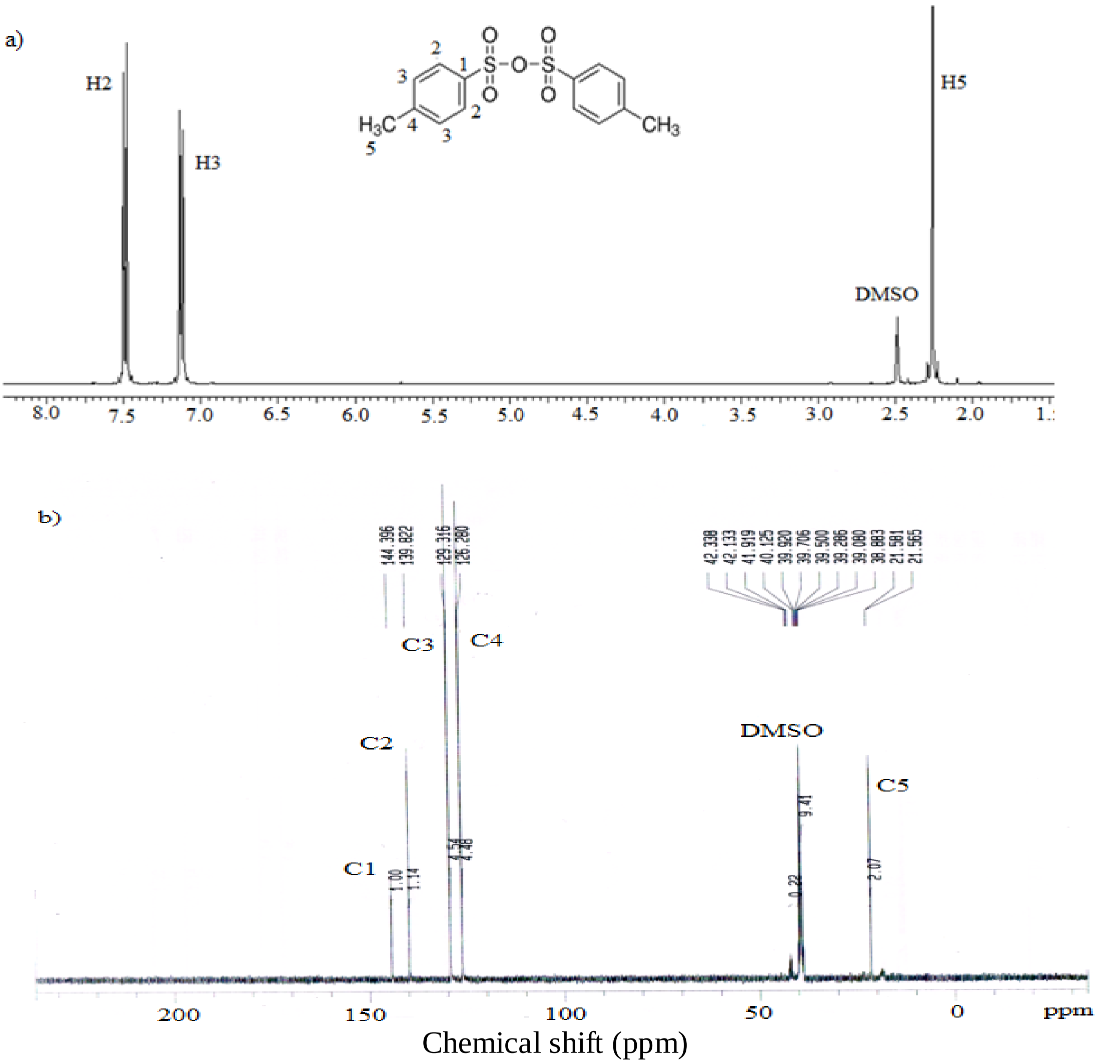

Figure 3.1: (a) ^{1}H NMR and (b) ^{13}C NMR spectrums of *p*-toluene sulfonic anhydride (Ts_2O)

(ii) Synthesis of 6-O-Monotosyl-6-deoxy-β-cyclodextrin (β-CDOTs)

β-CDOTs is the most important intermediate product in order to further functionalize the primary hydroxyl groups (C6) of β-CD, since tosylate is a good leaving group and can be easily substituted by other nucleophiles. The reaction was carried out with the presence of a base (NaOH), where the proton of C6 was removed in order to make O^-, which was a nucleophile, that was easily substituted, so when a CD reacted with the tosyl group in a basic medium, a monotosylation at C6 (β-CDOTs) was produced.

A typical reticulation reaction would proceed as follows: tosyl-β-cyclodextrin (CDOTs) was prepared according to Zhong and co-workers (Zhong et al., 1998), as shown in Scheme 2a. A suspension of β-CD (11.5 g, 10 mmol) and *p*-toluenesulfonic anhydride (Ts_2O) (4.9 g, 15 mmol) in 250 mL of water was stirred at room temperature for 2 H. A solution of NaOH (5.0 g in 50 mL of H_2O) was added, and after 10 min, the reaction mixture was filtered through the celite on the sintered glass funnel to separate the non reacting Ts_2O. The filtrate was brought to pH-8 by the addition of ammonium chloride (13.4 g), affording β-CDOTs as a precipitate that was collected after cooling at 4°C overnight and was used without further purification through chromatography. The degree of tolylation (DT) was determined via ^1H NMR spectroscopy (Figure 3.1a) (Gonil et al., 2011), which was based on the ratio of the areas of proton, as shown in Equation (3.1);

$$DT\ (\%) = \frac{(AR/4)}{([H1\text{-}H6)/7]\ x7)} x\ 100 \tag{3.1}$$

where DT(%) is the degree of tolylation, AR is the integral area of aromatic protons at chemical shift (δ) 7.8-7.4ppm, and H1-H6 are the integral areas of the CD protons at δ 5.9-

3.2ppm. The DT (%) was found to be less than 1; further suggesting that tosylation at primary hydroxyl of β-CD had successfully occurred. The obtained product was successfully characterized using several analytical techniques:

IR/KBr, cm^{-1} 3291 (OH), 2924 (C–H), 1646 (C=C), 1366 (SO_2 Assym), 1153 (SO_2 Sym). **^{1}H NMR/ppm**, **DMSO-D$_6$** H8 (7.74, d), H9 (7.43, d), OH-2-OH-3 (5.5–5.9, m), H1 (4,83, s), H1* (4.70, s), OH-6 (4.2–4.6, m), H3,H5,H6 (3.2–3.60, m), H2–H4 (2.9–3.2, m), H11 (2.32, s). **^{13}C NMR/PPM**, **DMSO-D$_6$** C7 (144.7), C10 (132.6), C9 (129.8), C8 (127.5), C1 (101), C4 (81.6), C2 (73), C3 (72.7), C5 (72.4), C6* (69.9), C6 (59.9), C11 (21.1). CHNS (%) C (37.63), H (6.68), S (1.30). DT (%) = 0.83. Percentage yield (60%). Melting point (170 °C). TLC: Eluent : 5:4:3 butanol / ethanol (95%) / water, R_f = 0.45.

The results showed that β-CDOTs had been successfully prepared. A new peak doublet of the doublet proton signal appeared around 4.7 ppm, and belonged to the H1* proton (Figure 3.2a) and carbon signal, (Figure 3.2b) C6*, 69.9 ppm belonged to the substituted CD. All the protons of β-CD still appeared after reaction with Ts_2O because the functionalization process occurred at only one of the primary hydroxyl groups of β-CD, as shown in Scheme 2a.

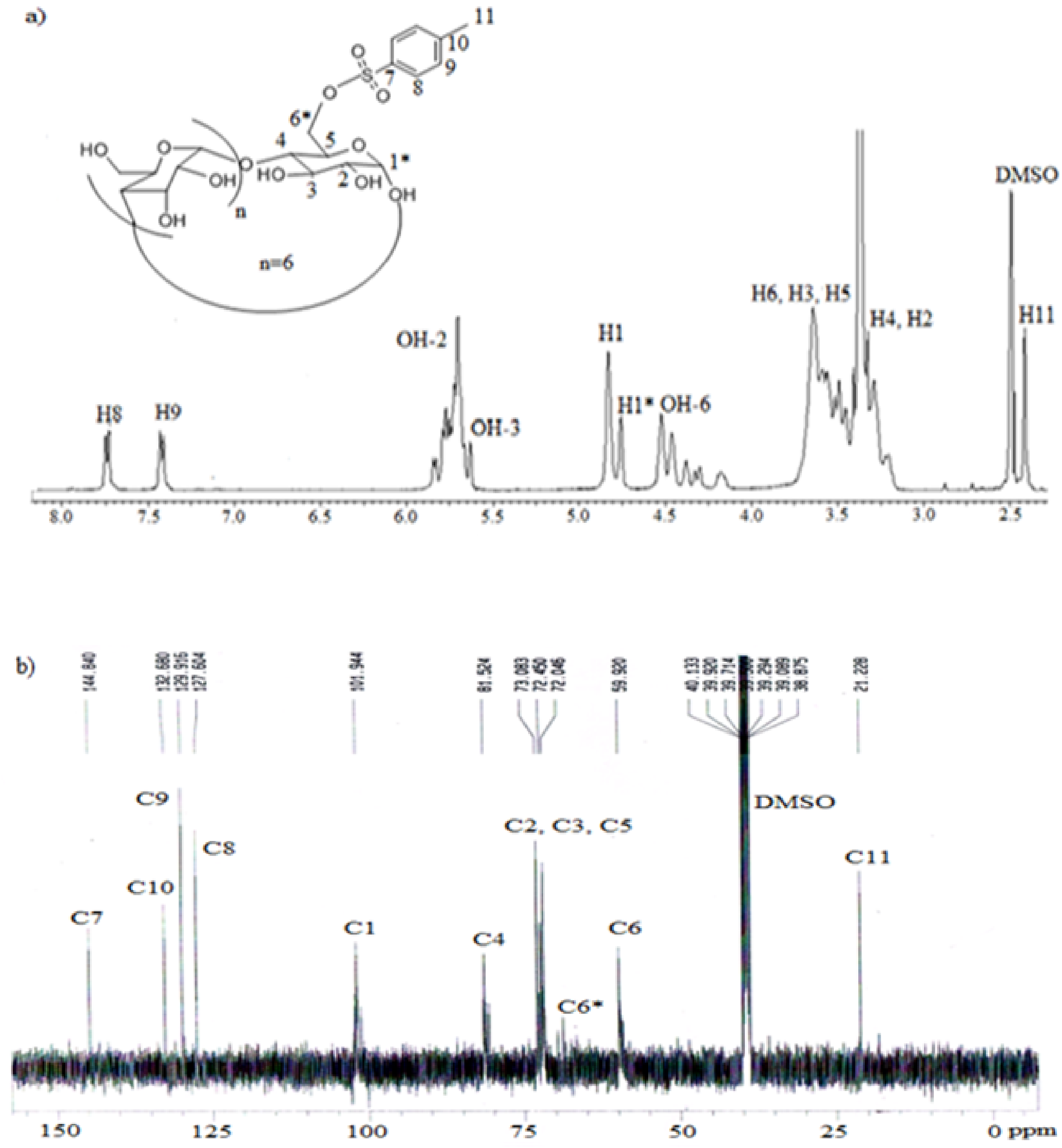

Figure 3.2: (a) ^{1}H NMR, and (b) ^{13}C NMR spectrums of β-CDOTs

(iii) Synthesis of Mono-6-deoxy-6-(3-benzylimidazolium)-β-CD (βCD-BIMOTs) monomer

Furthermore, the reaction was carried out by reacting β-CDOTs with 1-benzylimidazole (BIM). Since tosyl is a good leaving group, imidazole can easily undergo the nucleophilic substitution process. The reaction was carried out in the DMF solvent since β-CDOTs and BIM form a homogenous solution. The preparation of the mono-functionalized β-CD with BIM (βCD-BIMOTs) was done according to the following procedure (Ong et al., 2005), as shown in Scheme 2b: Freshly dried CDOTs (1.00g, 78mmol) and an appropriate amount of BIM (10 mole equivalent) in excess amount were dissolved in anhydrous DMF (40ml) and the solution was stirred at 90°C under an inert atmosphere. After two days, the resultant solution was cooled at room temperature and slowly added into acetone. Then, the mixture was stirred for 30 minutes, and thereafter, filtered and washed in excess amount of acetone. The product obtained was re-crystallized thrice from hot water to get the final product, as a white yellow precipitate.

Figure 3.3a shows the ^{1}H NMR spectrum of βCD-BIMOTs in the DMSO-D_6 solvent. The product formed was found to dissolve in water and several organic solvents (DMF, DMS0, and ethanol). The entire proton and carbon were assigned and the results are shown clearly in Figures 3.3a and 3.3b. Protons of imidazole ring (Hf, He, and Hd) appeared in the downfield region since the protons were deshielded upon functionalization. A new peak was observed in proton (H6*, 3.95 ppm) and carbon signal (C6*, 42.5 ppm), which belonged to the substituted CD. All the protons of β-CD still appeared after the reaction because the functionalization process occurred at only one of the primary hydroxyl groups of β-CD, as shown in Scheme 2b. The obtained product was successfully characterized using several analytical techniques:

IR/KBr, cm^{-1} 3297 (OH), 2922 (C–H), 1652 (C=C), 1152 (C–N). **^{1}H NMR/ppm**, **DMSO-D$_6$** Hf (9.3, s), He (7.94, s), Hd (8.20,s),Hc (7.49, s), Hb (7.74, t), Ha (7.46,s), Hg (5.18,s),H$_8$ (7.4, d), H$_9$ (7.1, d), OH-2–OH-3 (5.5–5.9, m), H1 (4,81, s), OH-6 (4.4–4.6, m), H6* (3.95), H3,H5,H6 (3.4–3.60), H2–H4 (3.2–3.4, m), H11 (2.07, s). **^{13}C NMR/PPM**, **DMSO-D$_6$** Ca (127), Cb (123.4), Cc (128.3), Cd (128), Ce (119), Cf (136.9), Cg (52), Ch (137.8), C7 (145.26), C10 (137.3), C9 (128.7), C8 (125.6), C1 (101.8), C4 (81.16), C2 (73.27), C3 (71.6), C5 (69.37), C6 (60.03), C6* (45.2),C11 (21.97). **CHNS (%)** C (38.2), H (6.67), S (0.47), N (1.0). Percentage yield (90%). Melting point (207 °C). TLC: TLC: Eluent : 5:4:3 butanol / ethanol (95%) / water R_f = 0.6

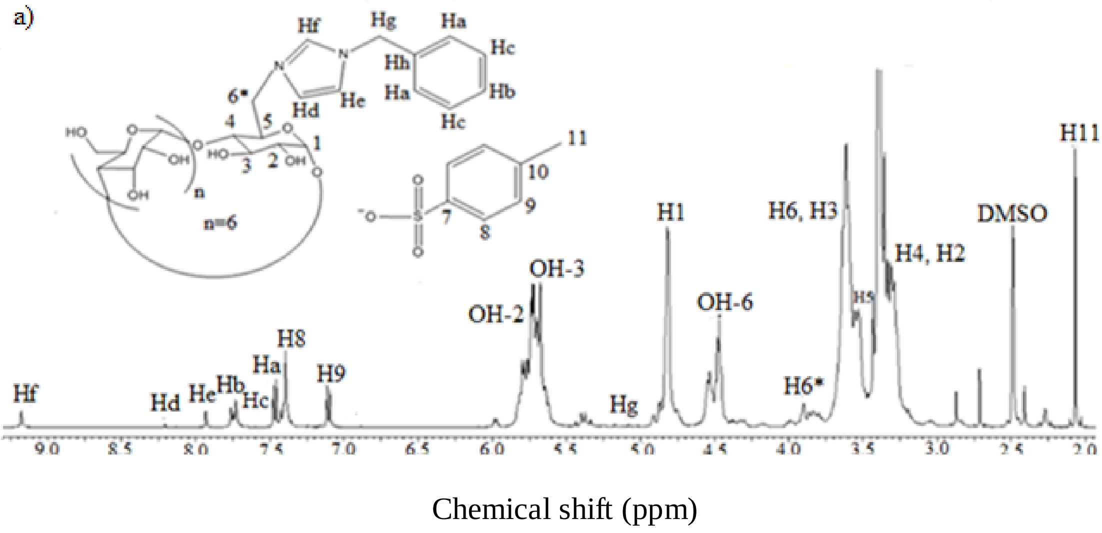

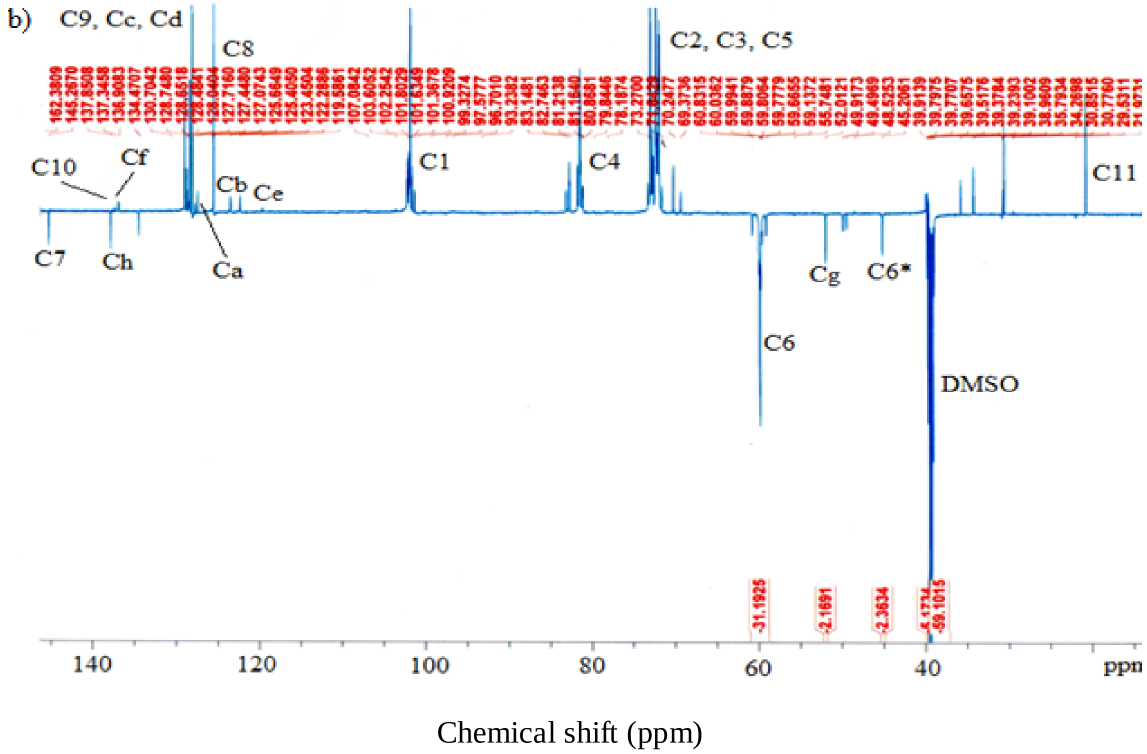

Figure 3.3: (a) ^{1}H NMR, and (b) ^{13}C NMR spectrums of βCD-BIMOTs

(iv) Synthesis of Insoluble βCD-BIMOTs-TDI

Insoluble β-Cyclodextrin functionalized ionic liquid polymer (βCD-BIMOTs-TDI) was prepared according to the method of Mahlambi and co-workers (Mahlambi et al., 2010), as shown in Scheme 2c. The polymerization reaction was monitored using FT-IR spectroscopy. Briefly, 0.69 mmol of βCD-BIMOTs was first dissolved in 30 mL of anhydrous DMF at room temperature, followed by the addition of Toluene 2,4-diisocyanate (TDI) (6.9 mmol) dropwise and the mixture was stirred for 24 H at 70 °C. The polymer formed was then precipitated with the addition of excess acetone. The solid form was allowed to settle down in acetone for 10 min to allow the removal of residual DMF from polymer, followed by filtration, and was washed with acetone and double distilled water to remove the non reactive cross linker, and was dried overnight under reduced pressure. The dried polymer was ground and sieved using a 53 µm sieve, before being used.

3.2.4 Synthesis of Insoluble β-CD-TDI

β-Cyclodextrin polymer (βCD-TDI) (without functionalization with IL) was synthesized for comparison purpose. The preparation of βCD-TDI was done by reacting 0.88 mmol of β-CD in 30 mL of anhydrous DMF at room temperature, followed by the addition of toluene 2,4-diisocyanate (TDI) (8.8 mmol of TDI) drop wise, and the mixture was stirred for 24 hours at 70 °C. The following procedures had been similar to the procedure in 3.2.3.4.

The polymerization reactions of the diisocyanate linker (TDI) with βCD-BIMOTs and βCD were monitored through IR spectroscopy. The obtained polymers were produced in high yields and were found to be insoluble in water, as well as in organic solvents (e.g., DMSO, D_2O, DMF, $CHCl_3$, and CH_3CN).

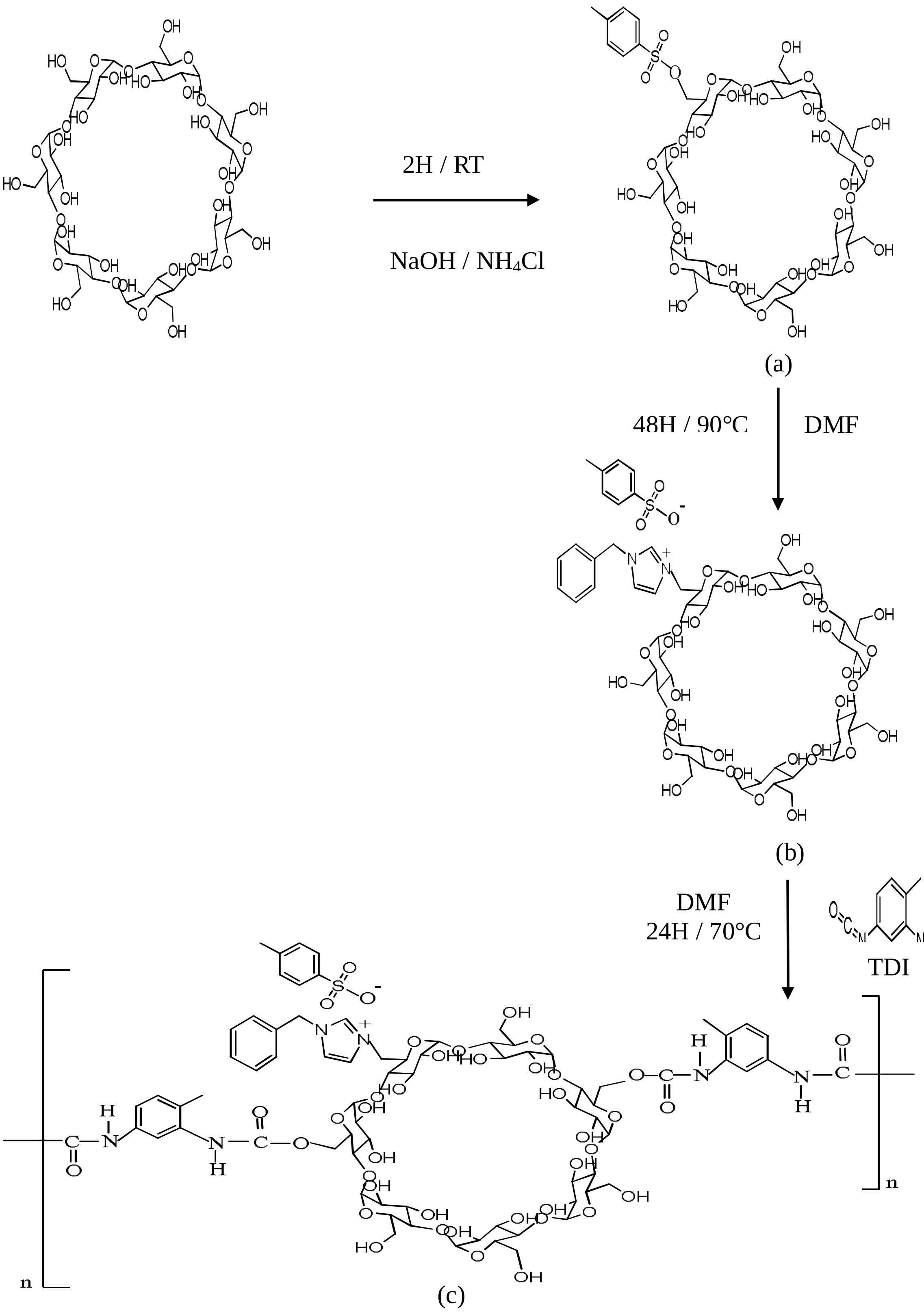

Scheme 2: Synthesis pathway of (a) β-CDOTs, (b) βCD-BIMOTs, and (c) βCD-BIMOTs-TDI (Raoov et al., 2014b)

3.2.5 Preliminary Sorption Experiments

In order to evaluate the performance of the synthesized polymers, preliminary sorption study was carried out. Experiment data were determined by the following batch method: In each experiment, 20 mg of dry polymer was mixed with 10 mL phenol (individual) at a known concentration in a tightly sealed flask. The solution was shaken for 2 hours on a shaker at room temperature. The adsorbents were removed by filtration and the residual concentration was determined using Shimadzu (Kyoto, Japan) Ultraviolet-Visible spectroscopy (UV-vis) recording spectrophotometer, equipped with 1 cm quartz cells for phenol compounds at different wavelengths (Table 3.3). The percentage of adsorbate adsorbed on the polymer (removal efficiency, R (%)) was calculated by the following equation:

$$R\% = \frac{C_o - C_e}{C_o} \times 100 \qquad (3.2)$$

where, C_o and C_e are the initial and equilibrium concentrations of solutions (mg/L), respectively.

Table 3.3: Wavelengths of phenols measured for UV-vis analysis

Phenol	Wavelength (nm)
2-CP	273.8
4-CMP	279.2
4-NP	316.0
2,4,6-TCP	295.0
2-NP	306.2
2,4-DNP	358.0
2,4-DCP	280.0

3.3 Results and discussion

β-Cyclodextrin functionalized ionic liquid polymer (βCD-BIMOTs-TDI) was characterized using various analytical instruments and was compared with β-Cyclodextrin polymer (βCD-TDI).

3.3.1 Characterization of the polymers

3.3.1.1 FT-IR Analysis

The spectrums of insoluble β-cyclodextrin polymers (βCD-BIMOTs-TDI and βCD-TDI) are shown in Figure 3.4. The absence of a peak at 2270 (1/cm) (corresponding to the isocyanate group) and the presence of carbamate linkage NHCO, was clearly observed, which indicated the completion of the reaction (Bhaskar et al., 2004). Main IR frequencies with assignments are shown in Table 3.4. The broad –OH stretching band of the β-CD around 3300 (1/cm) that corresponded with the multiple –OH functional groups, was reduced upon cross linking with TDI and its width was ascribed to the formation of inter and intramolecular hydrogen bonds. In the FT-IR spectrum of βCD-BIMOTs-TDI, the band at 1153 (1/cm) was attributed to the imidazolium groups, which further supported the anchoring of the ILs molecule onto the CD surface. Therefore, it had been concluded that the polymerization between βCD-BIMOTs and βCD with toluene 2,4-diisocyanate (TDI) had been completed and polymers (βCD-BIMOTs-TDI, βCD-TDI) were formed.

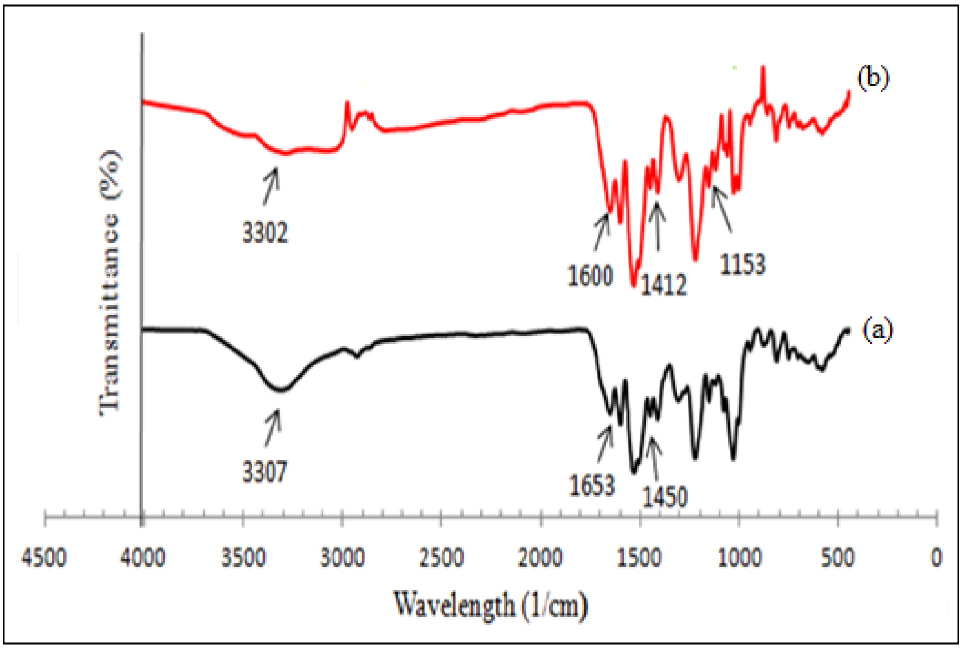

Figure 3.4: FT-IR analysis of (**a**) βCD-TDI, and (**b**) βCD-BIMOTs-TDI.

Table 3.4: Main IR frequencies with assignments

Samples	Wavelength (1/cm)	Assignments
βCD-TDI	3307	N–H and O–H stretch
	2270	Absence of isocyanate group
	1653, 1534	NHCO, carbamate linkage
	1450	Aromatic group in TDI
βCD-BIMOTs-TDI	3302	N–H, O–H stretch, and imidazole ring
	2270	Absence of isocyanate group
	1600, 1412	Aromatic group in TDI
	1535, 1651	NHCO, carbamate linkage
	1153	C–N stretch of imidazolium ring

3.3.1.2 XRD Analysis

Further evidence for the formation of the βCD-BIMOTs-TDI was obtained through the XRD, as demonstrated in Figure 3.5. Basically, no peaks were clearly visible in the XRD of the polymers, which was due to the change of cystalloids after cross linking with TDI. It was found that the peak at 2θ = 13° obviously decreased and broadened in βCD-BIMOTs-TDI, which indicated that the degree of crystallinity decreased more, as compared to the unmodified βCD-TDI (Zha et al., 2008). The lack of crystalline in the polymers might be due to the loss of regularity throughout the polymeric chains, which, in turn, was due to the introduction of bulky TDI molecules. Hence, in this study, it had been confirmed that βCD-TDI and βCD-BIMOTs-TDI are amorphous.

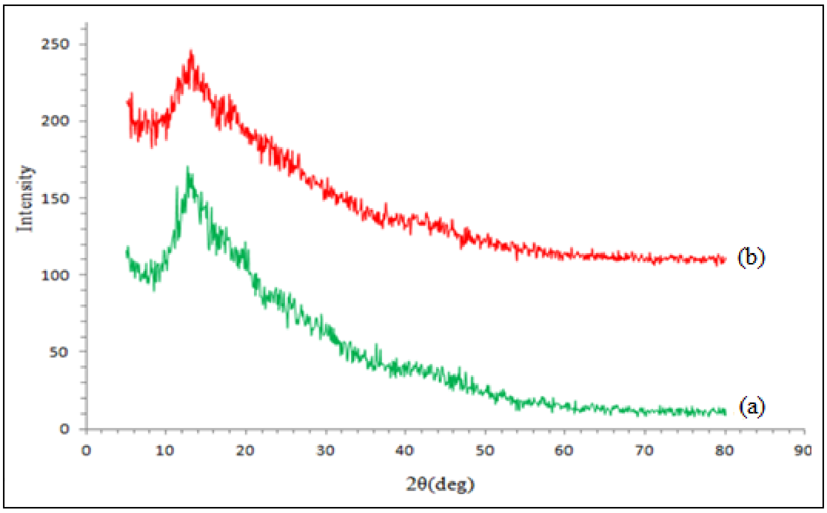

Figure 3.5: XRD analysis of (a) βCD-TDI, and (b) βCD-BIMOTs-TDI

3.3.1.3 Surface Morphology Studies

The surfaces morphology of βCD-BIMOTs-TDI was studied and compared with native βCD-TDI. The N_2 adsorption/desorption isotherm analysis (Figure 3.6) for βCD-BIMOTs-TDI exhibited a typical type-II isotherm with H_3 type hysteresis loop according to the IUPAC (Pierotti & Rouquerol, 1985), which indicated that the macroporous structure, with good pore connectivity, might be present in polymer compared to βCD-TDI, which exhibited a typical type-IV isotherm with a steep desorption branch and H_3 type hysteresis loop. Furthermore, the nitrogen amount adsorbed by βCD-BIMOTs-TDI increased very steeply at high relative pressure ($P/P_0 > 0.85$), which indicated the presence of macropores (Liu et al., 2000; Schroden et al., 2002; Zhang et al., 2008), and the results agree well with the IUPAC definition, which classifies the adsorbent pores into three: micropores (diameter < 2 nm), mesopores (2–50 nm), and macropores (>50 nm). Based on the BJH pore size distribution (calculated from Barret-Joyner-Halenda model) for dry βCD-BIMOTs-TDI, it exhibited that βCD-BIMOTs-TDI was a macroporous material with pore size of 77.6 nm and pore volume of 0.02435 cm^3/g (Table 3.5). Meanwhile, βCD-TDI represented micropores with pore size of 1.585 nm and pore volume of 0.02188 cm^3/g. The removal of solid particles, which were embedded on the surface of polymers by washing or etching led to the formation of pores. The presence of the macropores could be derived from the self-porogen effect during the polymerization process (Gokmen & Du Prez, 2012). In addition, the nitrogen desorption at 0.4 relative pressure (P/P_0) for βCD-BIMOTs-TDI, and 0.75 relative pressure (P/P_0) for βCD-TDI were found to be higher. These could be due to the heterogeneous surface of the polymers with many cavities (CD), imidazolium (βCD-BIMOTs-TDI), and isocyanate group, which made the desorption of nitrogen gas difficult.

Furthermore, βCD-BIMOTs-TDI exhibited low specific BET surface area (1.254 m^2/g) (dry state) after a chemical modification with IL, compared to the native βCD-TDI (2.401 m^2/g). Similar results were obtained in the preparation of macroporous IL material, which exhibited low surface area (Du et al., 2010). This phenomenon could be correlated with the covering of the adsorption sites by organic moieties immobilized on the mineral surface (cyclodextrin), which further hindered the access of N_2 molecules to the binding site (Alahmadi et al., 2012). The low surface area could also be from the usage of larger cation parts of IL (1-benzylimidazole) (Yoo & Lee, 2010). Table 3.5 shows the structural parameters of the samples.

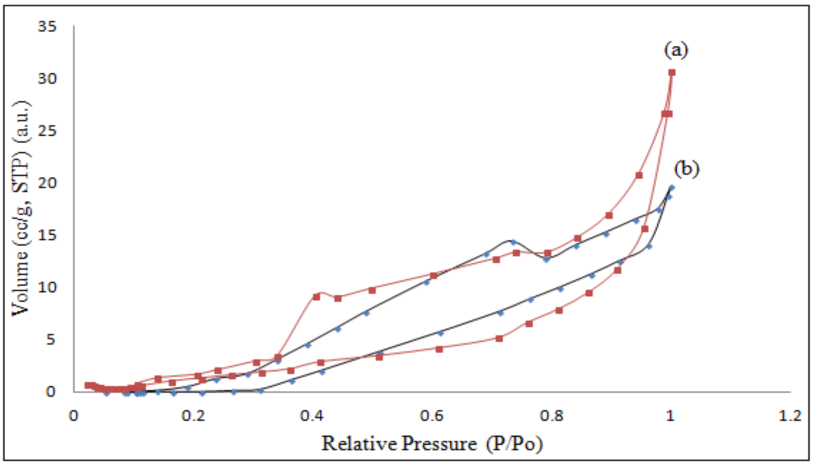

Figure 3.6: Nitrogen adsorption-desorption isotherms of (**a**) βCD-BIMOTs-TDI, and (**b**) βCD-TDI

Table 3.5: Structural parameters of the samples

Polymers	Surface area (m^2/g)	Pore volume (cm^3/g)	Pore diameter (nm)	Pore size distribution
βCD-TDI	2.401	0.02188	1.585	<2nm(micro pore)
βCD-BIMOTs-TDI	1.254	0.02435	77.66	>50nm(macro pore)

3.3.1.4 SEM Analysis

All the microscopic morphological structures were performed using the SEM in order to determine and compare the surface features of βCD-BIMOTs-TDI with native βCD-TDI. The SEM micrographs of the polymers are shown in Figure 3.7a and b. From the SEM micrographs, the presence of IL increased the pore size of the βCD-BIMOTs-TDI compared to βCD-TDI, and this observation was supported by the BJH result. βCD-TDI revealed a “shrinking” crystal structure. It exhibited the loss of sphericity, smooth surface, and reduced the size of particles, as shown in Figure 3.7a, while βCD-BIMOTs-TDI exhibited a totally different crystalline structure, which was not comparable with the morphology of the βCD-TDI. Different morphologies were observed for the IL material due to its unique properties. Basically, pore formation depends on the chemical structure of the polymer backbone, and the polymerization process (Salipira et al., 2008).

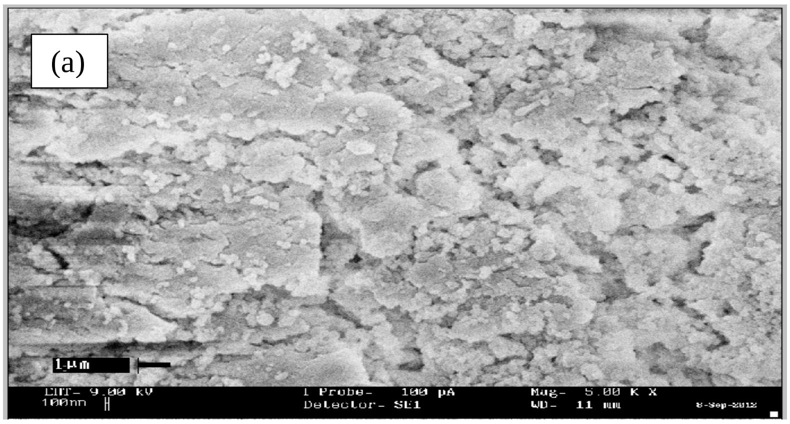

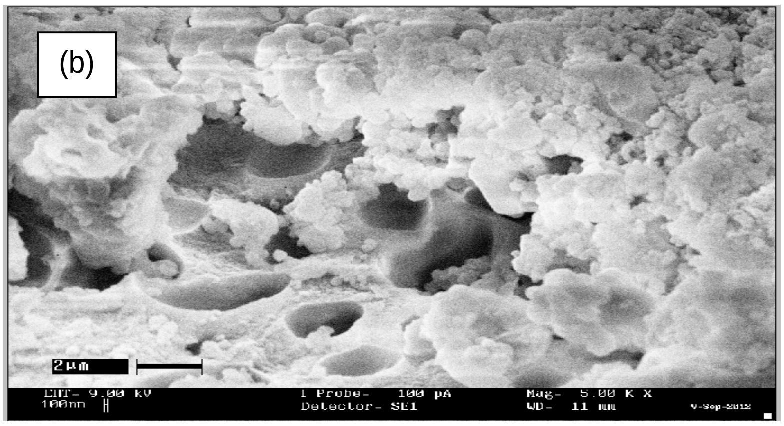

Figure 3.7: SEM analysis of (**a**) βCD-TDI, and (**b**) βCD-BIMOTs-TDI (Mag 5.00 KX)

3.3.1.5 Thermal Analysis of the Polymers

a) TGA

The TGA curves of βCD-BIMOTs-TDI and βCD-TDI polymers are shown in Figure 3.8. The thermal behaviours of the polymers (βCD-TDI, and βCD-BIMOTs-TDI) involved only a 3-step process. Generally, the first step could be interpreted due to the loss of water; the second and third steps might account for the most of the weight and had been associated with the formation of the residue of the CD polymer. Basically, the second degradation stage of βCD-BIMOTs-TDI polymer took place at a higher temperature (270–357 °C) with low weight loss (46%), and this result indicated that βCD-BIMOTs-TDI polymer was more stable than the unmodified βCD-TDI polymer, which took place at 260–365 °C with weight loss of 68%. Apart from that, high stability of βCD-BIMOTs-TDI polymer could be due to the strong electrostatic interaction between the BIM cation and OTs anion, which enabled this material to be used in high-temperature applications. The degradation and weight loss steps of the polymers are shown in Table 3.6.

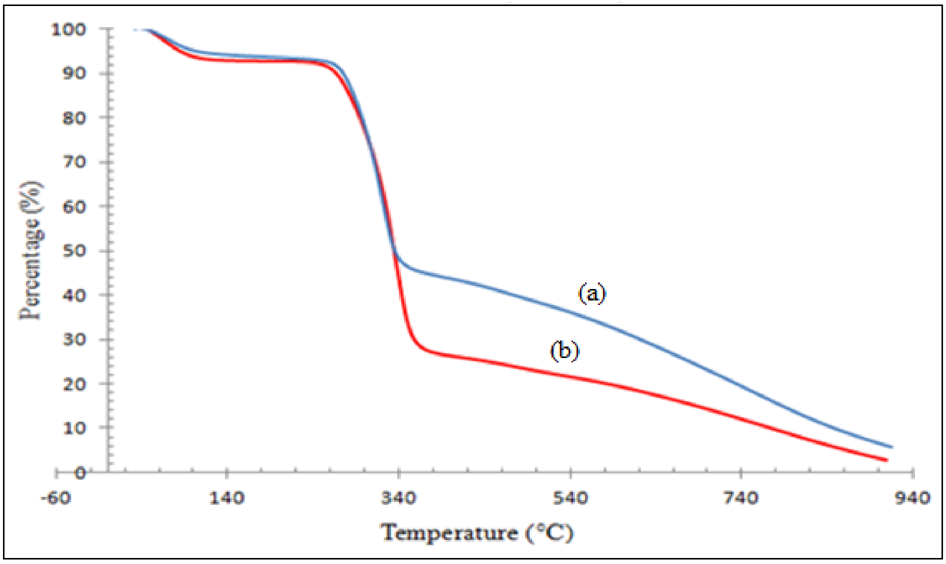

Figure 3.8: TGA analysis of a) βCD-BIMOTs-TDI and b) βCD-TDI

Table 3.6: TGA result of samples

Sample	**Region (°C)**	**Weight loss (%)**	**Assignment**
βCD-TDI	50–140	8	Water loss/Moisture
	260–365	68	Carbamate group and β-CD
	365–900	26	β-CD
βCD-BIMOTs-TDI	32–100	6	Water loss/Moisture
	270–357	46	Carbamate group, BIM, β-CD, OTs
	357–915	40	β-CD

b) Differential Scanning Calorimetry (DSC)

It can be observed in Figure 3.9, that the native βCD-TDI polymer, displayed different trends compared to βCD-BIMOTs-TDI polymer. βCD-TDI polymer involved four stages in the DSC analysis, while βCD-BIMOTs-TDI polymer only involved two stages (Table 3.7). Endothermic peak had been observed from about 50 °C due to loss of water, meanwhile, the second endothermic regions between 190 °C and 350 °C, were associated with the melting ranges of the samples. However, the difference could be observed in the βCD-TDI polymer at around 350 °C, where it showed the third endothermic peak due to the melting of the polymer and exothermic peak at 356 °C associated with curing (a process during which a chemical reaction or physical action took place) of the polymer due to the high degree of cross linking in the βCD-TDI polymer (Salipira et al., 2008). The second endothermic peak of βCD-BIMOTs-TDI polymer took place at a higher temperature (330 °C) compared to βCD-TDI polymer (323 °C). This result showed that the presence of IL increased the stability of the polymer compared to the native βCD-TDI polymer.

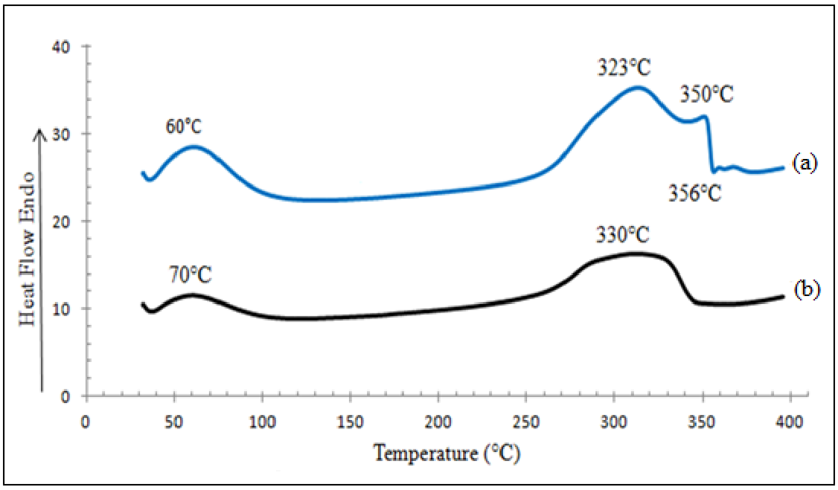

Figure 3.9: DSC analysis of (**a**) βCD-TDI, and (**b**) βCD-BIMOTs-TDI

Table 3.7: DSC analysis of the samples

Samples	Temperature (°C)	Peak (°C)	Exo/Endo	Assignment
βCD-TDI	38-93	60	Endothermic	Loss of water
	280-343	323	Endothermic	Melting of β-CD and TDI
	343-350	350	Endothermic	Melting of β-CD
	350-357	356	Exothermic	Curing process
βCD-BIMOTs-TDI	36-79	70	Endothermic	Loss of water
	252-343	330	Endothermic	Melting of β-CD, TDI, BIMOTs

3.3.2 Preliminary sorption Studies

Synthesized polymers have been applied in sorption studies in order to compare the performance of βCD-BIMOTs-TDI with native βCD-TDI. The removal capacities of the polymers for phenol compounds are presented in Figure 3.10. It was found that the βCD-BIMOTs-TDI polymer enhanced removal compared to the βCD-TDI polymer. The presence of IL in βCD-BIMOTs-TDI polymer basically increased the selectivity towards phenol. Furthermore, it is well known that β-CD can form inclusion complex with phenols (Hanna et al., 2003; Leyva et al., 2001b), so in this study, inclusion complex was formed as the cavity of β-CD was maintained in the polymerization process. Apart from that, the higher percentage of removal could be a result of the π–π interaction between the aromatic ring of phenols and imidazolium ring of βCD-BIMOTs-TDI. The formation of the inclusion complex and π–π interaction was proven and discussed in Section 4.3.10.

Meanwhile, the presence of macropores also enabled us to apply it for removal studies since it reduced the diffusion distance for analyte molecules to transport, simultaneously increased the adsorption and decreased mass transfer resistance. Hence, the provision of a more favourable and fast adsorption process (Du et al., 2010) was achieved. It could be speculated that βCD-BIMOTs-TDI can interact well with phenols because it possesses both the structural characteristics of benzylimidazolium and functional units of β-CD, and thus, it can be used in many areas for different applications.

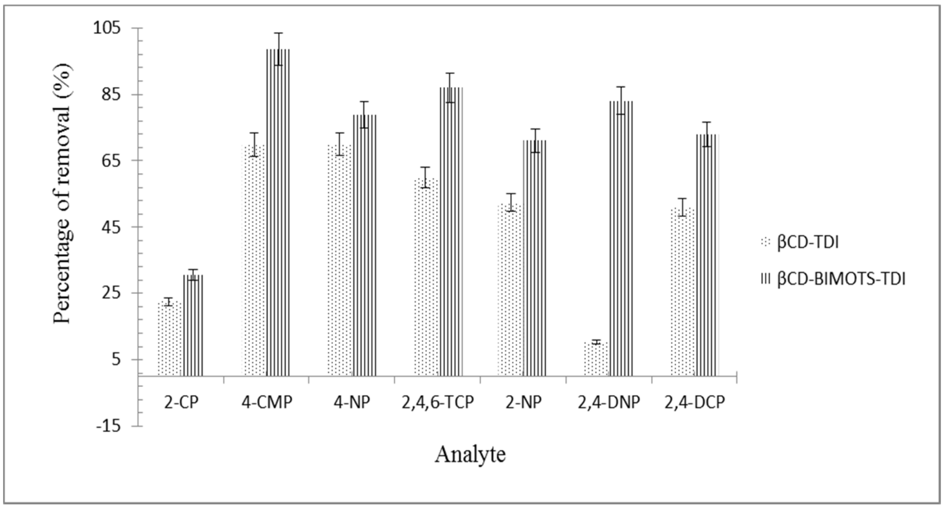

Figure 3.10: Preliminary batch sorption experiments. Removal condition: 25°C, 10 mL analyte solution, 20 mg sorbent, and 180 rpm. Equilibrium time (H): 2 hours

3.4 Conclusion

A macroporous βCD-BIMOTs-TDI had been successfully synthesized and characterized using various instruments, and the obtained results were compared with a native β-Cyclodextrin polymer (βCD-TDI). The SEM results showed that the βCD-BIMOTs-TDI revealed macropores with lower BET surfaces area upon the functionalization with the IL while βCD-TDI exhibited micropores with higher BET surfaces area. In addition βCD-BIMOTs-TDI showing high sorption capacities towards all the studied phenol compounds compared to βCD-TDI.

CHAPTER 4

RESULTS AND DISCUSSION

Part 2: Comparative studies on adsorptive removal of phenols by macroporous βCD-BIMOTs-TDI: Adsorption Isotherm, Kinetic study, and Thermodynamics

4.1 Introduction

In this chapter, the macroporous βCD-BIMOTs-TDI was used for the removal of 3 different types of phenol compounds (2,4-DCP, 2,4,6-TCP, and 2,4-DNP) since this material have attracted tremendous research interests (Dai et al., 2000) and we pursued our interests for the adsorptive studies. Apart from that, adsorption techniques have been considered to be among the most effective approaches to remove pollutants from effluents. The adsorption properties were demonstrated and compared through several batch mode adsorption experiments. Hence, the adsorption mechanism was proposed by considering the inclusion of complex and π-π interaction between modified β-CD functionalized ionic liquid (βCD-BIMOTs) and one selected phenol compound (2,4-DCP molecule).

4.2 Experimental

4.2.1 Materials

4.2.1.1 Adsorbents

It was found in Chapter three; the macroporous cyclodextrin functionalized ionic liquid polymer (βCD-BIMOTs-TDI) gave the highest removal percentage for all the studied phenol compounds. Thus, this material was selected as an adsorbent to investigate the adsorption parameters of 2,4-DCP, 2,4,6-TCP, and 2,4-DNP.

4.2.1.2 Adsorbate

2,4-dichlorophenol (2,4-DCP), 2,4,6-trichlorophenol (2,4,6-TCP), and 2,4-dinitrophenol (2,4-DNP) were chosen as representative adsorbates for this part of research and were purchased from Sigma Aldrich (Steinheim, Germany). The properties of these phenols are listed in Table 3.2.

4.2.2 Adsorption studies

2,4-DCP, 2,4,-TCP, and 2,4-DNP were selected as model analytes for batch adsorption studies and were determined by the following batch method: in each experiment, 20 mg of βCD-BIMOTs-TDI was mixed with 10 mL of an aqueous solution of analyte at a known concentration (10 mg/L) in a tightly sealed vial. The solution was shaken for 2 hours on a shaker (180 rpm) at room temperature. After the adsorption process, the adsorbent was separated by filtration and the residual concentration was determined using Shimadzu Ultraviolet-Visible spectroscopy (UV–Vis), equipped with 1 cm quartz cells at 280 nm (2,4-DCP), 295 nm (2,4,6-TCP) or 358 nm (2,4-DNP) respectively. The percentage of removal, R (%), and the amount of analyte adsorbed per unit mass of the adsorbent (q_e) were calculated using Eq. 4.1 and Eq. 4.2.

The percentage of adsorbate adsorbed by the polymer (removal efficiency, R (%)) was calculated by the following equation:

$$R\% = \frac{C_o - C_e}{C_o} \times 100 \qquad (4.1)$$

and the amount of analyte adsorbed per unit mass of the adsorbent (q_e) was calculated as follows:

$$q_e = \frac{(C_o - C_e)V}{W} \qquad (4.2)$$

where, C_o and C_e are the initial and equilibrium concentrations of solutions (mg/L), respectively. V (L) is the volume of the solution and W (g) is the mass of the dry adsorbent used.

4.2.2.1 Effect of pH solution

The effect of pH was studied in the range of pH (3-10) at room temperature. The desired pH was adjusted with 0.01 M HCL and 0.01 M NaOH using pH meter (Model Ella Instrument). The analytes initial concentrations were fixed at 10 mg/L in 10mL of analyte solution with the sorbent dosage of 20 mg.

4.2.2.2 Effect of contact time

The effect of contact time was studied at different time intervals (0-180 min) at room temperature. The initial concentrations of the analytes were fixed at 10 mg/L in 10mL of analyte solution with sorbent dosage of 20 mg at pH 6 for 2,4-DCP and 2,4,6-TCP, while pH 4 for 2,4-DNP respectively.

4.2.2.3 Effect of concentration

The equilibrium studies were conducted at different adsorbate's initial concentrations with sorbent dosage of 20 mg in 10 mL of analyte solution. The experiments were done at 298, 318, and 338 K, respectively.

4.2.3 Synthesis and characterization of modified β-CD functionalized ionic liquid - 2,4-DCP (βCD-BIMOTs-2,4-DCP) inclusion complex

In order to study the interaction between βCD-BIMOTs-TDI and phenols, thus inclusion complex was prepared and studied between modified β-CD functionalized ionic liquid (βCD-BIMOTs) and with one selected phenol compound studied in this part (2,4-DCP). The inclusion complex (βCD-BIMOTs-2,4-DCP) was prepared using the conventional kneading method (Cwiertnia et al., 1999). Equimolar amounts of BCD-BIMOTs and 2,4-DCP was kneaded with mortar and pestle in minimal ethanol to form a homogeneous paste. The complex was kneaded for approximately 30 min and dried to constant mass. After drying, white powder complex was obtained and characterized using ^{1}H NMR and 2D NMR. The calculated yields were about 90%.

4.3 Results and discussion

4.3.1 Effect of pH

An optimization of the pH value plays a vital role in the adsorption studies. The degrees of ionization and speciation of chlorophenols depend on the pH of the solution, which subsequently lead to the change in the adsorption kinetics and equilibrium point (Sathishkumar et al., 2009). Thus, the behaviour of adsorbate and adsorbent are connected with pH. The effects of pH ranging from 3.0 to 10.0 were tested on the adsorption of 2,4-DCP, 2,4,6-TCP, and 2,4-DNP by βCD-BIMOTs-TDI, as shown in Figure 4.1, and the results showed that the sorption was strongly pH-dependent. It could be seen from Figure 4.1 that the total amount of adsorption increased significantly with an increase in pH from 3 to 6 for 2,4-DCP and 2,4,6-TCP, while 3 to 4 for 2,4-DNP. The percentage (%) of removal reached maximum at pH 6.0 for 2,4-DCP with 82% of removal, and 2,4,6-TCP with 85% removal, and then, decreased with an increase of pH from 6.0 to 10.0. Meanwhile, the percentage of removal of 2,4-DNP reached a maximum at pH 4.0 with 88% of removal, and then, decreased as the pH increased from 4.0 to 10.0. The obtained results could be due to the sorption mechanism, which was probably simultaneously dominated by the Van Der Waals force, inclusion complex, and hydrogen bonding (Li et al., 2012b). It is well known that β-CD molecules have a remarkable capacity to form inclusion complexes with phenols (Leyva et al., 2001b; Liu et al., 2010), therefore, in this study, inclusion complex formation could be the main interaction apart from other interactions since the cavity of β-CD was maintained in the polymerization process. Apart from that, strong π-π interaction between the imidazolium ring of IL and phenol molecules could be the reason for high removal at pH 6 for 2,4-DCP and 2,4,6-TCP, and pH 4 for 2,4-DNP.

In a solution of low pH, more protons would be available in order to protonate the 2,4-DCP (pKa = 7.85), 2,4,6-TCP (pKa = 7.42) and 2,4-DNP (pKa = 3.96) molecules, but protonation of phenol compounds had been very difficult to achieve because it needed very strong acidic condition (pH 1 or pH 2) and phenol compounds preferred to be in molecular form when pH < pKa. In addition, β-CD does not deprotonate when pH < 12 (Gaidamauskas et al., 2009) therefore, β-CD existed in molecular form and the positive charge on imidazole ring remained in this studied pH range. In addition, electrostatic repulsion between the positively charged sorbent surface (βCD-BIMOTs-TDI) and protonated phenols reduced the adsorption capacity at low pH medium even though π-π interaction existed between phenols and IL ring.

Apart from that, at higher pH medium, 2,4-DCP, 2,4,6-TCP, and 2,4-DNP molecules preferred to be in deprotonated form, as shown in Eq. 4.3:

$$POH \leftrightarrow PO^- + H^+ \quad K_a = \frac{[PO^-][H^+]}{[POH]} \qquad (4.3)$$

where POH and PO^- represent the molecular and dissociated ionic species of 2,4-DCP, 2,4,6-TCP, and 2,4-DNP respectively. K_a is the dissolution constant of 2,4-DCP, 2,4,6-TCP, and 2,4-DNP. A decline pattern at higher pH medium could be due to the higher concentration of hydroxyl groups, which competed with the phenol molecules and led to lower adsorption of phenols on βCD-BIMOTs-TDI (Yang et al., 2011). In addition, the protonated and deprotonated forms of 2,4-DCP, 2,4,6-TCP, and 2,4-DNP molecules were not in favour to form inclusion complex with the cavity of β-CD (Li et al., 2012b).

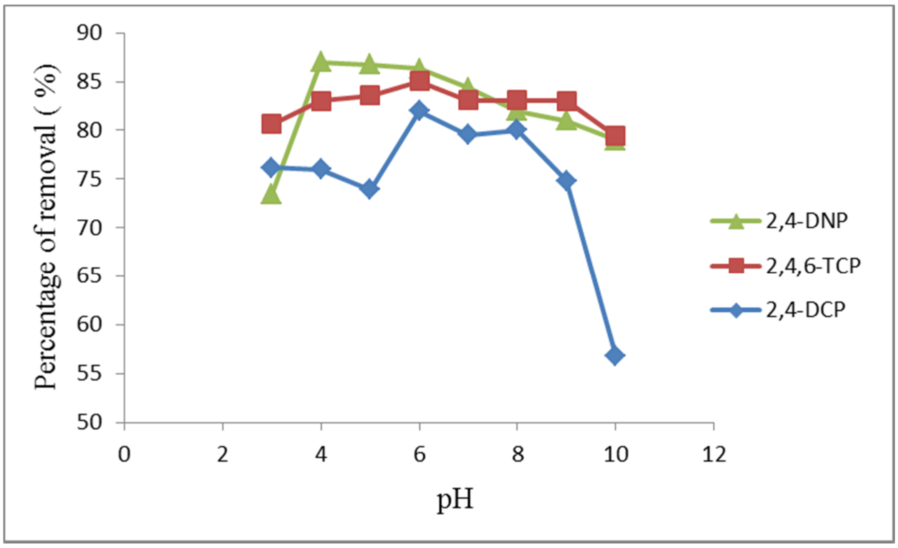

Figure 4.1: Effects of initial pH on 2,4-DCP, 2,4,6-TCP, and 2,4-DNP (condition: sorbent: 20 mg; initial concentration: 10 mg/L; volume: 10 mL; temperature 298K).

4.3.2 Effect of contact time

The effect of contact time (0-180 min) on removal percentages of 2,4-DCP, 2,4,6-TCP, and 2,4-DNP on βCD-BIMOTs-TDI were investigated, as shown in Figure 4.2. It is apparent from Figure 4.2 that the percentage of removal of 2,4-DCP, 2,4,6-TCP, and 2,4-DNP were rapid for the first 40 min since more adsorption sites were available and 2,4-DCP, 2,4,6-TCP, and 2,4-DNP could easily interact with these sites due to the presence of the macropores. Thus, the diffusion distance for 2,4-DCP, 2,4,6-TCP, and 2,4-DNP transports were reduced, and the adsorption process increased (Du et al., 2010). The removal was found to be optimum at 120 min with 81% of 2,4-DCP, 82% of 2,4,6-TCP, and 87% of 2,4-DNP. The removal processes were carried out for 180 min and they were found to be constant. Therefore, 120 min was selected for the entire studied phenol compounds as the equilibrium point and were used throughout the study.

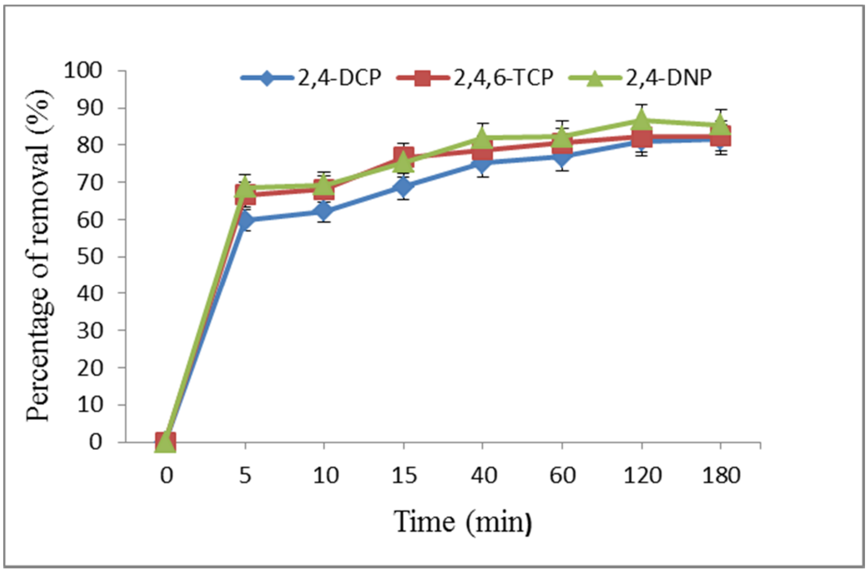

Figure 4.2: Effects of initial time on 2,4-DCP, 2,4,6-TCP, and 2,4-DNP (condition: sorbent: 20 mg; initial concentration: 10 mg/L; volume: 10 mL; sample pH at 6, and temperature 298K).

4.3.3 Effect of initial concentration (C_0)

Figure 4.3 represents the effect of the initial concentration of 2,4-DCP, and 2,4,6-TCP on βCD-BIMOTs-TDI in the range of 5-100 mg/L, and 2,4-DNP in the range of 5-60 mg/L at 298 K, 318 K, and 338 K respectively. The initial concentration provided an important driving force to overcome all the mass transfer resistance of 2,4-DCP, 2.4.6-TCP, and 2,4-DNP between the aqueous and solid phases (Kilic et al., 2011). Apart from that, the presence of macroporous on the surface of βCD-BIMOTs-TDI was beneficial in reducing mass transfer resistance and had become favourable for fast 2,4-DCP, 2,4,6-TCP, and 2,4-DNP adsorption (Du et al., 2010).

The percentages of removal for 2,4-DCP and 2,4,6-TCP were found to be optimum at 20 mg/L with 80% and 10 mg/L with 91%. Meanwhile, 2,4-DNP showed an optimum removal at 5 mg/L about 92%, and then decreased as concentration increased and reached equilibrium at 50 mg/L. It was observed that the βCD-BIMOTs-TDI adsorbed phenolic species in the order of 2,4-DNP > 2,4,6-TCP > 2,4-DCP. Higher percentage of removal was observed at lower concentration could be due to the availability of more active sites on the adsorbent than the numbers of phenol ions in the solution, while at higher concentration, phenol ions are more than the active sites.

The decrease in the percentage of removal as concentration increased was significant for 2,4-DNP and 2,4,6-TCP molecules, and this indicated that the βCD-BIMOTs-TDI materials had become saturated as the concentration increased. Apart from that, complexation between phenols and β-CD molecule were influenced by the molecular structure and hydrophobicity of phenols compounds (Sun et al., 2010b). The hydrophobic properties of phenols increase as the amount of chlorine increases. Water-octanol distribution constant (log k_{ow}) represents the hydrophobicity of a compound (Saitoh et al., 2002). Thus, in the present study, the order of hydrophobicity followed the order of 2,4,6-TCP (log $k_{ow =}$ 3.69) > 2,4-DCP (log k_{ow} = 3.08) > 2,4-DNP (log $k_{ow =}$ 1.53). Therefore, in this study, the removal of 2,4-DNP decreased as the concentration increased, could be due to less hydrophobic and had not been able to form stable inclusion complex with the hydrophobic cavity of β-CD at high concentration of 2,4-DNP. Apart from that, a decrease in the removal percentage of 2,4,6-TCP as concentration increased could be due to its larger molecular structure and could not fit well into the hydrophobic cavity of β-CD at higher concentration even though more hydrophobic than 2,4-DCP and 2,4-DNP .

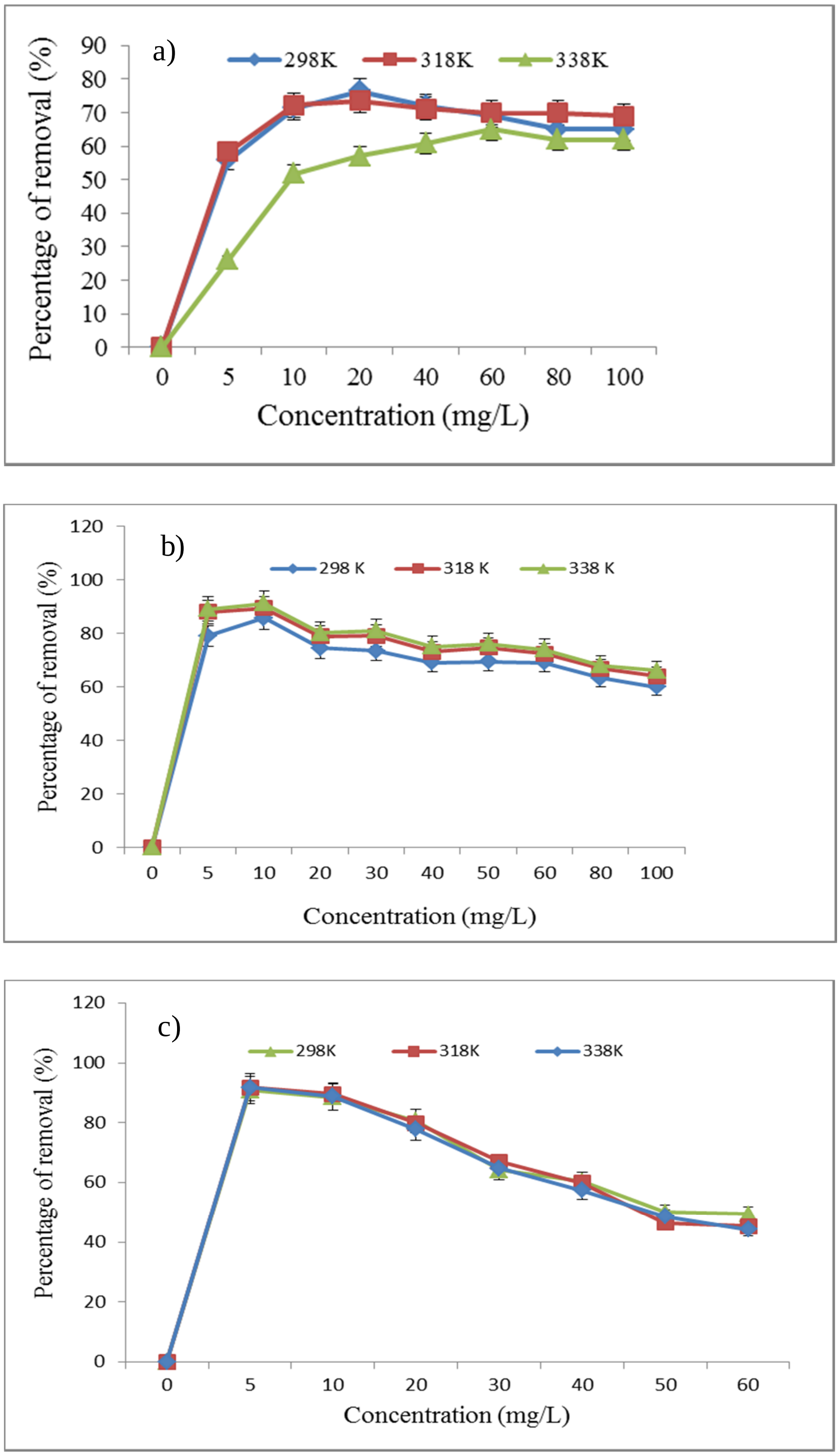

Figure 4.3: Effects of initial concentration of a) 2,4-DCP, b) 2,4,6-TCP, and c) 2,4-DNP (condition: sorbent: 20 mg; initial concentration: 10 mg/L; volume: 10 mL; sample pH at 6, and temperature 298K).

4.3.4 Effect of solution temperature

The adsorption capacity, qe (mg/g) of 2,4-DCP, 2,4,6-TCP, and 2,4-DNP on βCD-BIMOTs-TDI were shown in Figure 4.4a, 4.4b, and 4.4c. As shown in Figure 4.4a, adsorption capacity of 2,4-DCP was found to decrease at higher temperature (Figure 4.4a) in all the concentrations examined (5-100 mg/L) that could be attributed to the exothermic reaction due to the increase in the percentage of the desorption of 2,4-DCP from the distorted active sites of the adsorbent. At lower concentration, no significant difference on adsorption capacity between 298 K and 318 K was observed, but at higher concentration (80 mg/L, 100 mg/L), adsorption capacity was found to be optimum at 318 K. When the temperature increased, the proportion of 2,4-DCP at equilibrium decreased. Therefore, the reaction must be carried out at a temperature that is high enough to achieve equilibrium rapidly, but not too high as to restrict the proportion of 2,4-DCP. Hence, in this study, 298 K and 318 K were found to be the suitable temperatures for the removal of 2,4-DCP using βCD-BIMOTs-TDI.

Meanwhile, the adsorption capacity, qe (mg/g) of 2,4,6-TCP on βCD-BIMOTs-TDI, was found to increase (Figure 4.4b) in all the concentrations examined (5-100 mg/L) with the increase of temperature that could be attributed to the endothermic reaction. Apart from that, no significant difference could be observed at lower concentration (5-40 mg/L) for the removal of 2,4-DNP (Figure 4.4c), but at higher concentration (60 mg/L), binding capacity was found to increase as the temperature increased from 298 K to 338 K, which could be due to endothermic reaction.

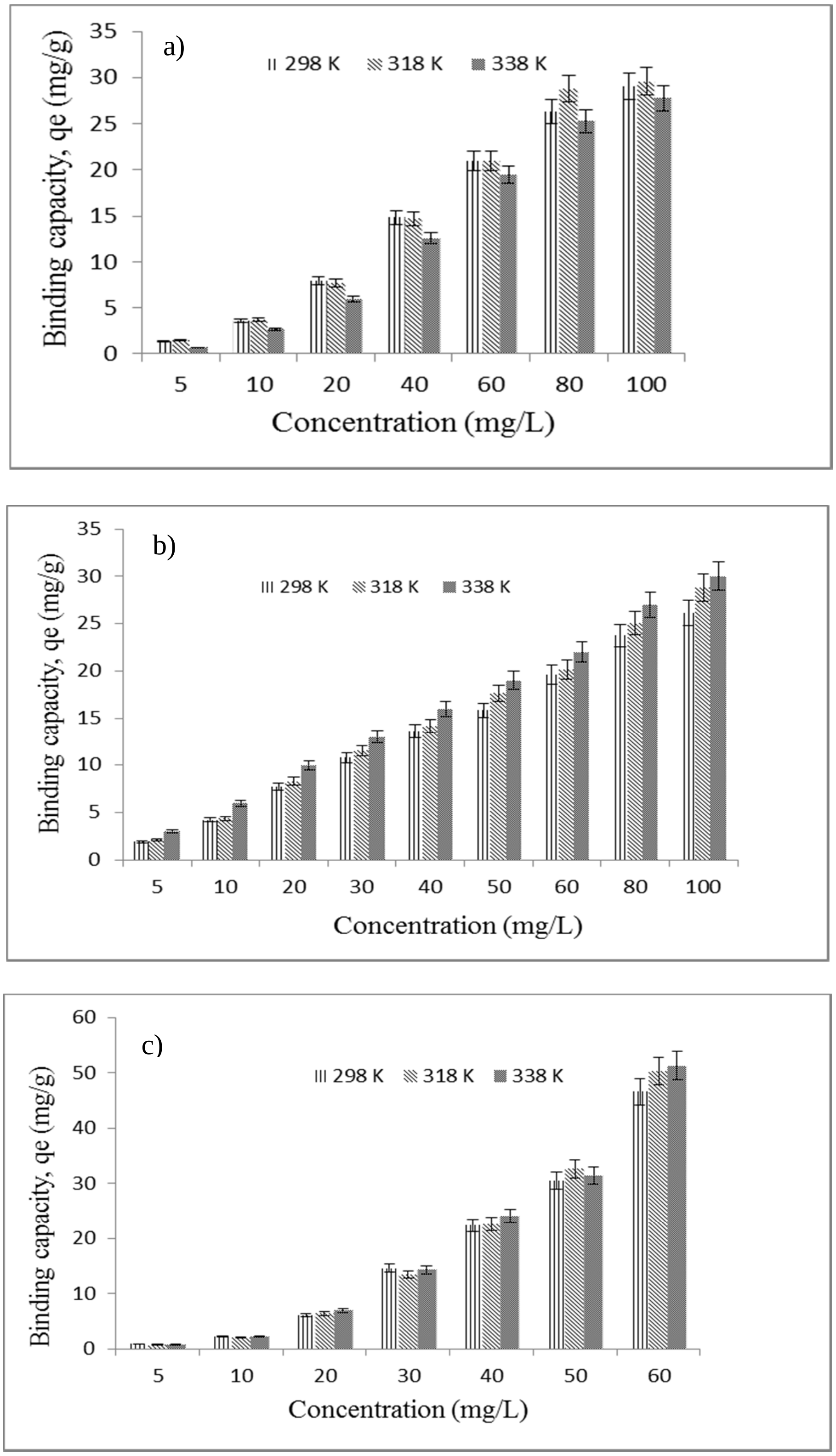

Figure 4.4: Effects of solution temperature on a) 2,4-DCP, b) 2,4,6-TCP, and c) 2,4-DNP (condition: sorbent: 20 mg; volume: 10 mL; sample pH at 6).

4.3.5 Adsorption kinetic model

Several kinetic models were used to investigate the mechanism of adsorption and kinetic parameters, the sorption data of 2,4-DCP, 2,4,6-TCP, and 2,4-DNP on βCD-BIMOTs-TDI using pseudo first order (Febrianto et al., 2009; Memon et al., 2011) (Figure 4.5a), pseudo second order (Ho et al., 2000; Bingjun Pan et al., 2008) (Figure 4.5b), Elovich (Figure 4.5c), film diffusion (Figure 4.5d), and intra particles diffusion (Figure 4.5e) (Weber & Morris, 1963) models. The characteristics and equations used are described in Section 2.4.2.

The normalized standard deviation value, Δq (%) and relative error (%) were obtained to determine the suitability of the model to describe the adsorption kinetics, which is defined as

$$\Delta q\ (\%) = \sqrt{\frac{[(q_{exp}-q_{cal})\ /\ q_{exp}]^2}{N-1}}\ \times 100 \qquad (4.4)$$

$$\text{Relative error (\%)} = 100 \left| \frac{q_{exp}-q_{cal}}{q_{exp}} \right| \qquad (4.5)$$

where N represents the number of data points, while q_{exp} and q_{cal} (mg/g) are the experimental and calculated adsorption capacities, respectively. The lower the value of Δq and relative error (%), the better the model fits (Castro López et al., 2012; Shaarani & Hameed, 2011). Besides, the accuracy and validity of the kinetic models were compared quantitatively and the results are shown in Table 4.1 with correlation coefficient R^2, normalized standard deviation (Δq (%)), and relative error (%) for the adsorption of 2,4-DCP, 2,4,6-TCP, and 2,4-DNP on βCD-BIMOTs-TDI. Referring to Table 4.1, the pseudo second order kinetics model was found to fit well for all the phenols species studied with lower Δq values (2,4-DCP = 0.798%, 2,4,6-TCP = 0.491%, and 2,4-DNP = 0.214%), and relative errors (2,4-DCP = 2.111%, 2,4,6-TCP = 1.298%, and ,2,4-DNP = 0.567%). These were in tandem with R^2 values ranging from 0.9996-1 (Figure 4.5b), which further proved that the adsorption of 2,4-DCP, 2,4,6-TCP, and 2,4-DNP on the βCD-BIMOTs-TDI followed the pseudo second order model. This consistency could be further proven by the closeness of the calculated and experimental q_e value. In comparison, there was a large difference between the experimental and the calculated adsorption capacity for 2,4-DCP, 2,4,6-TCP, and 2,4-DNP represented by Δq (%), indicating a poor pseudo first order fit to the experimental data. This indicated that most of the 2,4-DCP, 2,4,6-TCP, and 2,4-DNP molecules were adsorbed onto the surface of βCD-BIMOTs-TDI by the chemisorption mechanism, which involved valence forces through the sharing or exchange of electrons (Vimonses et al., 2009) and the adsorption mechanism might depend on both the adsorbate and the adsorbent (Pavan et al., 2008). It could also be seen from pseudo second order data that the adsorption rate of phenol compounds $k_{2,}$ on βCD-BIMOTs-TDI was found to be in the order of 2,4-DNP > 2,4,6-TCP > 2,4-DCP. Additionally, the initial adsorption rates, h, had been also consistent with this order. Previously, several authors showed the successful application of pseudo second order model for representation of experimental kinetics data of phenols adsorption (Li et al., 2012a; Pan et al., 2011).

To further prove that the sorption was based on chemisorptions, the Elovich's model was employed (Figure 4.5c) (Castro López et al., 2012). Good fit with $R^2 > 0.9$, for 2,4-DCP, 2,4,6-TCP, and 2,4-DNP adsorption on βCD-BIMOTs-TDI with the closeness of experimental and calculated adsorption capacity, further supported the fact that the adsorption process was based on chemisorptions. In conclusion, the models fit the kinetic data for the adsorption of 2,4-DCP, 2,4,6-TCP, and 2,4-DNP, in the order of pseudo second order kinetics > Elovich > pseudo first order kinetics.

Hence, to further investigate and understand the mechanism of adsorption process and to determine the rate controlling step, which mainly depended on external diffusion/film, followed by intra particle or pore diffusion, and finally, sorption into the interior sites of the adsorbent. The final process was very rapid, hence the sorption of the adsorbate on the sorbent might be governed by external and/or intra particle diffusion (Bhatnagar & Minocha, 2009). Based on the obtained plots, external diffusion was not applicable in these adsorption experiments since the plots did not give zero intercept, as shown in Figure 4.5d with R^2 ranging from 0.6900 to 0.7928 based on the obtained result in Table 4.1.

Apart from that, Figure 4.5e represents plots of linear form of the intra particle diffusion model. The results showed that the intercept did not pass through the origin, and the correlation coefficient values (R^2) were less than 0.99 (Table 4.1) for the adsorption of 2,4-DCP, 2,4,6-TCP, and 2,4-DNP on βCD-BIMOTs-TDI, suggesting that the intraparticle diffusion was involved in the sorption process, yet it was not the rate of controlling step. Furthermore, larger c value (3.2982) indicated better adsorption mechanism of 2,4,6-TCP on βCD-BIMOTs-TDI adsorbent. Bratnagar and Minocha (2009) reported similar results earlier in light of the removal of chlorophenol from water. Hence, both external and intraparticle diffusion simultaneously occurred during the adsorption process but they were not rate determining steps.

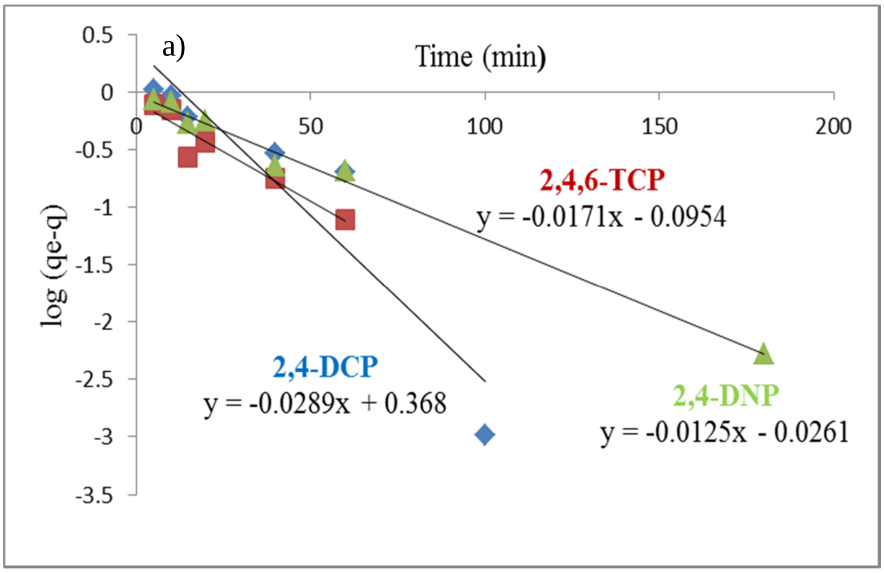
a)
Time (min)
log (qe-q)
0.5
0
-0.5
-1
-1.5
-2
-2.5
-3
-3.5
0
50
100
150
200
2,4,6-TCP
y = -0.0171x - 0.0954
2,4-DCP
y = -0.0289x + 0.368
2,4-DNP
y = -0.0125x - 0.0261

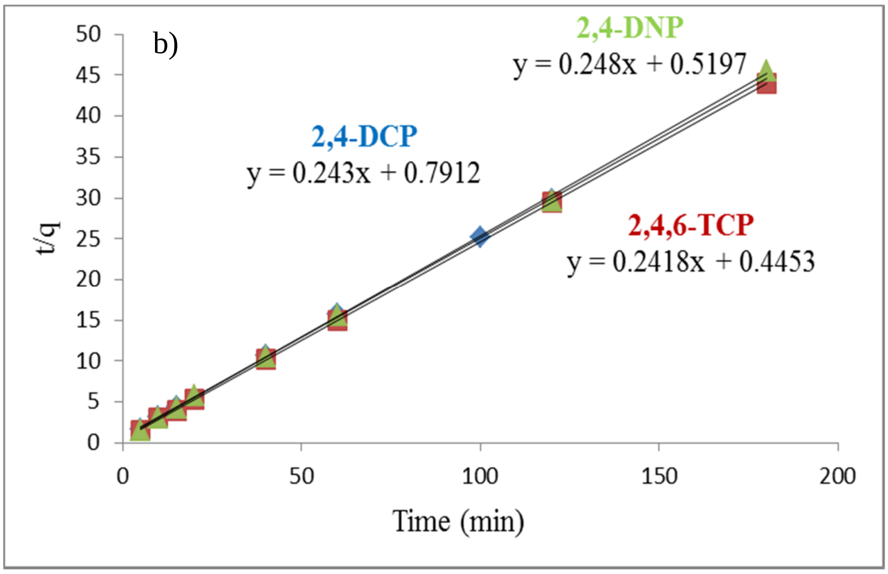
b)
t/q
50
45
40
35
30
25
20
15
10
5
0
0
50
100
150
200
Time (min)
2,4-DNP
y = 0.248x + 0.5197
2,4-DCP
y = 0.243x + 0.7912
2,4,6-TCP
y = 0.2418x + 0.4453

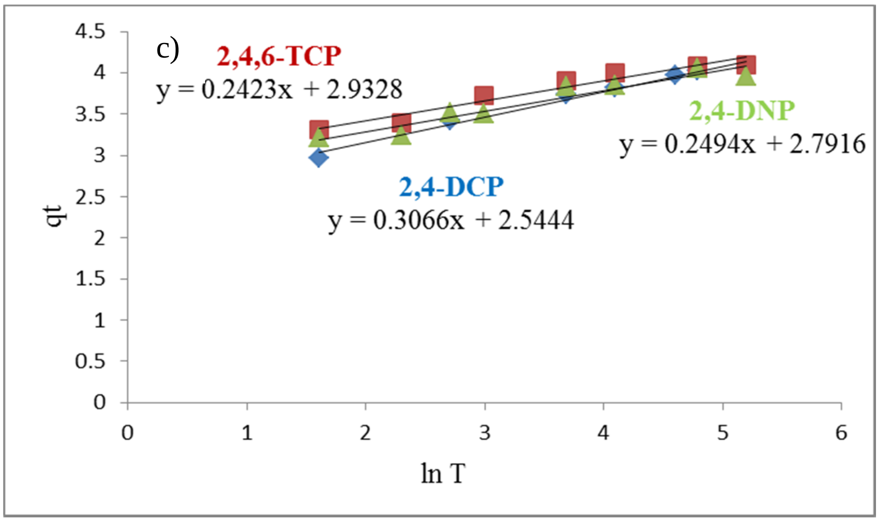
c)
2,4,6-TCP
y = 0.2423x + 2.9328
2,4-DNP
y = 0.2494x + 2.7916
2,4-DCP
y = 0.3066x + 2.5444
qt
ln T
0
0.5
1
1.5
2
2.5
3
3.5
4
4.5
0
1
2
3
4
5
6

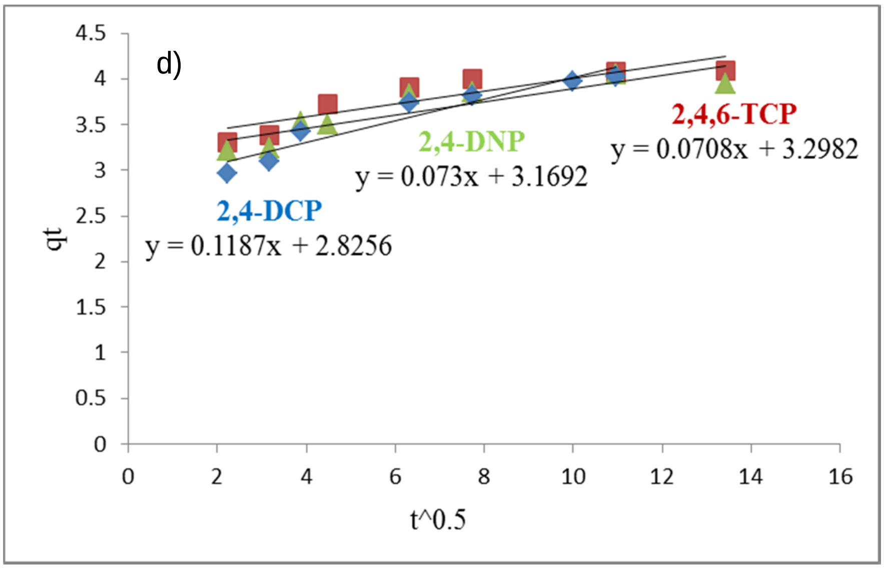
d)
2,4,6-TCP
y = 0.0708x + 3.2982
2,4-DNP
y = 0.073x + 3.1692
2,4-DCP
y = 0.1187x + 2.8256
qt
t^0.5
0
0.5
1
1.5
2
2.5
3
3.5
4
4.5
0
2
4
6
8
10
12
14
16

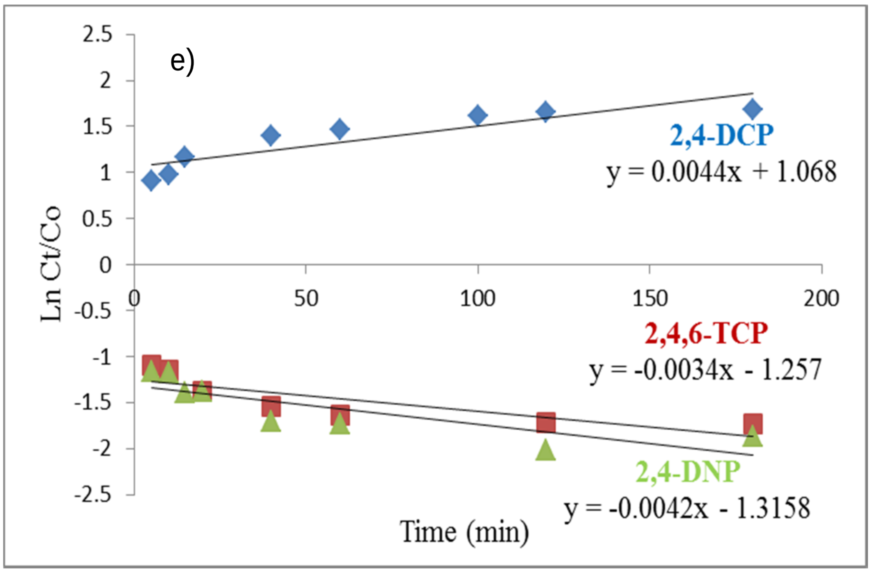

Figure 4.5: a) Pseudo first order plot, b) Preudo second order model plot, c) Elovich plot, d) External diffusion plot, and e) Intraparticle plot for adsorption of 2,4-DCP, 2,4,6-TCP, and 2,4-DNP on βCD-BIMOTs-TDI at 298 K

Table 4.1: Kinetic parameter for the adsorption of phenol compounds on βCD-BIMOTs-TDI.

Kinetic models	Parameters	2,4-DCP	2,4,6-TCP	2,4-DNP
	q_e, exp (mg/g)	4.025	4.083	4.055
Pseudo first order kinetic model	q_e, cal (mg/g)	2.330	0.803	0.942
	k_1 (min^{-1})	0.067	0.039	0.029
	Δq (%)	18.830	35.926	34.332
	Relative error (%)	42.112	80.333	76.769
	R^2	0.8748	0.9113	0.9917
Pseudo second order kinetic model	q_e, cal (mg/g)	4.110	4.136	4.032
	k_2 (g/mg min)	0.075	0.118	0.131
	h (mg/g min)	1.264	2.246	19.235
	$t^{1/2}$ (min)	3.250	1.842	2.096
	Δq (%)	0.798	0.491	0.214
	Relative error (%)	2.111	1.298	0.567
	R^2	**0.9998**	**1**	**0.9996**
Elovich's equation	q_e, cal (mg/g)	3.000	4.093	3.986
	β (g/mg)	3.262	4.127	4.009
	α (mg/g min)	1232.79	42873.00	18087.00
	Δq (%)	10.400	0.010	0.643
	Relative error (%)	25.470	0.245	1.702
	R^2	**0.9798**	**0.9421**	**0.9199**
External diffusion	k_{ext} (1/min)	-0.0044	0.0034	0.0042
	c	-1.0680	-1.2570	-1.3158
	R^2	0.7928	0.6900	0.6991
Intraparticle diffusion model	K (mg/g min)	0.1187	0.0708	0.0730
	c (mg/g)	2.8256	3.2982	3.1692
	R^2	0.9192	0.8031	0.8022

4.3.6 Adsorption isotherm

In order to describe further the interaction between the adsorbent and adsorbates, adsorption isotherm was studied at all temperatures (298 K, 318 K, and 338 K). The linearised forms of Langmuir (Figure 4.6), Freundlich (Figure 4.7), Temkin (Figure 4.8) and Dubinin-Radushkevich's (D-R) (Figure 4.9) isotherm models were applied to fit the equilibrium data. Table 4.2 shows the adsorption of isotherm constant for 2,4-DCP, 2,4,6-TCP, and 2,4-DNP on βCD-BIMOTs-TDI at three varying temperatures.

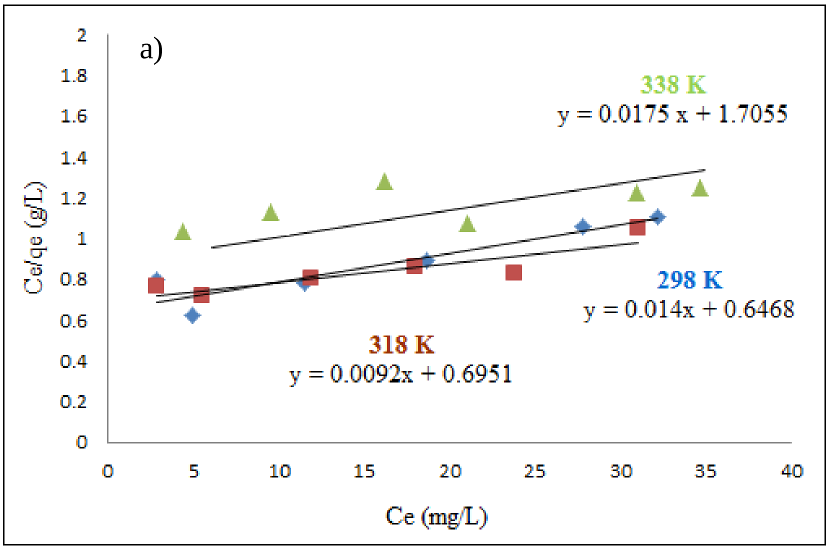

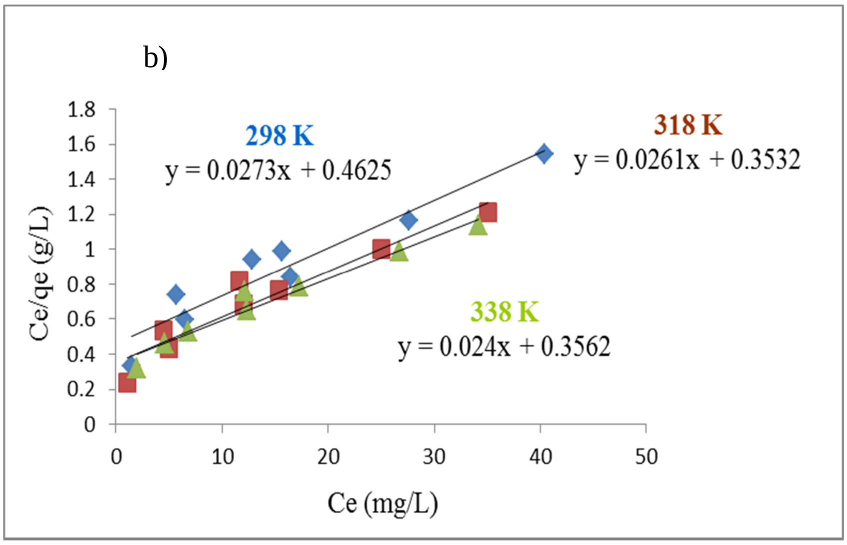

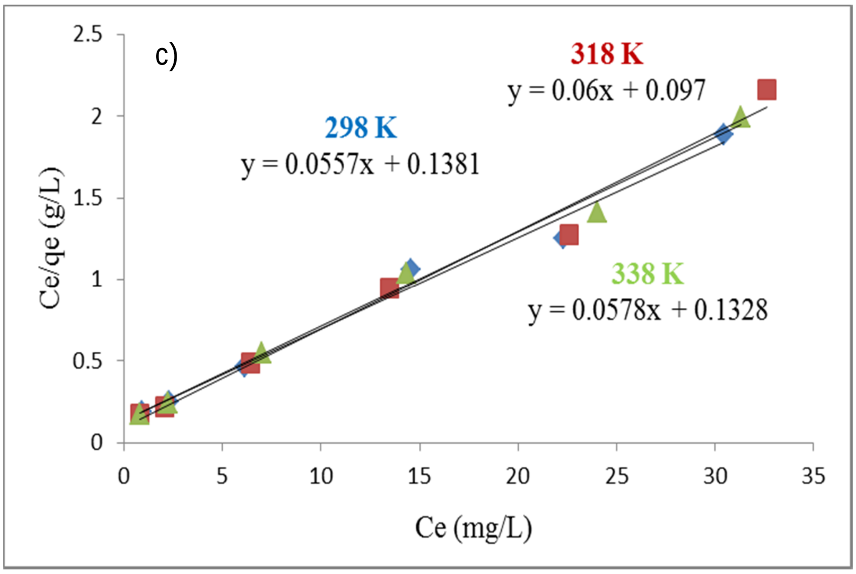

Figure 4.6: Langmuir's isotherm model for the adsorption of a) 2,4-DCP, b) 2,4,6-TCP, and c) 2,4-DNP on βCD-BIMOTs-TDI at 298, 318, and 338 K.

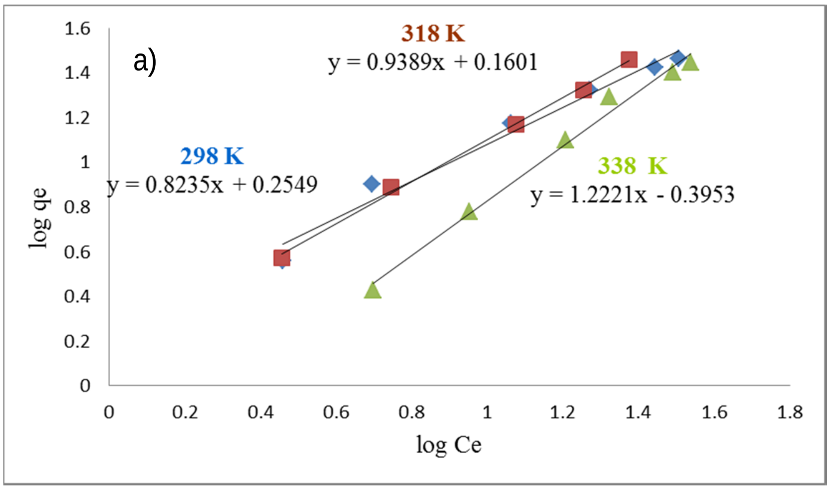
a)
318 K
y = 0.9389x + 0.1601
298 K
y = 0.8235x + 0.2549
338 K
y = 1.2221x - 0.3953
log qe
1.6
1.4
1.2
1
0.8
0.6
0.4
0.2
0
0
0.2
0.4
0.6
0.8
1
1.2
1.4
1.6
1.8
log Ce

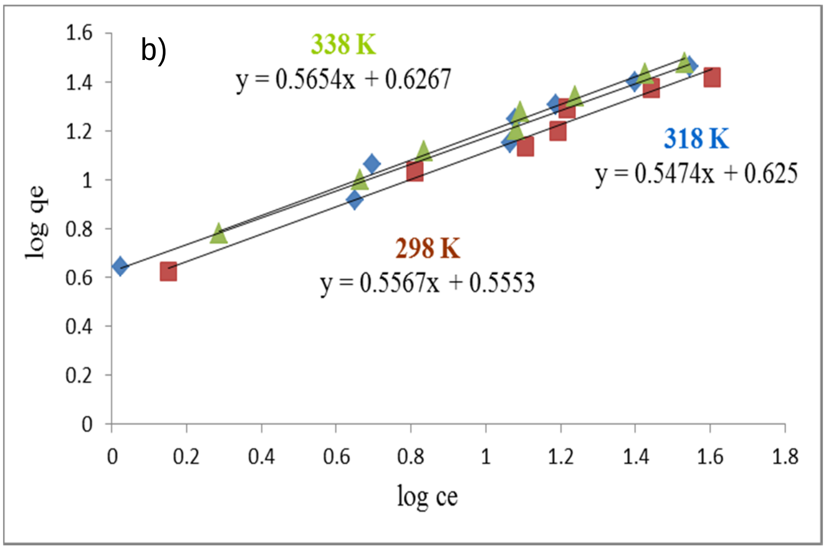
b)
338 K
y = 0.5654x + 0.6267
318 K
y = 0.5474x + 0.625
298 K
y = 0.5567x + 0.5553
log qe
1.6
1.4
1.2
1
0.8
0.6
0.4
0.2
0
0
0.2
0.4
0.6
0.8
1
1.2
1.4
1.6
1.8
log ce

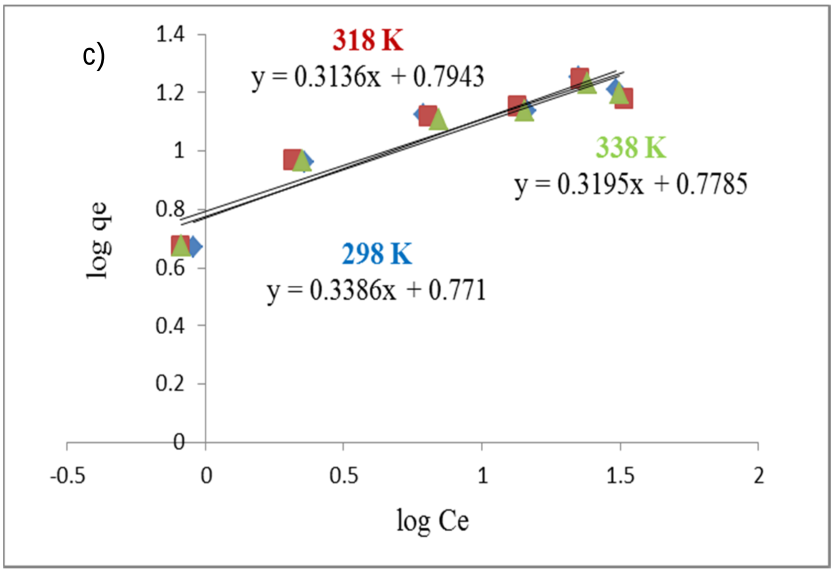

Figure 4.7: Freundlich's isotherm model for the adsorption of a) 2,4-DCP, b) 2,4,6-TCP, and c) 2,4-DNP on βCD-BIMOTs-TDI at 298, 318, and 338 K.

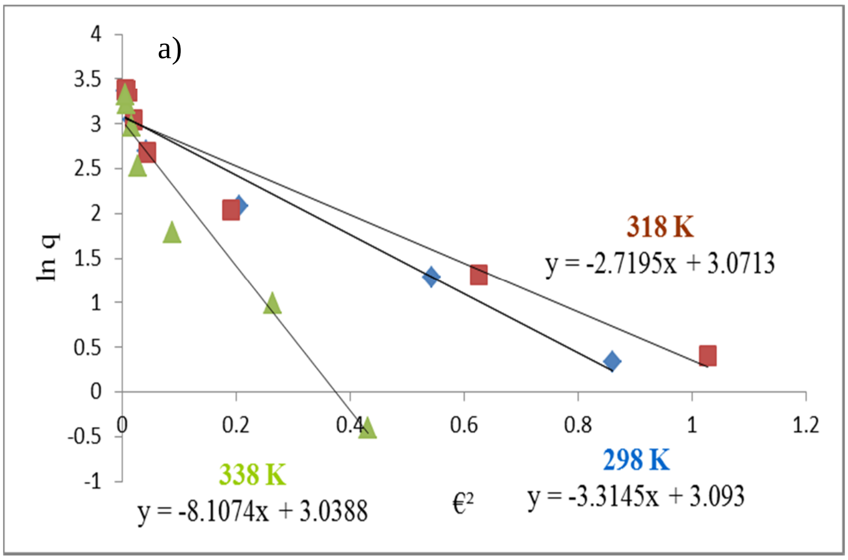

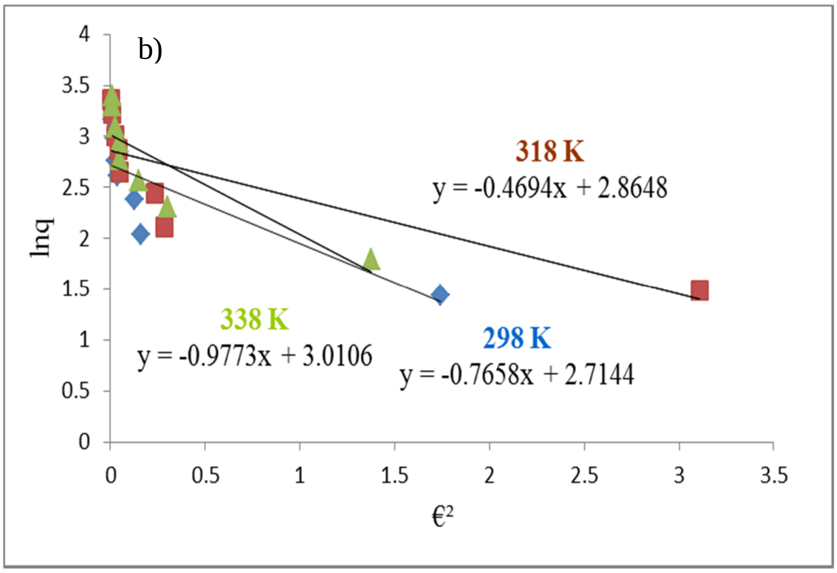

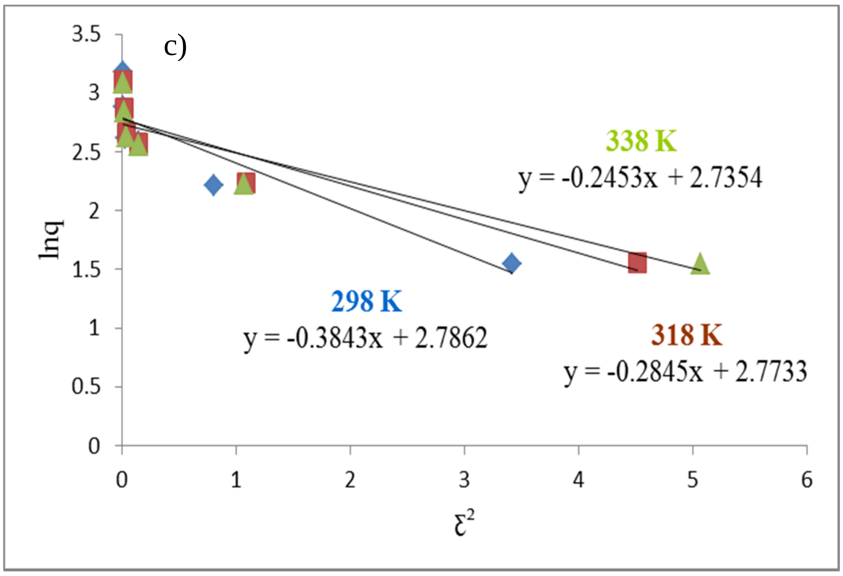

Figure 4.8: Dubinin-Radushkevich’s isotherm model for the adsorption of a) 2,4-DCP, b) 2,4,6-TCP, and c) 2,4-DNP on βCD-BIMOTs-TDI at 298, 318, and 338 K.

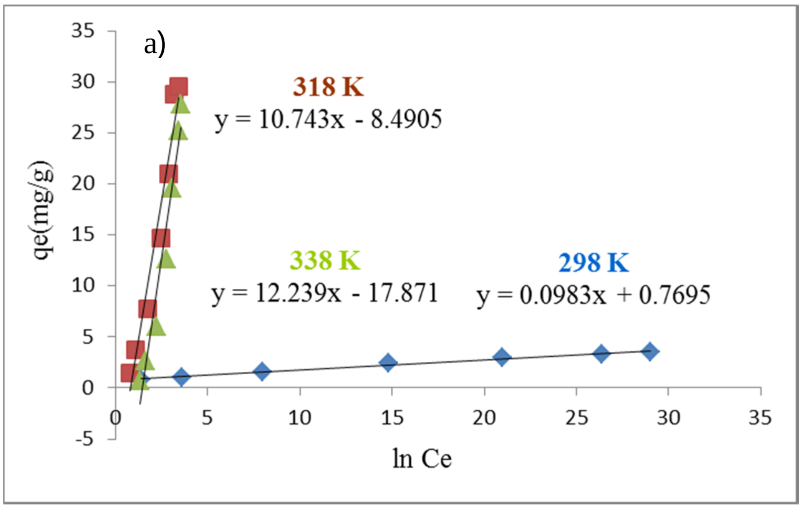
a)
318 K
y = 10.743x - 8.4905
338 K
y = 12.239x - 17.871
298 K
y = 0.0983x + 0.7695
qe(mg/g)
ln Ce
35
30
25
20
15
10
5
0
-5
0
5
10
15
20
25
30
35

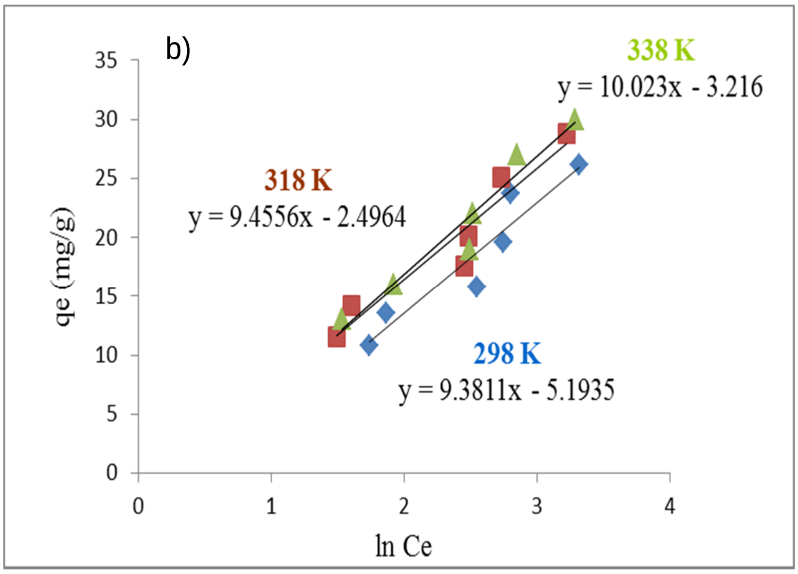
b)
338 K
y = 10.023x - 3.216
318 K
y = 9.4556x - 2.4964
298 K
y = 9.3811x - 5.1935
qe (mg/g)
ln Ce
35
30
25
20
15
10
5
0
0
1
2
3
4

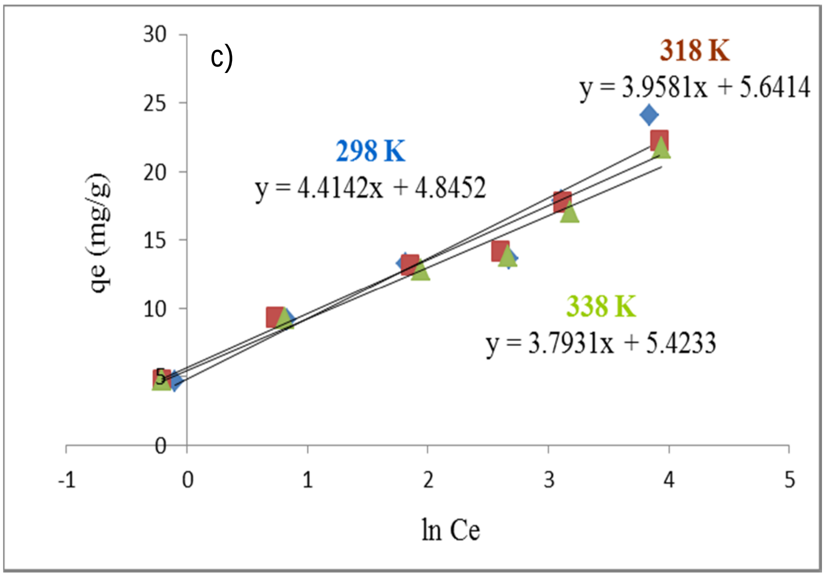

Figure 4.9: Temkin's isotherm model for the adsorption of a) 2,4-DCP, b) 2,4,6-TCP, and c) 2,4-DNP on βCD-BIMOTs-TDI at 298, 318, and 338 K

4.3.7 Fitting of the isotherm models

4.3.7.1 Fisher parameter

The different types of adsorption isotherm models were compared using the Fisher test (equation 4.6). The best model selected for the experimental data was the one with the highest value of the Fisher parameter, F_{calc} (Ajnazarova & Kafarov, 1985).

$$F_{calc} = \frac{(n-1)\sum_{i=1}^{n}\left(q_{\exp,i} - \overline{q_{\exp}}\right)^2}{(n-1)\sum_{i=1}^{n}\left(q_{\exp,i} - q_{t,i}\right)^2} \tag{4.6}$$

where $q_{exp,i}$ and $q_{t,i}$ are the experimental and calculated values for each data point, respectively. $\overline{q_{exp}}$ is the mean value of the vector $q_{exp,\ i}$, while l is the number of adjusted parameters of the model, and n is the number of data points.

The standard error of estimation (SEE) was calculated using equation 4.7:

$$SEE = \frac{100}{n} \cdot \sum_{i=1}^{n} \frac{\left| q_{\exp,i} - q_{t,i} \right|}{q_{\exp,i}} \tag{4.7}$$

The experimental equilibrium data for the adsorption of 2,4-DCP, 2,4,6-TCP, and 2,4-DNP on βCD-BIMOTs-TDI at best conditions at different temperatures are shown in Table 4.2. The benefits of the fit and adequacy of the studied models were estimated by R^2 and Fisher tests respectively. Adsorption isotherms of 2,4-DCP and 2,4,6-TCP on βCD-BIMOTs-TDI were better fitted by the Freundlich's model with $R^2 > 0.97$ for all the studied temperatures, as shown in Figure 4.7. This fact has been further supported by higher F_{calc} and lower *SEE* values for all the temperatures studied, as shown in Table 4.2, compared to the other three isotherm models. This shows that βCD-BIMOTs-TDI has a heterogeneous surface with many cavities (cyclodextrin), imidazolium ring, and isocyanate group. Therefore, it can be expected that the sorption system with different types of interactions (such as inclusion complex, hydrogen bonding, Van Der Waals forces, and π-π interaction) were involved. K_F, Freundlich constant for the adsorption capacity of 2,4-DCP showed a decrease with the rise of temperature determined as 1.799, 1.446, and 0.402 for 298K, 318K, and 338K respectively, which indicated that the adsorption process was exothermic. In comparison, K_F values were found to increase for 2,4,6-TCP, ranging from 3.592-4.234, indicated that the sorption process was endothermic. The n values (indicator for adsorption intensity) calculated from the Freundlich's model were in the range of $1 < n < 10$, for the adsorption of 2,4-DCP at 298K and 318K, which indicated that the adsorption process was favourable at lower temperature, while as for 2,4,6-TCP, the n values were found to be above the range at all the studied temperature that indicated the favourability of the sorption process on βCD-BIMOTs-TDI. Apart from that, the obtained K_F values indicated that the adsorption of phenol compound on βCD-BIMOTs-TDI were in the order or 2,4-DNP > 2,4,6-TCP > 2,4-DCP. Similar result was reported in the previous work for the removal of chlorophenols using β-CD-polyamidoamine copolymer (Li et al., 2012a). Besides, n values of Freundlich's isotherm for 2,4-DCP and 2,4,6-TCP were found to be more than 1, except for n value of 2,4-DCP at 338K (0.818), indicating the adsorption process was a chemical process (Sun et al., 2010b).

Apart from that, the sorption of 2,4,6-TCP had been better than 2,4-DCP on βCD-BIMOTs-TDI and this might be explained mainly from inclusion effect and hydrogen bonding between sorbent and adsorbates. β-CD have higher affinity for 2,4,6-TCP due to the higher hydrophobicity compared to 2,4-DCP and could form stable inclusion complex. Meanwhile, the strength of the hydrogen bonding depends on the number and position of chlorine atoms. The number of chlorine atoms in 2,4,6-TCP was more than 2,4-DCP (Li et al., 2012b), so the order of the strength of hydrogen bonds was 2,4,6-TCP > 2,4-DCP. Thus, 2,4,6-TCP molecules reacted with adsorption sites via binding to the active sites in the polymer network, forming hydrogen and inclusion complex with the cavity of β-CD.

In addition, the βCD-BIMOTs-TDI showed high adsorption activity towards phenol compounds with low pka value, and the sequence of the pKa values of these compounds are: 2,4-DNP (3.96) < 2,4,6-TCP (7.42) < 2,4-DCP (7.85). Thus, the adsorption of phenols compounds onto βCD-BIMOTs-TDI improved with the nitro functional group in the molecule of phenol. As both nitro and chloro groups are electron withdrawing groups, the π-π interactions are enhanced with the increase in the number of these groups. The nitro group has stronger electron-withdrawing ability than chloro group, hence the π-π interactions between 2,4-DNP and βCD-BIMOTs-TDI are stronger than chlorophenols.

The adsorption of 2,4-DCP was also found to fit well with Temkin's isotherm with $R^2 > 0.95$ for all studied temperature, supported by the higher F_{calc} values and lower *SEE* values, indicating that the heat of adsorption of all the molecules in the layer would decrease linearly with coverage and the adsorption was characterized by a uniform distribution of binding energies, up to some maximum binding energy.

On the other hand, the Langmuir's model was basically intended for a homogeneous system, while the Freundlich's model was suitable for a highly heterogeneous surface, being the system more heterogeneous as 1/n value was closer to 0 for the adsorption of 2,4,6-TCP on βCD-BIMOTs-TDI. The obtained experimental data (1/n between 0.547 and 0.565) suggested that although some degree of heterogeneity was present, a more homogeneous surface could be assumed. The Langmuir's isotherm was found to fit quite well with the experimental data with high correlation coefficient ($R^2 > 0.91$) for all the studied temperatures. The maximum monolayer adsorption (q_m) was 41.670 with R_L value of 0.460 for the adsorption of 2,4,6-TCP onto βCD-BIMOTs-TDI at 338K. The obtained R_L values, which were greater than zero and less than unity for the studied temperatures, suggested that the adsorption process was favourable at all studied temperatures. The calculated value of $\beta < 1.0$ from Dubinin-Radushkevich's isotherm model for the adsorption of 2,4,6-TCP represented a rough surface with many cavities and further supported the fit of isotherm data for Freundlich's model, which suggested a heterogeneous surface. Hence, it can be concluded that adsorption of 2,4,6-TCP by βCD-BIMOTs-TDI followed a multisorption process, where both monolayer and bilayer adsorptions were present simultaneously in the surfaces of the sorbent, but the former adsorption was more predominant.

The adsorption of 2,4-DNP was found to fit well with Langmuir's model, which was basically intended for a homogeneous system with R^2 values ranging from 0.9840-0.9918, supported with higher F_{calc} and lower *SEE* values for all the studied temperature. This phenomenon could be explained by electrophilic property of oxygen in $–NO_2$ of 2,4-DNP, which made the nitrogen atom to face difficulty to form hydrogen bonding with β-CD. Therefore, it was difficult for 2,4-DNP to tightly adsorb around β-CD. Other than that, π-π interactions between the aromatic rings of 2,4-DNP and βCD-BIMOTs-TDI had been very important in the adsorption of 2,4-DNP compounds on βCD-BIMOTs-TDI. The electron density of aromatic ring should be taken into account for its effect on π-π interactions. Basically, substituted groups could either strengthen or weaken the electron cloud distribution on aromatic rings and it depends on their dipolar properties. 2,4-DNP was expected to have stronger effects on π-π interactions because of its high dipole moment (3.51 debye). Thus, the isotherms studies of 2,4-DNP deviated substantially from 2,4-DCP and 2,4,6-TCP (Pan et al., 2005). Therefore, the adsorption of 2,4-DNP was on the monolayer adsorptions on a homogenous surface with uniform energies of adsorption for all the binding sites with no further adsorption process would occur if the site was occupied by a solute. The maximum monolayer adsorption (q_m) values were in the range of 16.67-17.95 with R_L values ranging from 0.047-0.075, which were greater than zero and less than unity for the studied temperatures, suggesting that the adsorption process was favourable at all studied temperatures. The Temkin's isotherm model also fit quite well with the adsorption of 2,4-DNP on βCD-BIMOTs-TDI with $R^2 > 0.93$ for all studied temperature. The Temkin constant b_T, related to heat of sorption, was found to increase from 561.275 to 740.85 for all studied temperature.

As a conclusion, the applicability of the isotherm models to the adsorption behaviours was judged by using the correlation coefficient (R^2) values, and Fisher parameters (F_{calc} and *SEE*). Therefore, the adsorption equilibrium data fitted the isotherm models in the order of Freundlich > Temkin > Dubinin-Radushkevich > Langmuir for the adsorption of 2,4-DCP. Meanwhile, the adsorption of 2,4,6-TCP followed the order of Freundlich > Langmuir > Temkin > Dubinin-Radushkevich. In comparison, the adsorption of polar 2,4-DNP followed the order of Langmuir > Temkin > Freundlich > Dubinin-Radushkevich.

Table 4.2: Details of isotherm constants and correlation coefficient of determination for various adsorption isotherms for the adsorption of 2,4-DCP, 2,4,6-TCP, and 2,4-DNP onto βCD-BIMOTs-TDI

Adsorbate	Isotherms	Parameters		
		Temperature (K)		
		298 K	318 K	338 K
2,4-DCP	Langmuir			
	q_m (mg/g)	71.43	108.70	57.14
	b (L/mg)	0.022	0.013	0.010
	R^2	0.8618	0.7679	0.5538
	R_L	0.362	0.490	0.556
	Fcalc	1101.400	838.600	526.000
	SEE	0.479	0.418	0.388
	Freundlich			
	K_F ((mg/g) (L/mg)1/n)	1.799	1.446	0.402
	n	1.214	1.065	0.818
	1/n	0.824	0.939	1.222
	R^2	**0.9758**	**0.9974**	**0.9895**
	Fcalc	1168.528	1098.496	1113.359
	SEE	0.179	0.175	0.223
	Dubinin-Radushkevich			
	q_m (mg/g)	22.04	21.57	20.88
	β (mol^2/kJ^2)	3.315	2.720	8.107
	E	0.388	0.429	0.2483
	R^2	0.9595	0.9265	0.9504
	Fcalc	275.400	347.700	335.600
	SEE	0.150	0.133	0.306
	Temkin			
	K_T (L/mg)	2.506 x 10^3	0.450	0.242
	b_T(kJ/mol)	25.200	0.246	0.223
	R^2	0.9856	0.9562	0.9522
	Fcalc	943.900	606.500	726.800
	SEE	0.080	0.346	0.685
	Langmuir			
	q_m (mg/g)	36.63	38.31	41.67
	b (L/mg)	0.059	0.074	0.067
	R^2	0.9162	0.9154	0.9610
	R_L	0.380	0.351	0.460
	Fcalc	199.308	181.842	173.253
	SEE	0.106	0.113	0.092

Table 4.2 (Continued)

2,4,6-TCP	Freundlich			
	K_F ((mg/g) (L/mg)$^{1/n}$)	3.592	4.217	4.234
	n	1.796	1.827	1.769
	1/n	0.557	0.547	0.565
	R^2	**0.9820**	**0.9761**	**0.9914**
	Fcalc	326.918	223.935	220.067
	SEE	0.094	0.122	0.098
	Dubinin-Radushkevich			
	q_m (mg/g)	15.10	17.55	20.30
	β (mol^2/kJ^2)	0.766	0.469	0.977
	E (kJ/mol)	0.810	1.030	0.715
	R^2	0.6839	0.6577	0.7195
	Fcalc	164.089	192.863	195.540
	SEE	0.001	0.009	0.012
	Temkin			
	K_T (L/mg)	0.575	0.768	0.726
	b_T(kJ/mol)	264	279	280
	R^2	0.8968	0.9239	0.9468
	Fcalc	158.863	154.634	344.845
	SEE	0.155	0.161	0.083
2,4-DNP	Langmuir			
	q_m (mg/g)	17.95	16.67	17.30
	b (L/mg)	0.403	0.619	0.435
	R^2	**0.9847**	**0.9840**	**0.9918**
	R_L	0.075	0.047	0.068
	Fcalc	214.553	237.938	212.815
	SEE	0.063	0.056	0.059
	Freundlich			
	K_F ((mg/g) (L/mg)1/n)	5.902	6.005	6.227
	n	2.953	3.189	3.130
	1/n	0.339	0.314	0.319
	R^2	0.8911	0.8711	0.9139
	Fcalc	131.736	127.655	134.854
	SEE	0.084	0.082	0.079
	Dubinin-Radushkevich			
	q_m (mg/g)	16.219	16.010	15.419
	β (mol^2/kJ^2)	0.384	0.285	0.245
	E	1.141	1.326	1.428
	R^2	0.824	0.8576	0.8406
	Fcalc	282.965	272.201	264.867
	SEE	0.591	0.046	0.050
	Temkin			
	K_T (L/mg)	2.997	1.621	4.179
	b_T(kJ/mol)	561.275	667.96	740.85
	R^2	0.9325	0.9750	0.9678
	Fcalc	80.113	612.678	146.183
	SEE	0.107	1.815	0.095

4.3.8 Comparison of different sorbents

Table 4.3 lists the comparison of the sorption amount (q_e) of 2,4-DCP, 2,4,6-TCP, and 2,4-DNP on various adsorbents at different equilibrium times (q_t). The q_e of βCD-BIMOTs-TDI for 2,4-DCP, 2,4,6-TCP, and 2,4-DNP had been relatively high and were comparable with previous works. Thus, βCD-BIMOTs-TDI is considered as a promising sorbent for the removal of 2,4-DCP, 2,4,6-TCP, and 2,4-DNP.

Table 4.3: Comparison of βCD-BIMOTs-TDI with other method

Adsorbates	Sorbent	Sorbent dose (g/L)	C_o (mg/L)	q_e (mg/g)	q_t (hours)	Ref.
2,4-DCP	β-cyclodextrin/attapulgite composites	2	100	19.04	12	(Pan et al., 2011)
	β-cyclodextrin epichlorohydrin polymer	2	98	15.7	2	(Li et al., 2010)
	γ-cyclodextrin epichlorohydrin polymer	2	98	9.8	2	(Li et al., 2010)
	Aged-refuse	50	100	1.53	6	(Xiaoli & Youcai, 2006)
	βCD-BIMOTs-TDI	1	100	**29.58**	2	**This work**
2,4,6-TCP	Cibacron Blue F3GA carrying microbeads	5	500	18.6	1	(Li et al., 2010)
	Coconut shell activated carbon (CSAC)	5	100	19.94	3.5	(Xiaoli & Youcai, 2006)
	Commercial grade activated carbon (CAC)	5	100	19.53	3.5	(Xiaoli & Youcai, 2006)
	βCD-BIMOTs-TDI	1	100	**30**	2	**This work**
2,4-DNP	PHEMA microbeads	0.1	400	16.2	1	(Denizli et al., 2002)
	Bentonite	-	5-30	3.92	-	(Koumanova & Yaneva, 2006)
	βCD-BIMOTs-TDI	1	60	**51.27**	2	**This work**

4.3.9 Adsorption Thermodynamics

The obtained thermodynamic parameters for the adsorption of 2,4-DCP, 2,4,6-TCP, and 2,4,-TCP listed in Table 4.4 and Figure 4.10 show the thermodynamic plots. The ΔG° values were found to be negative for these adsorption studies for all studied phenols, except for 2,4-DCP at 338 K, which indicated that the process was thermodynamically feasible, spontaneous, and chemically controlled (Kilic et al., 2011) at lower temperature. The largest absolute values of ΔG° for 2,4,6-TCP and 2,4-DNP compared to 2,4-DCP suggested the most spontaneous nature of the adsorption processes on βCD-BIMOTs-TDI. In addition, the values of ΔG° for 2,4-TCP and 2,4-DNP were found to increase as the temperature increased, indicating high driving force, and hence, resulted in high adsorption capacity compared to the adsorption of 2,4-DCP on βCD-BIMOTs-TDI.

Meanwhile, the negative value of ΔH° (-18.10) indicated that the adsorption process of 2,4-DCP was exothermic and this finding is supported by the decrease of the K_f value uptake capacity of the sorbent with the rise of temperature (Table 4.2). In comparison, the positive values of ΔH° (40.27, 2.38) indicated that the adsorption process of 2,4,6-TCP and 2,4-DNP were endothermic and this finding is supported by the increase of the K_f value uptake capacity of the sorbent with the rise of temperature (Table 4.2). ΔH° value also gave indication on the type of adsorption process that took place, either physical or chemical process (Ahmed & Theydan, 2012). The obtained ΔH° values in this study were not in the range of physisorption. Therefore, chemisorption had taken place for the adsorption of 2,4-DCP, 2,4,6-TCP, and 2,4-DNP on βCD-BIMOTs-TDI.

A negative value of ΔS°(-55.99) was obtained for the adsorption process of 2,4-DCP, due to the decrease in randomness at the solid/solution interface (Aydın, & Aksoy, 2009). Meanwhile, a positive value of ΔS° was obtained for the adsorption of 2,4,6-TCP and 2,4-DNP, indicating that the reorientation or restructuring of water around the solute of surface was very unfavourable since it disturbed the existing water structure and imposed a new and more ordered structure on the surrounding water molecules. As a result of adsorption of 2,4,6-TCP and 2,4-DNP on the surface of βCD-BIMOTs-TDI, the liberation of the solvent molecules from the solvated shells had been more predominated in the studied system, and thus, the degree of freedom of the water molecule increased. Therefore, the positive value of entropy suggested the increased randomness at the solid-solution interface during the adsorption of 2,4,6-TCP and 2,4-DNP (Iqbal & Ashiq, 2007).

Table 4.4: Thermodynamic parameters for 2,4-DCP on βCD-BIMOTs-TDI.

	T (K)	**ΔG° (kJ/mol)**	**ΔH° (J/mol)**	**ΔS° (J/K mol)**
2,4-DCP	298 318 338	-1.16 -0.86 1.14	-18.10	-55.99
2,4,6-TCP	298 318 338	-40.05 -42.74 -45.43	40.27	134.53
2,4-DNP	298 318 338	-6.50 -6.94 -7.37	2.38	21.82

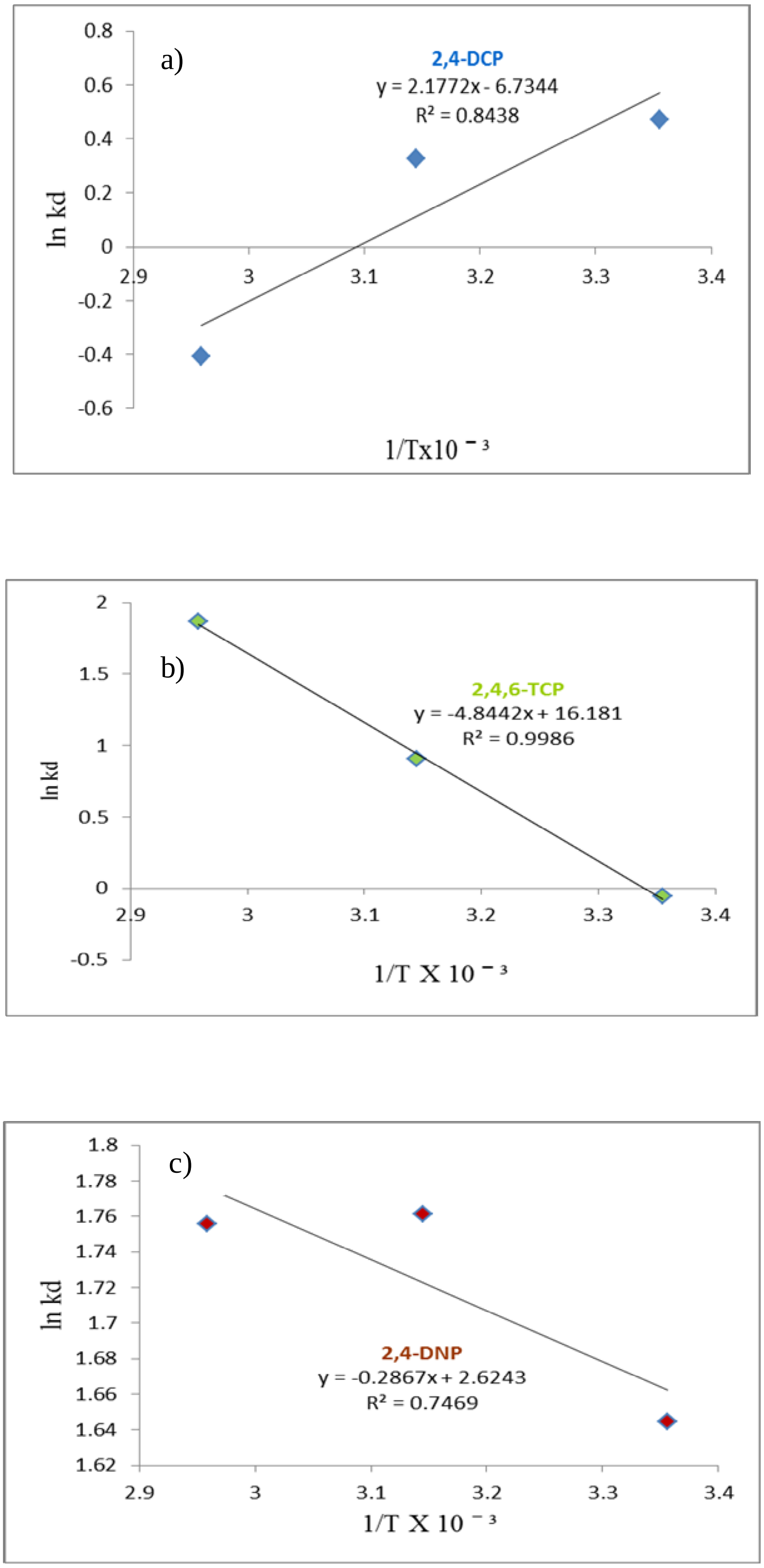

Figure 4.10: Thermodynamic plot for a) 2,4-DCP, b) 2,4,6-TCP and c) 2,4-DNP

4.3.10 Adsorption behaviour of βCD-BIMOTs via inclusion complex

In order to prove the formation of inclusion complex and π–π interaction between the modified β-CD functionalized ionic liquid (βCD-BIMOTs) with one selected phenol compound (2,4-DCP), ^{1}H NMR and 2D NOESY experiments were carried out. The analysis of the inclusion complex between the modified β-CD (β-CD-BIMOTs) and the 2,4-DCP was indeed very crucial in this work, since the cavity of β-CD was maintained during the polymerization process. Furthermore, the findings have supported that inclusion complex formation had been one of the main interactions between both the adsorbent and adsorbate in this adsorption process. Hence, in order to evaluate the geometry of inclusion formation of β-CD-BIMOTs and 2,4-DCP, ^{1}H NMR (Figure 4.11) and 2D NOESY measurements (Figure 4.12) (DMSO-D_6, 25°C,600 MHz) were performed on a AVN600 spectrometer. The obvious downfield shift of the protons on the inner cavity of β-CD-BIMOTs, *i.e.*, H3 and H5, had been observed due to the anisotropic shielding by the ring current from the aromatic rings of 2,4-DCP (Table 4.5) compared to other protons. Besides, when 2,4-DCP entered into the hydrophobic cavity of β-CD-BIMOTs, the change of the micro-environment in 2,4-DCP protons led to the upfield shift (Hb-p and Hc-p). Meanwhile, H5 proton of β-CD-BIMOTs changed from doublet to singlet upon the formation of inclusion complex, as shown in Figure 4.11. The presence of proton signals belonging to both β-CD-BIMOTs and 2,4-DCP molecules could be observed in the ^{1}H NMR spectrum of 2,4-DCP-βCD-BIMOTs (Figure 4.11c), which strongly suggested that the new inclusion complex was formed.

The formation of inclusion complex was further proven by the 2D NOESY analysis (Figure 4.12) since 2D NMR is a powerful tool for investigating intermolecular interactions and for gaining more information on the conformation of the inclusion complex (Li et al., 2003). 2D NOESY experiment provided an upper limit (ca. 5Å) on the distance between protons' cross peaks under favourable condition. The cross peaks in the spectra, indicated in Figure 4.12, originated from the interaction of the protons of 2,4-DCP and β-CD-BIMOTs. The cross peaks of β-CD-BIMOTs (3.5–3.6 ppm, H-3, H-5) and 2,4-DCP (7.4–6.9 ppm, Ha-p, Hb-p) demonstrated strong intensity. Hence, from the 2D NOESY spectra, we can conclude that the aromatic ring of 2,4-DCP had been accommodated in the β-CD cavity. The cross peak around 7-8 ppm, which belonged to BIMOTs and 2,4-DCP, showed that there was an interaction between the BIMOTs ring and 2,4-DCP (Figure 4.12) and this could be due to both the π-π interaction and electrostatic attraction. Moreover, the formation of inclusion complex in this study depended on the pH medium of aqueous solution, as discussed in Section 4.3.1. Protonation and deprotonation of phenol compounds were unfavourable for the formation of the inclusion complex. Therefore, the proposed mechanism was based on the pH medium of the solution, as shown in Figure 4.13. A similar phenomenon was reported by Huh et al. (2002) in the study of inclusion complex in β-CD.

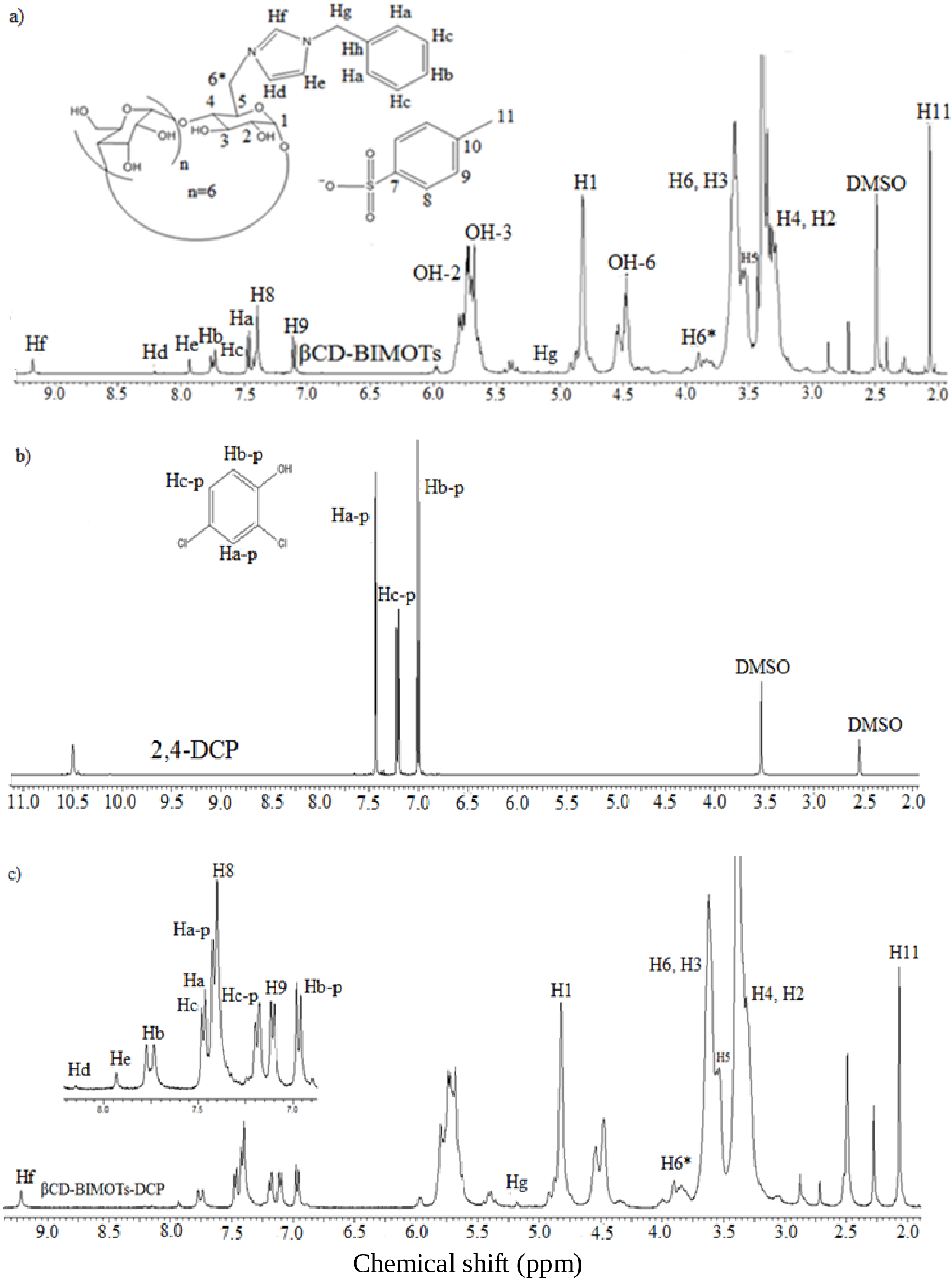

Figure 4.11: ^{1}H NMR spectrum of a) βCD-BIMOTs, b) 2,4-DCP and c) βCD-BIMOTs-DCP.

Table 4.5: Chemical shift (§) of βCD-BIMOTs, 2,4-DCP, and βCD-BIMOTs-DCP

	βCD-BIMOTs (§)	2,4-DCP (§)	β-CD-βCD-BIMOTs-DCP (§)	Δ§
H1	4.8330		4.8345	+0.0015
H2	3.3030		3.3102	+0.0072
H3	3.5450		3.6231	**+0.0781**
H4	3.3268		3.3239	-0.0029
H5	3.3980		3.5567	**+0.1587**
H6	3.6298		3.6359	-0.0061
H8	7.4175		7.4138	-0.0037
H9	7.1269		7.1135	-0.0134
H11	2.0868		2.0834	+0.0034
Ha	7.4597		7.4829	+0.0232
Hb	7.7450		7.7454	+0.0004
Hc	7.4914		7.4957	+0.0043
Hd	8.2100		8.1502	-0.0598
He	7.9458		7.9480	+0.0026
Hf	9.2031		9.2226	+0.0195
Hg	5.1880		5.2032	+0.0152
Ha-p		7.4334	7.4300	-0.0034
Hb-p		7.0258	6.9765	**-0.0493**
Hc-p		7.2095	7.1135	**-0.0960**

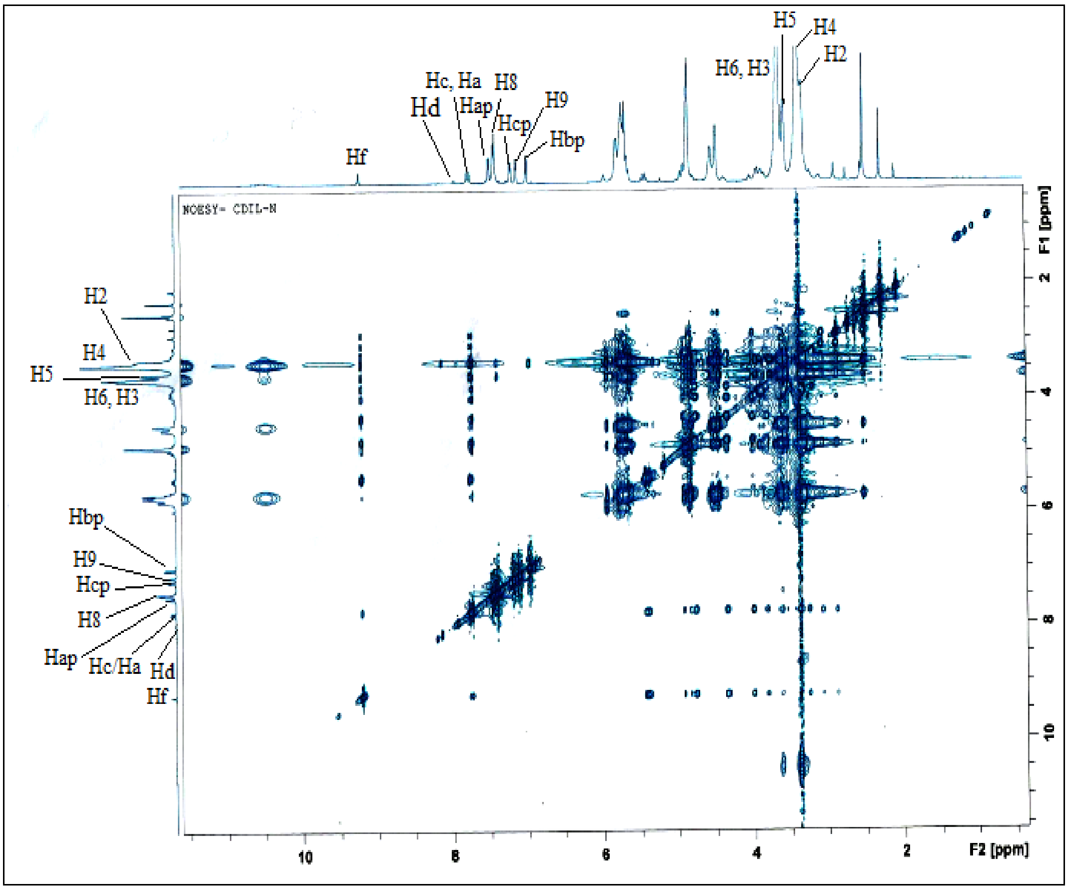

Figure 4.12: The two-dimensional NOESY spectrum of βCD-BIMOTs-DCP complex in DMSO-D_6

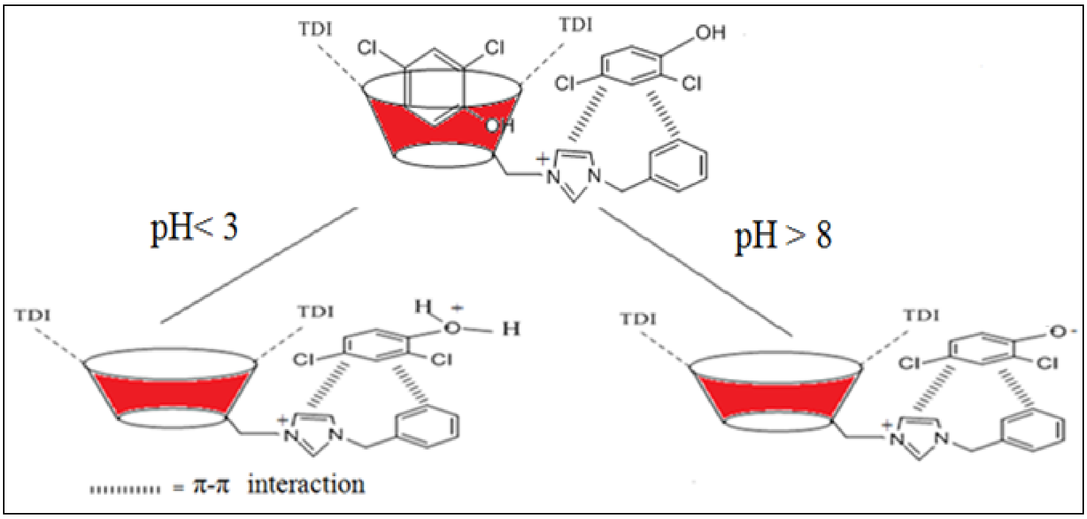

Figure 4.13: Schematic illustration of the pH-dependent adsorption/complexation of 2,4-DCP with βCD-BIMOTs-TDI

4.4 Conclusion

In the present investigation, cyclodextrin functionalized ionic liquid polymer (βCD-BIMOTs-TDI) was successfully evaluated as an adsorbent for adsorption of 2,4-DCP, 2,4,6-TCP, and 2,4-DNP from an aqueous solution. The optimum removal was observed at pH 6 for the adsorption of 2,4-DCP and 2,4,6-TCP, while pH 4 was selected for the adsorption of 2,4-DNP. Kinetic analysis showed that the pseudo second order equation provided better correlation for the adsorption of 2,4-DCP, 2,4,6-TCP, and 2,4-DNP with correlation coefficient (R^2) values that ranged from 0.9996-1 for the adsorption data with 120 min being the equilibrium time. Based on the obtained results, the adsorption process on βCD-BIMOTs-TDI was in the order of 2,4-DNP > 2,4,6-TCP > 2,4-DCP. Meanwhile, both film and intraparticle diffusion simultaneously occurred during the adsorption process of 2,4-DCP, 2,4,6-TCP, and 2,4-DNP onto βCD-BIMOTs-TDI, but they were not rated as determining step. The Langmuir, Freundlich, Temkin, and Dubinin-Radushkevich's isotherm models were used to study the sorption phenomena, and Freundlich's isotherm fitted well with this adsorption process ($R^2>0.97$ for all studied temperature) for the adsorption of 2,4-DCP and 2,4,6-TCP. In comparison, Langmuir's model was found to fit well with the adsorption of 2,4-DNP on βCD-BIMOTs-TDI. Meanwhile, the negative value of ΔH° (-18.10) indicated that the adsorption process of 2,4-DCP was exothermic, while the positive values of ΔH° (40.27 and 2.38) indicated that the adsorption process of 2,4,6-TCP and 2,4-DNP were endothermic. Eventually, the adsorption mechanism was proposed by considering inclusion complex and π-π interaction between βCD-BIMOTs with 2,4-DCP in a pH medium.

CHAPTER 5

RESULTS AND DISCUSSION

Part 3: The application of βCD-BIMOTs-TDI as an adsorbent for SPE with phenols

5.1 Introduction

Sample pre-treatment is very important and it is a laborious step in chemical analysis, especially when dealing with environment sample, due to the complex matrices of environment samples and extremely low concentration of the contaminants. Thus, the most common and conventional technique for the analysis of environmental samples is the solid phase extraction (SPE), which is a widely used technique for environmental sample pre-treatment due to its high recoveries, short extraction time, high enrichment factor, low consumption of organic solvent, and ease of automation (Rodriguez-Mozaz et al., 2007).

In this work, a new SPE method was demonstrated using βCD-BIMOTs-TDI polymer as an adsorbent. Due to high toxicity and the widespread of environmental occurrences, phenols were selected as model analytes in this study (Elci et al., 2011; Mussmann et al., 1994; Padilla-Sánchez et al., 2011). Even though many works have been published on the development of new SPE sorbent for extraction of phenols (El-Sheikh et al., 2010; Feng et al., 2009; Liu et al., 2011c; Qi et al., 2010), this is the first study to report on the application of βCD-BIMOTs-TDI as an adsorbent in SPE for the determination of phenols.

5.2 Experimental

5.2.1 Standard, reagents, and chemicals

The preparation steps of βCD-BIMOTs-TDI and βCD-TDI have been clearly mentioned in Section 3.2.3. Thus, these materials were selected as adsorbents for SPE for extraction of phenols. 2-chlorophenol (2-CP), 2-nitrophenol (2-NP), 2,4-dichlorophenol (DCP), 4-chlorophenol (4-CP), 4-chloro-3-methylphenol (4-CMP), and 2,4,6-Trichlorophenol (TCP) were purchased from Sigma Aldrich (Steinheim, Germany) (Fig. 1). All the solvents and chemicals used were of analytical and chromatographic grades, respectively. They were used as received. Double distilled water was used throughout the study. Chromabond C-18 sorbent, spherical hydrophobic polystyrene-divinylbenzene adsorbent resin (HR-X), and polystyrene-divinylbenzene adsorbent resin (HR-P) were purchased from Macherey-Nagel (Duren, Germany). HPLC grade of solvents were purchased from Fisher Scientific (Leicestershire, UK). The standard stock solutions of phenols (1000 mg/L) were prepared in methanol and were stored in a dark amber glass at 4 °C to prevent degradation. The working solution was freshly prepared by diluting the stock solutions with water.

5.2.2 Solid phase extraction (SPE)

5.2.2.1 GC-FID analysis

Agilent 7890A GC system with an Agilent 5975C Series GC/FID from Agilent Technologies Inc. (Santa Clara, CA, USA) was used to analyse the phenols. HP-5MS GC column (30m x 0.32 mm i.d. and 0.25µm film thickness) was used. Helium, as a carrier gas, was used at a flow rate of 1.0 mL min-1.

5.2.2.2 Chromatographic conditions

Both the injection port and detector temperatures were set at 260 °C. The gas chromatography temperature profile was set at 35-220 °C, starting at 35 °C (held for 1 min) and was ramped at 35°C min^{-1}- 220°C min^{-1} (held for 8 min). The sample (1 µL) was injected manually into the injection port under splitless mode.

5.2.2.3 SPE procedure

βCD-BIMOTs-TDI (100 mg) was placed in a 3 mL SPE polypropylene cartridge using upper and lower frits to avoid adsorbent loss. 12-port SPE vacuum manifold from Thermo Fischer Scientific (Waltham, MA, USA) was used to place the filled SPE cartridge (Figure 5.1). Prior to extraction, the cartridges were conditioned by passing 5 mL of methanol and 5 mL of water, respectively. 15 mL of spiked sample (5 mg/L of each phenol at pH 6) was passed through the cartridge at a flow rate of 0.5 mL min^{-1} for optimization process and concentration was determined using calibration curve (0.2 mg/L to 10 mg/L). The prepared sorbent material in the cartridge was not allowed to dry at any moment. After the sample loading procedure, the SPE cartridge was then dried by passing air for 30 min. The retained phenols were then eluted from the adsorbent with 2 ml of methanol, and finally, injected to GC-FID for analysis. Seven parameters were studied to perform better extractions:

a) Effect of sample pH

The samples’ pH was studied from 3 to 10. The desired pH was adjusted with 0.01 M HCL and 0.01 M NaOH using pH meter (Model Ella Instrument). The extraction procedures were similar to those mentioned in Section 5.2.2.3.

b) Effect of sample volume

The sample volume was studied from 1mL to 75 mL of spike sample at 5 mg/L of each phenol compound at pH 6. The extraction procedures were similar to those mentioned in Section 5.2.2.3.

c) Effect of eluting solvent

Various different solvents were used as eluting solvents, such as methanol, dichloromethane, hexane, ethanol, acetonitrile, ethyl acetate, and acetone. The extraction procedures were similar to those mentioned in Section 5.2.2.3.

d) Effect of elution volume

Different volumes of elution were studied from 2 mL to 20 mL. The extraction procedures were similar to those mentioned in Section 5.2.2.3.

e) Effect of washing

Effect of washing was studied with 0.2 mL to 1 mL of hexane. The extraction procedures were similar to those mentioned in Section 5.2.2.3.

f) Effect of drying

Effect of drying was done similar to the procedures mentioned in Section 5.2.2.3 without the washing step.

g) Effect of modifier

Effect of modifier was studied with the addition of 1% to 20% of acetic acid in the 2 mL of methanol during elution step. The extraction procedures were similar to those mentioned in Section 5.2.2.3.

For comparison purpose, the βCD-TDI SPE, C-18 SPE, HR-X SPE, and HR-P SPE were packed in 3 mL cartridges for extraction and a similar procedure as the βCD-BIMOTs-TDI SPE was followed. The percentage of recovery (% R) during optimization process was calculated by using the following formula (Ariffin & Anderson, 2006):

$$\% \mathrm{R} = \left(\frac{\mathrm{C_{a}, final}}{\mathrm{C_{s}, initial}} \right) \times 100\% \qquad (5.1)$$

where:

C_a, final = the final concentration of analyte in the acceptor phase

C_s, initial = the initial analyte concentration in the sample

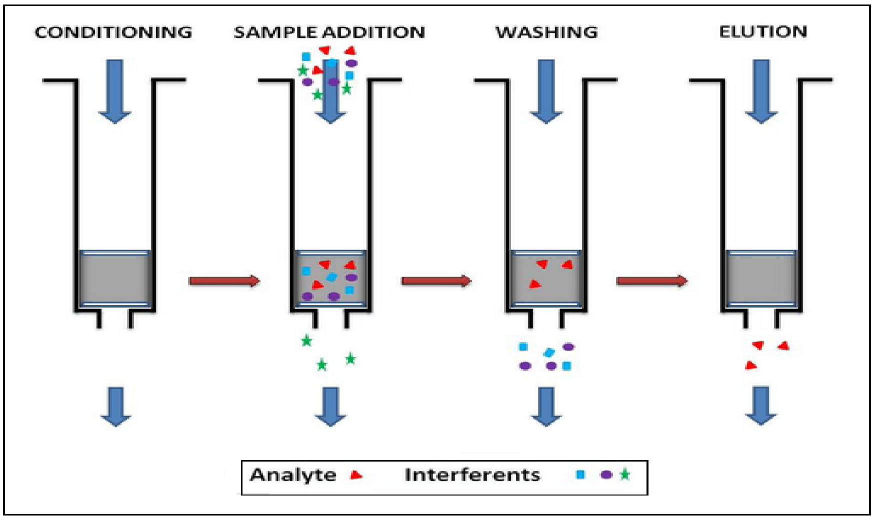

Figure 5.1: Schematic diagram of SPE procedure

5.2.3 Real sample analysis

5.2.3.1 Determination of phenols in real samples

Tap water samples were collected from a water tap in the lab (Universiti Malaya). Meanwhile, river water samples were collected in glass bottles from Taman Jaya, Petaling Jaya, Kuala Lumpur, Malaysia. The collected samples were filtered using 0.45 µm Millipore cellulose membrane, right after sampling. The pre-cleaned bottles were covered with aluminium and stored in the dark at 4°C prior to analysis.

5.2.3.2 Spike sample

Besides, in order to access matrix effects, 0.5 mg/L and 1 mg/L of phenols were spiked to the river and tap water and their concentrations were determined by SPE (calibration range from 0.2 mg/L to 10 mg/L) using βCD-BIMOTs-TDI adsorbent. The concentration of the phenols was obtained from the peak area of each analytes and was substituted into the calibration equation to obtain the concentration.

5.2.4 Method validation

5.2.4.1 Linearity and Precision

Linear range calibration curves were plot in the range of 0.01 µg/L to 6.00 µg/L, with correlation coefficients (R^2) ranging from 0.9904-0.9978. The repeatability to find the precision of the developed method was evaluated by three injections of spiked DI water with 0.1 µg/L of each phenol was performed and expressed as relative standard deviation (RSD, %). Standard deviation (SD) and RSD, % were calculated using the following formula:

$$SD = \sqrt{\frac{\sum\left(x - \bar{x}\right)^2}{n-1}} \tag{5.2}$$

$$RSD = \frac{SD}{\bar{x}} \times 100\% \tag{5.3}$$

where $\bar{x}$ represents mean, x is the result of every run, and n is the number of measurements (repeatability).

5.2.4.2 Limit of detection (LOD) and Limit of quantification (LOQ)

The limits of detection and quantification were determined from the SD of blank response (σ) and its slope (S) from the linear range curve using Eqs. 5.4 and 5.5 (Shrivastava & Gupta, 2011) :

$$\mathrm{LOD} = 3(\sigma/S) \tag{5.4}$$

$$\mathrm{LOQ} = 10(\sigma/S) \tag{5.5}$$

The detection limits can be defined as the lower concentration of the interested compound, which could be detected by GC-FID and should be lower than the maximum residue limits (MRL) in real samples. Meanwhile, the LOQ were considered as the lowest recovery with acceptable results.

5.2.4.3 Recovery

The percentage of recoveries (% R) for real sample was calculated by using the following equation:

$$\%\,\mathrm{R} = \frac{\text{Concentration of spike sample – concentration unspike sample}}{\text{Concentration of spike added}} \times 100 \tag{5.6}$$

5.3 Results and discussion

5.3.1 SPE optimization

5.3.1.1 Sample pH

The extraction of phenols depends on the pH value of the sample solution because it is presented in different states according to different pH medium (Yang et al., 2011). Moreover, as the solubility of the acidic/basic target analytes is affected together with dissociation equilibrium, an adjustment of the pH will enhance the extraction process (Miskam et al., 2014). Therefore, in this study, the effect of sample pH on the recoveries was investigated in the range of 3 to 10, as shown in Figure 5.2. The obtained result illustrated that the sample pH greatly affected the adsorption of all the phenols on βCD-BIMOTs-TDI within the examined pH ranges. The best result was observed at pH 6, with recoveries of 80%, 43%, 88%, 75%, 84%, and 57% for 2-CP, 2-NP, DCP, 4-CP, 4-CMP, and TCP, respectively, and therefore, pH 6 medium was selected for the other extraction processes in this work.

The obtained results can be explained by using the adsorption mechanism, which is dominated by the inclusion complex, hydrogen bonding, and Van Der Waals force (Li et al., 2012b). Furthermore, all the studied phenols are found to be neutral at pH 6 and able to form inclusion complexes with hydrophobic cavity of CD (Leyva et al., 2001a). Thus, in this study, the inclusion complex formation could be the main interaction since the cavity of β-CD was maintained during the polymerization process apart from other interactions.

Apart from that, low and high pH medium were unsuitable for the extraction process in this study because at low pH medium, the phenols were in protonated form, meanwhile, at high pH medium, they were in deprotonated form. It is well known that hydrophilic guest (protonated or deprotonated) would not be able to form inclusion complex with CD (Li et al., 2012b), thus, neutral pH medium was the most suitable, even though strong π-π interaction between imidazolium ring of the IL and the phenol molecules was present at both high and low pH medium. Furthermore, chlorophenols and nitrophenols were found to be ionisable when pH>pKa (the pka values are listed in Table 3.2). Therefore, pH 6 was the best condition for this extraction process.

In addition, such results can be explained in accordance with the anion-exchange mechanism of phases based on benzyl imidazolium tosylate functionalized on β-CD. The ionization of the analytes were suppressed, minimizing the ionic interaction at low pH medium, while at high pH, the phenols compounds were fully negatively charged, and this favoured their interaction with the positively charged IL. However, due to high concentration of hydroxyl groups, which competed with the phenol molecules, there were lower adsorption and recoveries of phenols on βCD-BIMOTs-TDI (Yang et al., 2011). Therefore, the recoveries were also in accordance with the ability of anion-exchange, and therefore, pH 6 medium was used for the entire extraction process.

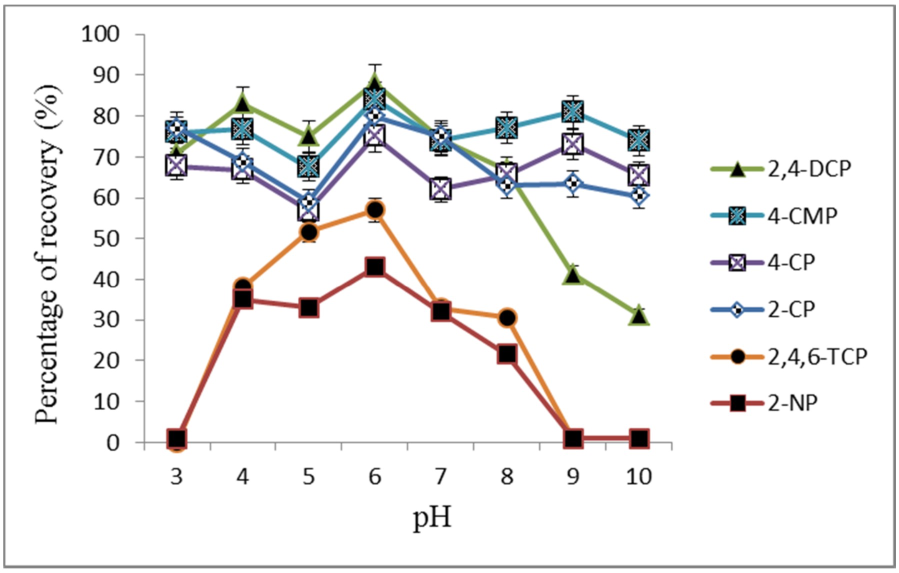

Figure 5.2: Effect of sample pH of analytes mixture on the recovery of phenols. Extraction condition: 5 mL methanol + 5 mL water as conditioning solvent, 10 mL sample loading volume, and 2 ml of methanol as elution solvent.

5.3.1.2 Sample loading volume

The optimization process was carried out in order to investigate the effect of sample volume, as the cartridge was loaded with 1-75 mL aqueous solution of phenols. Basically, for SPE satisfactory, the recoveries should obtain high sensitivity and enrichment factor. Thus, it was necessary to determine the breakthrough volume. As shown in Figure 5.3, the recoveries were increased as the sample volume increased, but optimum percentage of recovery was observed at 15 mL of sample volume. Therefore, 15 mL of sample volume was regarded as the breakthrough volume. The recoveries were low at low sample volume due to the limited phenols aqueous medium to adsorb the βCD-BIMOTs-TDI, while at high sample volume, the recoveries were also low due to the fact that in the presence of larger amounts of solvent, it would result in less interaction between the phenols and βCD-

BIMOTs-TDI, and hence, resulted in lower adsorption and recoveries (Yang et al., 2011). In addition, low recoveries at high sample volume could be also due to the sorbent breakthrough that was exceeded (Miskam et al., 2014). As a result, on the basis of optimization, a sample volume of 15 mL was selected as the optimal sample volume for this extraction process.

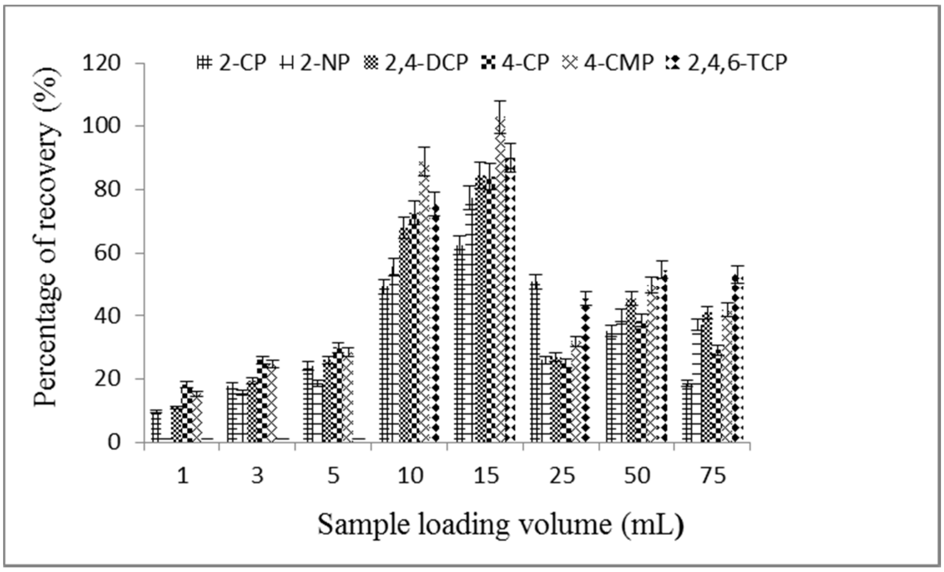

Figure 5.3: Effect of different sample loading volume on recovery of phenols. Extraction condition: 5 mL methanol + 5 mL water as conditioning solvent, sample at pH = 6, and 2 ml of methanol as elution solvent.

5.3.1.3 Elution step

In SPE, the eluting step is very important in order to desorb the retained phenols on βCD-BIMOTs-TDI with a suitable solvent. In this study, seven eluting solvents of different polarities, namely methanol, dichloromethane, hexane, ethanol, acetonitrile, ethyl acetate, and acetone, were investigated to identify the best eluting solvent. Strong elution solvents are able to displace all the analytes from the sorbent in a small volume (Poole et al., 2000). So, polar solvents, such as methanol, acetonitrile, ethanol, and acetone, were the best candidates, as the solvent strengths were higher compared to non polar solvents (dichloromethane, hexane, and ethyl acetate). As shown in Figure 5.4, hexane showed poor eluting capability towards all the studied phenols and it indicated the strong affinity of phenols towards βCD-BIMOTs-TDI. As shown in Figure 5.4, higher extraction recovery was achieved with methanol for all the studied phenols in the range of 76-113% compared to other solvents. This had been due to the properties of the methanol, which is a protic solvent and is able to elute polar phenols that may have hydrogen bonding with the hydroxyl/carboxyl groups on the βCD-BIMOTs-TDI surface more effectively than aprotic solvent, such as acetonitrile (Liu et al., 2011b). Therefore, methanol was the most effective eluent as it gave the highest recoveries for all the studied phenols.

The eluent volume was optimized from 2-20 mL; the efficient elution could only be achieved with no less than 2 mL of methanol (Figure 5.5). The recoveries for all the phenols decreased as the eluent volume increased as the samples were diluted. Thus, 2 mL of methanol was used as eluent solvent for the extraction of the phenols.

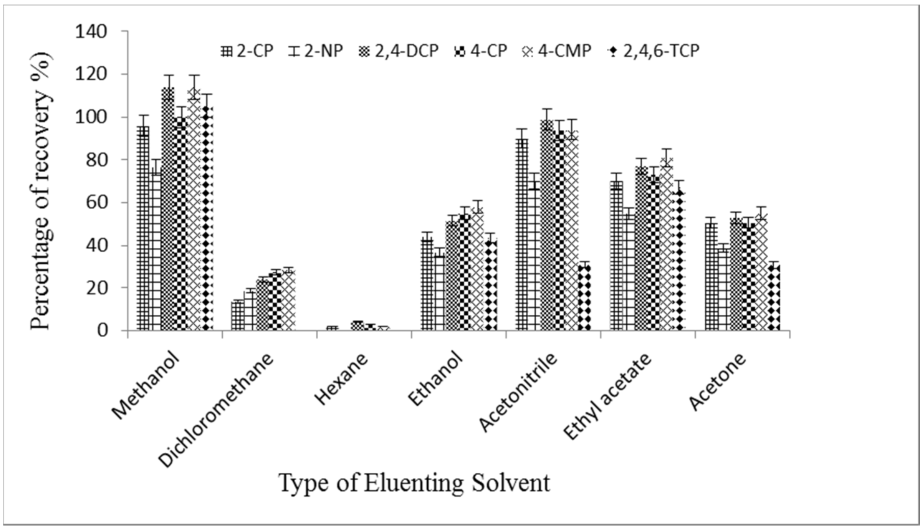

Figure 5.4: Effect of eluting solvent on recovery of phenols. Extraction condition: 5 mL methanol containing 5 mL water as conditioning solvent, sample at pH = 6, and 2 ml of methanol as elution solvent.

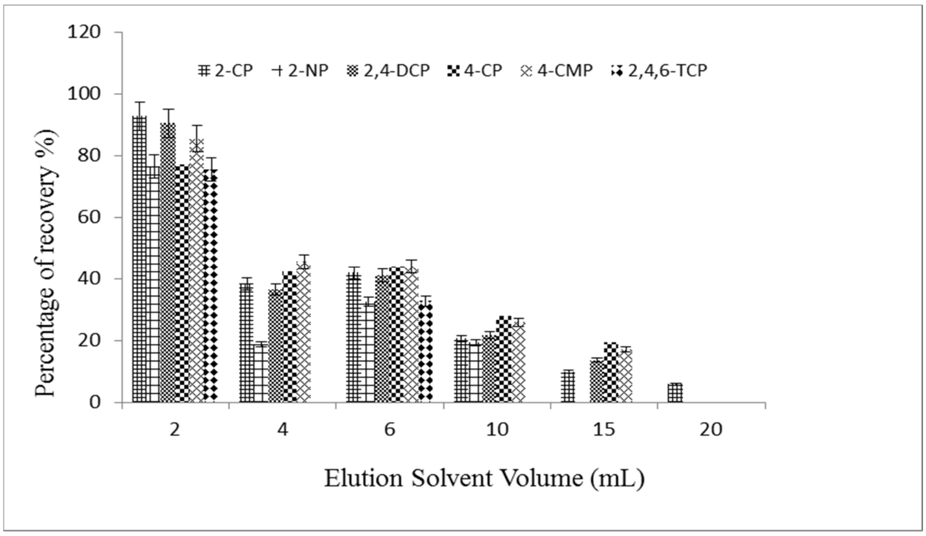

Figure 5.5: Volume of eluting solvent on recovery of phenols. Extraction condition: 5 mL methanol containing 5 mL water as conditioning solvent, sample at pH = 6, and 2 ml of methanol as elution solvent.

5.3.1.4 Washing step

The βCD-BIMOTs-TDI sorbent was rinsed with hexane, after the sample was loaded into the cartridges since hexane had poor eluting capability of phenols from βCD-BIMOTs-TDI sorbent, and therefore, it was used as a washing solvent in order to identify if the washing step increased the recovery of the retained phenols, and to displace any undesired matrices without displacing the analyte of interest. Furthermore, the collected washing solvent was also analysed with the GC-FID and the results indicated that the hexane solution did not elute the phenols effectively from the cartridge. Therefore, hexane was used as a washing solvent in this study since it was a weak solvent and could not displace the phenols during the extraction process (Wan Ibrahim et al., 2012).

As shown in Figure 5.6, the volume of hexane was optimized from 0.2 mL to 1 mL, and the results showed that washing with 0.2 mL of hexane yielded higher percentage of recovery. Meanwhile, the drying step was introduced prior to the elution step to replace the washing solvent since the drying step reduced the volume of the solvent that retained in the sorbent after the sample loading step. Thus, the sorbent was allowed to dry with air for 30 min, which was considerably sufficient to remove the entire sample solvent, which might be trapped in the sorbent pores. As expected, the extraction recoveries for all the studied phenols had been higher compared to the washed sorbent with solvents. Therefore, the 30 minute of drying step was used throughout the subsequent analysis.

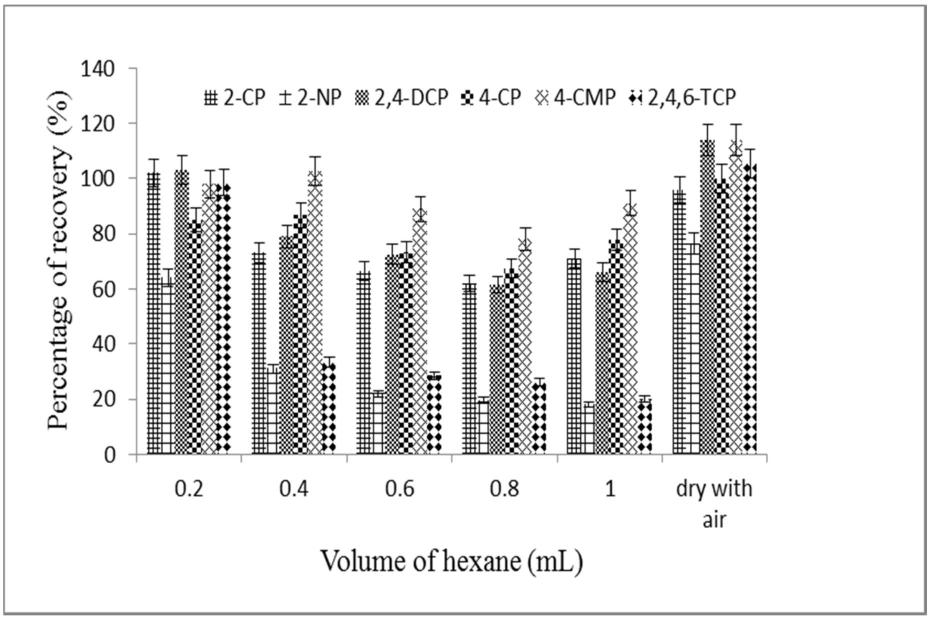

Figure 5.6: Effect of washing on the recovery of phenols. Extraction condition: 5 mL methanol + 5 mL water as conditioning solvent, sample at pH = 6, and 2 ml of methanol as elution solvent.

5.3.1.5 Effect of modifier

A study on the effect of modifier was carried out in order to identify if it increased the extraction recoveries of the retained phenols on βCD-BIMOTs-TDI, especially 2-nitrophenol (2-NP). Thus, the effect of modifier was looked into with the addition of 1% to 20% of acetic acid in 2 mL of elution solvent (methanol). The obtained result is shown in Figure 5.7, whereby 1% of acetic acid gave the highest extraction recovery for all the studied phenols. In addition, a significant difference could be observed from Figure 5.8, whereby a comparison was done with and without the addition of 1% of acetic acid in the 2 mL of eluent solvent (methanol). The significant result could be seen, especially in the extraction recovery of 2-NP, which was increased up to 114 %. Therefore, the addition of acetic acid in the eluent solvent as a modifier played an important role in desorbing phenols from the βCD-BIMOTs-TDI. This is because, acetic acid would compete with the phenols for the functional groups in the binding sites, but too much of acetic acid would not benefit the elution step (Feng et al., 2009). The complete elution of the analytes also guaranteed the reusability of this SPE cartridge. Thus, between the extraction processes, the cartridges were washed with methanol containing 1% of acetic acid and water to ensure that the cartridges could be made available immediately for the next extraction.

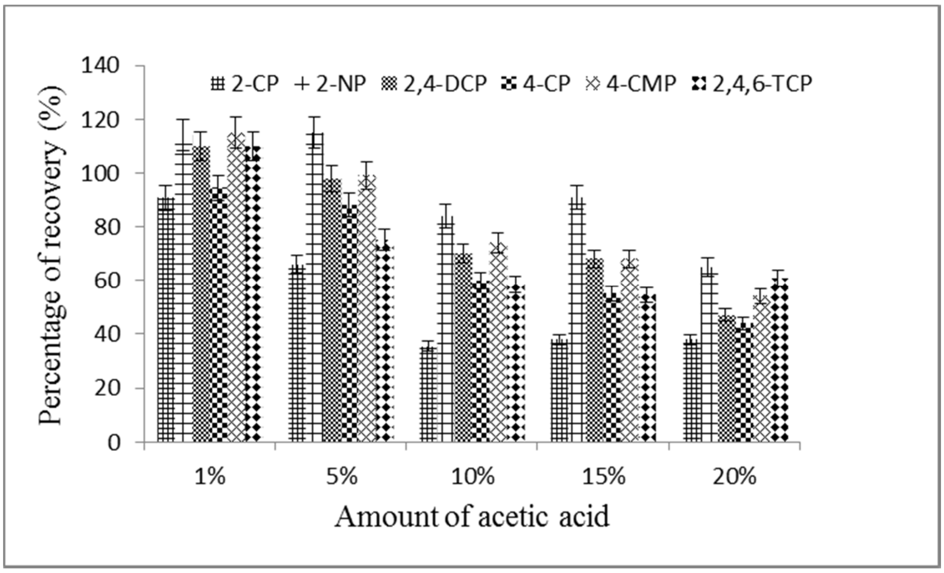

Figure 5.7: Effect of modifier on recovery of phenols. Extraction condition: 5 mL methanol + 5 mL water as conditioning solvent, sample at pH = 6, and 2 ml of methanol as elution solvent.

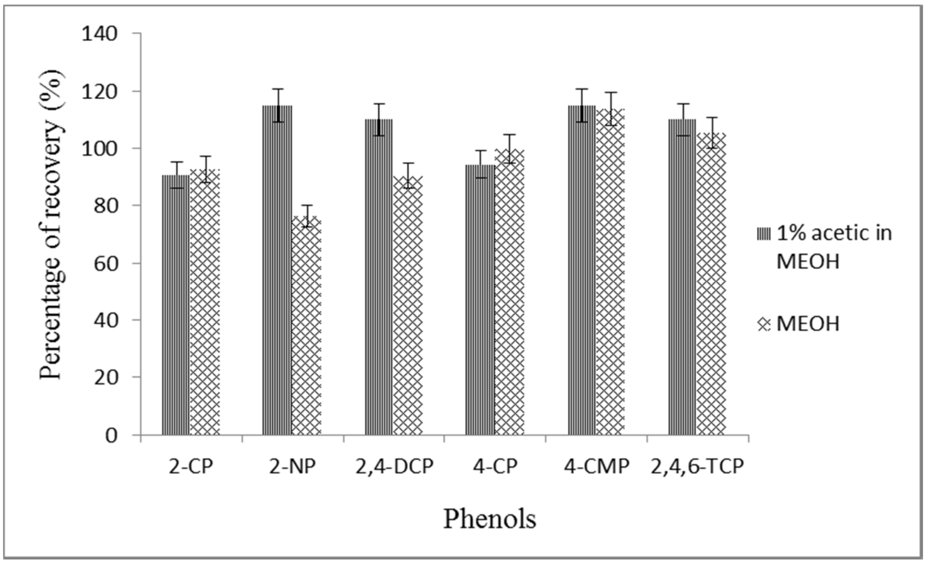

Figure 5.8: Effect of modifier on recovery of phenols. Extraction condition: 5 mL methanol + 5 mL water as conditioning solvent, sample at pH = 6, and 2 ml of methanol as a elution solvent.

5.3.2 Comparison with other adsorbents

For the purpose of comparison, the SPE performance of βCD-BIMOTs-TDI adsorbent with unmodified βCD-TDI and some commonly available adsorbent materials, such as C-18 silica, spherical hydrophobic polystyrene-divinylbenzene adsorbent resin (HR-X) (spherical particles 85 µm, pore size 55-60 Å, surface area 1000 m^2/g), and polystyrene-divinylbenzene adsorbent resin (HR-P) (specific surface 1200 m^2/g, particle size 50-100 µm), were evaluated. In order to conduct these comparisons, the same amounts (100 mg) of different adsorbents were packed in 3 mL SPE cartridges. Optimization of extraction condition was carried out for βCD-TDI, C18 silica, HR-P, and HR-X adsorbents. The optimized condition was applied to extract the phenols using SPE, and the results are shown in Figure 5.9. The obtained results showed that the βCD-BIMOTs-TDI sorbent yielded the highest recoveries (103-114%) of phenols among these studied sorbents. This result definitely justified the worth of βCD-BIMOTs-TDI as an SPE adsorbent.

The recovery of HR-X was also higher among all the studied phenols, which were in the ranges of 60.6-115%. Notably, no phenols was found in the washing solutions for HR-X, indicating that HR-X had good sorption capacity for the phenols, but lower recoveries were obtained compared to βCD-BIMOTs-TDI sorbent due to too stable adsorption and strong affinity of phenols towards the HR-X adsorbent.

The extraction process was easier to be conducted with C18 silica compared to βCD-BIMOTs-TDI adsorbent, but the adsorption was poorer. Phenols could be detected in the washing solution after the phenols were loaded on the C18 cartridge, indicating that 100 mg of the C18 silica had been insufficient for the retention of phenols, especially for 2-CP, 2-NP, and 4-CP, as their recoveries were too low (25%, 38% and 29%) compared to TCP, CMP, and DCP that showed that C18 silica had poor sorption capacity for polar compounds. Higher sorption capacities of C18 towards TCP, CMP, and DCP were observed due to the increase in the number of chloro substituent, which further increased the hydrophobicity (Saitoh et al., 2002). Thus, the obtained results of the present study clearly indicated that the hydrophobic interaction was predominant between C18 silica and the phenols. Hence, in order to increase the adsorption capacity with C18 silica, the mass of the adsorbent must be increased, but it would increase the cost of the analysis and it was unfavourable for instrument miniaturization, and meanwhile, the performance of HR-P was even poorer than C18 silica, as this could be due to the shortage of sorption capacity.

The performance of βCD-TDI sorbent was tested in order to investigate the effectiveness of modified βCD-BIMOTs-TDI. The extraction recoveries were low (32%-57%) for the βCD-TDI adsorbent. The presence of IL ring in the βCD-BIMOTs-TDI enhanced the selectivity of the phenols towards the βCD cavity compared to the unmodified βCD-TDI. Since strong π-π interaction and inclusion complex formation were the main interactions between the βCD-BIMOTs-TDI and the phenols, especially in the βCD-TDI sorbent, only weak inclusion interaction was present between the adsorbent and the analyte. Thus, the extraction recovery was low for the βCD-TDI compared to βCD-BIMOTs-TDI. Apart from that, complete elution of phenols from βCD-BIMOTs-TDI adsorbent was achieved due to its unique surface morphology and chemical structure compared to other adsorbents. These hydrophilic groups enhanced the water-wettability of βCD-BIMOTs-TDI and the retention and elution of polar compounds (phenols). Besides, phenols also can readily access the macropores on the surfaces of βCD-BIMOTs-TDI and favour the adsorption and elution process during SPE. This unique characteristic makes βCD-BIMOTs-TDI a powerful adsorbent material for the extraction of phenols.

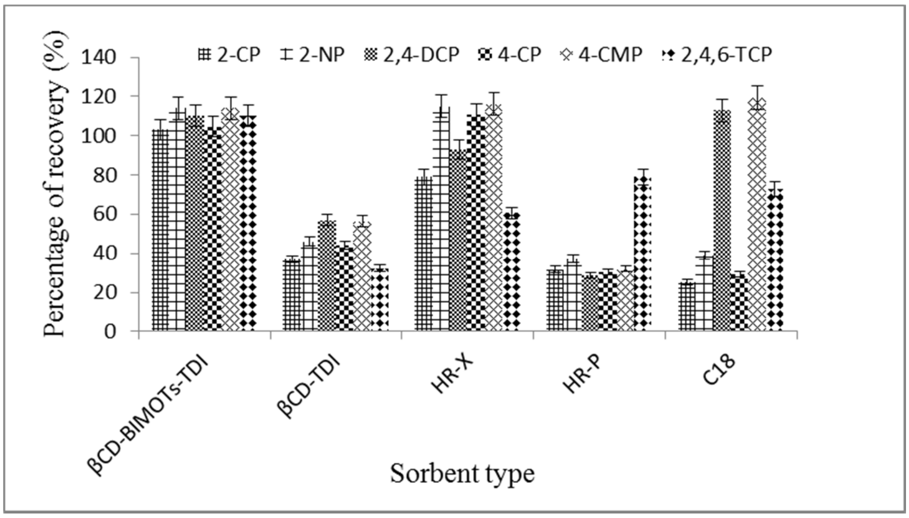

Figure 5.9: Comparison of the performance of βCD-BIMOTs-TDI with other adsorbents (βCD-TDI, HR-X, HR-P and C-18) for the SPE of six phenols. The SPE cartridges were packed with 100 mg adsorbent in all cases. Extraction condition: 5 mL methanol + 5 mL water as conditioning solvent, 15 mL of sample solution at pH 6 containing 5 mg/L of each phenol, and 2 mL methanol containing 1% of acetic acid as eluent solvent.

5.3.3 Analytical performance of the proposed method

The optimized parameters for the extraction of phenols using βCD-BIMOTs-TDI were sampled at pH 6, 5 mL methanol + 5 mL water as conditioning solvent, 15 mL sample loading volume, and 2 mL of methanol containing 1% of acetic acid as the elution solvent prior to the GC-FID analysis. A series of experiments were designed to obtain linear ranges, precision, detection limits, and other characteristics of the developed method. Good linearity with correlation coefficient (R^2) ranging from 0.9904-0.9978 was obtained for this method and the results are tabulated in Table 5.1. Based on a signal-to-noise ratio of 3, the LODs were in the range of 0.23-0.35 µg/L, while the signal-to-noise ratio of 10 and the LOQs were in the range of 0.70-1.18 µg/L. The obtained LOD value in this study had been below the legal tolerance level for each phenol in drinking water (0.5 µg/L), according to the European Community Directive, and Japanese Ministry of Health, Labour and Welfare, that stated the maximum contaminant level for phenols in drinking water is 5 µg/L. The repeatability was obtained by performing three extractions at the concentration of 0.1 µg/L under optimal conditions with 100 mg of sorbent. The relative standard deviations (RSDs) were in the range of 1.0% to 3.4% respectively, and these excellent results indicated that the developed method was simple, yet provided a sensitive procedure for the determination of phenols at trace levels.

Table 5.1: Analytical performance data of the proposed method

Analyte	Linear range (µg/L)	R^2	LOD (µg/L)	LOQ (µg/L)	RSD (%) (n=3)
2-CP	0.01-6.00	0.9916	0.35	1.18	2.9
2-NP	0.01-5.00	0.9904	0.29	0.97	3.4
DCP	0.01-6.00	0.9916	0.24	0.79	1.3
4-CP	0.02-6.00	0.9917	0.33	1.08	1.8
4-CMP	0.02-6.00	0.9955	0.23	0.70	2.2
TCP	0.02-6.00	0.9978	0.25	0.82	1.0

5.3.3.1 Real water sample analysis

The applicability of the method for phenols was validated using real environmental aqueous samples, which were river water and tap water, with the proposed method. The pH of all the real samples was adjusted to 6 before SPE. None of the target analytes were detected in these water samples under optimized condition described and these samples were then spiked with phenols at a concentration of 0.5 mg/L and 1 mg/L in order to investigate the effect of the sample matrices. As shown in Table 5.2, the recoveries of the spiked phenols in the river and tap water samples were satisfactory, which were between

87%-116%, and RSDs (0.1-1.7%) lower than 5% were achieved. The typical chromatograms of river water samples at the concentration level of 0.5 mg/L and 1 mg/L for phenols are demonstrated in Figure 5.10.

Table 5.2: The recoveries and RSDs of phenols in real environmental samples with a spiked concentration of 0.5 mg/L and 1 mg/L for each analyte.

Analyte	Tap water		River water	
	Concentration added (mg/L)	Recovery (%)/RSDs	Concentration added (mg/L)	Recovery (%)/RSDs
2-CP	0.5	111.7 (0.1)	0.5	101.9 (0.6)
	1	91 (0.2)	1	107.9 (1.1)
2-NP	0.5	116 (0.4)	0.5	116.3 (0.2)
	1	100.8 (0.4)	1	98 (1.1)
DCP	0.5	104 (0.3)	0.5	96 (0.2)
	1	90 (1.1)	1	87 (1.7)
4-CP	0.5	88 (0.1)	0.5	100 (0.2)
	1	100.8 (0.2)	1	98.8 (0.5)
4-CMP	0.5	115.1 (1.3)	0.5	115.2 (0.2)
	1	93 (0.7)	1	91.5 (0.5)
TCP	0.5	99.6 (0.3)	0.5	105.6 (0.4)
	1	104 (0.3)	1	103.7 (0.5)

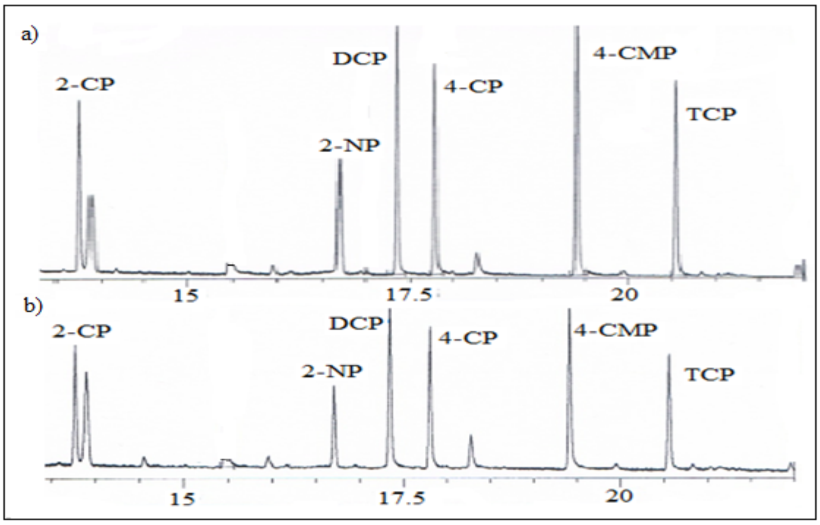

Figure 5.10: Chromatogram obtained from the analysis of river water using βCD-BIMOTs-TDI SPE for phenols (Carrier Helium: 33cm/sec, constant flow, Oven:35 °C for min,

35-220 °C at 8 °C/min: Splitless, 250 °C, FID, 300 °C, and Spiking concentration a) 1 mg/L, and b) 0.5 mg/L.

5.3.3.2 Comparison of the represented method with other methods

The proposed method in this study was compared with the previous study for the determination of phenols in water samples. The analytical methods developed previously are summarized in Table 5.3 for the determination of phenols in water. All of these results from this study indicated that the proposed method was fast, reproducible, and provided a simple technique with low LOD and RSD values with good extraction recoveries.

Table 5.3: Comparison of the represented method with other methods for the determination of phenols

	Determination				
Clean-up	Technique	Recoveries (%)	RSD (%)	LOD (μg/L)	References
SPME (PANI, 50°C, 50 min, NaCl)	GC-FID	69-111	8.0-15.0	0.7-58	(Bagheri et al., 2005)
HS-SPME	GC-FID	94-105	4.0-5.0	14-32	(Portillo et al., 2006)
SPE	CE-CL	79-92	2.0	20-82	(Tsukagoshi et al., 2002)
SPE	GC-MS/SIM	-	6	16-22	(López-Vidal & Arce, 2005)
SPE	FI-Amperometric biosensor	-	2.6-3.8	19-66	(Campuzano et al., 2003)
βCD-BIMOTs-TDI-SPE	**GC-FID**	**87-116**	**0.1-1.7**	**0.23-0.35**	**Current study**

5.4 Conclusion

In this work, the βCD-BIMOTs-TDI was successfully applied as an adsorbent for SPE, coupled with GC-FID, for extraction of six selected phenols in tap and river water samples. The βCD-BIMOTs-TDI-SPE method offered an interesting and effective option for the analysis of phenols in environmental water samples. Higher recoveries were achieved with βCD-BIMOTs-TDI compared to other adsorbents due to its unique morphology and chemical structure. The βCD-BIMOTs-TDI adsorbent also exhibited some advantages, such as high affinity towards phenols, good compatibly with different types of solvents, good repeatability, and no impact on sorbent drying. The performance of βCD-BIMOTs-TDI was successfully applied and compared with several other adsorbents and they exhibited low detection limit (0.23-0.35 µg/L) compared to the other previously reported methods. Thus, it is believed that this adsorbent can be a promising material for SPE.

CHAPTER 6

CONCLUSION AND FUTURE RECOMMENDATIONS

6.1 Conclusion

A new macroporous β-Cyclodextrin functionalized ionic liquid polymer (βCD-BIMOTs-TDI) had been successfully synthesized, characterized, and compared with a native β-Cyclodextrin polymer (βCD-TDI). The βCD-BIMOTs-TDI was characterized using various tools and the results obtained were compared with βCD-TDI. The SEM results showed that the presence of IL increased the pore size, while the BET results showed that the βCD-BIMOTs-TDI had 1.254 m^2/g surface area, and the BJH pore size distribution results revealed that the polymer exhibited macropores with a pore size of 77.66 nm. Meanwhile, βCD-TDI represented micropores with pore size of 1.585 nm and pore volume of 0.02188 cm^3/g. Higher BET surface area was obtained for βCD-TDI (2.401 m^2/g) and the obtained results showed that the surface area of the βCD-BIMOTs-TDI decreased upon the functionalization with IL or after the chemical modification with IL, compared to the native βCD-TDI. Based on the preliminary sorption study, 2,4-dichlorophenol (2,4-DCP), 2,4,6-trichlorophenol (2,4,6-TCP), and 2,4-dinitrophenol (2,4-DNP) with enhanced capacity towards βCD-BIMOTs-TDI were selected for batch adsorption study.

The newly prepared macroporous βCD-BIMOTs-TDI was evaluated as an adsorbent for adsorption of 2,4-DCP, 2,4,6-TCP, and 2,4-DNP from an aqueous solution. The optimum removal was observed at pH 6 for the adsorption of 2,4-DCP and 2,4,6-TCP, while pH 4 was selected for the adsorption of 2,4-DNP. Pseudo second order equation provided better correlation for the adsorption of the studied phenols with R^2 values ranging from 0.9996-1 for the adsorption data with 120 min being the equilibrium time. The Langmuir, Freundlich, Temkin, and Dubinin-Radushkevich's isotherm models were used to study the sorption phenomena and Freundlich's isotherm fitted well with this adsorption process with correlation coefficient (R^2) > 0.97 for all the studied temperature for the adsorption of 2,4-DCP and 2,4,6-TCP. In comparison, Langmuir's model was found to fit well with the adsorption of 2,4-DNP on βCD-BIMOTs-TDI. Besides, the thermodynamics analysis showed that the adsorption process of 2,4-DCP was exothermic, while the positive values of $\Delta H°$ indicated that the adsorption process of 2,4,6-TCP and 2,4-DNP were endothermic. Hence, the adsorption mechanism was proposed by considering inclusion complex and π-π interaction between βCD-BIMOTs-TDI with one selected phenol compound (2,4-DCP). The amount of sorptions (q_e) by 2,4-DCP, 2,4,6-TCP, and 2,4-DNP were compared with various adsorbents at different equilibrium times (q_t). The obtained qe of βCD-BIMOTs-TDI for 2,4-DCP, 2,4,6-TCP, and 2,4-DNP were relatively high and had been comparable with previous works. Therefore, βCD-BIMOTs-TDI can be considered as a promising sorbent for the removal of 2,4-DCP, 2,4,6-TCP, and 2,4-DNP.

βCD-BIMOTs-TDI was further applied as an adsorbent in SPE. A new SPE method was developed with the extraction of six different phenols. Six phenols, as model analytes, were extracted on a βCD-BIMOTs-TDI SPE cartridge, and then, were eluted with 2 mL of methanol containing 1% acetic acid. The optimum experimental condition was 15 mL of sample volume (sample at pH 6) and 2mL of methanol containing 1% acetic acid as an eluent solvent. The eluent concentration was determined by using GC-FID. Under optimized condition, high sensitivity (detection limits 0.23-0.35 µg/L) and good recoveries (87%-116%) were achieved with satisfactory relative standard deviation (RSDs) (0.1-

1.7%). The developed βCD-BIMOTs-TDI-SPE was then compared with native βCD-TDI-SPE and other commercially available adsorbents and the obtained results showed that the βCD-BIMOTs-TDI exhibited higher extraction recovery due to the unique structure and properties. Finally, the βCD-BIMOTs-TDI was applied as an SPE sorbent for phenols determination under optimized condition, in river and tap waters, prior to the GC-FID separation. The obtained result was successfully compared with other reported work from the literature and the comparison showed that the LOD values and percentages of RSD from the present study had been extremely good.

6.2 Future direction

A further study on the properties and application of βCD-BIMOTs-TDI is in need since this polymer exhibits unique morphology and higher adsorption capacity towards organic compounds. Therefore, the application of this polymer should be tried with other organic compounds, which are polar and/or non polar, since it achieved good results with polar and non polar compounds in the present study. Furthermore, it can also be applied as an adsorbent for metal since the presence of IL in the polymer can act as a chelating agent to form complex interaction with metal in order to trap it. The current developed SPE method had been sensitive enough, but the solvent consumption was not economical. Therefore, the application of βCD-BIMOTs-TDI as an adsorbent in microextraction is in need since minimum solvent usage is needed for the extraction process to be more economical.

Reference

Abay, İ., Denizli, A., Bişkin, E., & Salih, B. (2005). Removal and pre-concentration of phenolic species onto β-cyclodextrin modified poly (hydroxyethylmethacrylate–ethyleneglycoldimethacrylate) microbeads. *Chemosphere, 61*(9), 1263-1272.

Aguilera-Herrador, E., Lucena, R., Cárdenas, S., & Valcárcel, M. (2010). The roles of ionic liquids in sorptive microextraction techniques. *TrAC Trends in Analytical Chemistry, 29*(7), 602-616.

Ahmed, G. H. G., Laíño, R. B., Calzón, J. A. G., & García, M. E. D. (2014). Magnetic nanoparticles grafted with β-cyclodextrin for solid-phase extraction of 5-hydroxy-3-indole acetic acid. *Microchimica Acta*, 1-8.

Ahmed, M. J., & Dhedan, S. K. (2012). Equilibrium isotherms and kinetics modeling of methylene blue adsorption on agricultural wastes-based activated carbons. *Fluid Phase Equilibria, 317*, 9-14.

Ahmed, M. J., & Theydan, S. K. (2012). Equilibrium isotherms, kinetics and thermodynamics studies of phenolic compounds adsorption on palm-tree fruit stones. *Ecotoxicology and environmental safety, 84*, 39-45.

Ajnazarova, S., & Kafarov, V. (1985). Metodi optimisatsi eksperimenta v khimicheskoy teknologui. *Vishaia Shkola, Moscow*.

Alahmadi, S. M., Mohamad, S., & Maah, M. J. (2012). Synthesis and characterization of mesoporous silica functionalized with calix [4] arene derivatives. *International Journal of Molecular Sciences, 13*(10), 13726-13736.

Altenor, S., Carene, B., Emmanuel, E., Lambert, J., Ehrhardt, J.-J., & Gaspard, S. (2009). Adsorption studies of methylene blue and phenol onto vetiver roots activated carbon prepared by chemical activation. *Journal of Hazardous Materials, 165*(1), 1029-1039.

Ariffin, M. M., & Anderson, R. A. (2006). LC/MS/MS analysis of quaternary ammonium drugs and herbicides in whole blood. *Journal of Chromatography B, 842*(2), 91-97.

Ashnagar, A., Naseri, N. G., & Khanaki, B. (2007). Study of the β-cyclodextrin imipramine hydrochloride inclusion complex and determination of its stability constant (K) by UV-Visible spectroscopy. *Journal of Chemistry, 4*(4), 550-558.

Asouhidou, D. D., Triantafyllidis, K. S., Lazaridis, N. K., & Matis, K. A. (2009). Adsorption of Remazol Red 3BS from aqueous solutions using APTES- and cyclodextrin- modified HMS-type mesoporous silicas. *Colloids and Surfaces A: Physicochemical and Engineering Aspects, 346*(1–3), 83-90. doi: http://dx.doi.org/10.1016/j.colsurfa.2009.05.029

Badruddoza, A., Tay, A., Tan, P., Hidajat, K., & Uddin, M. (2011). Carboxymethyl-β-cyclodextrin conjugated magnetic nanoparticles as nano-adsorbents for removal of copper ions: synthesis and adsorption studies. *Journal of Hazardous Materials, 185*(2), 1177-1186.

Badruddoza, A. Z. M., Hazel, G. S. S., Hidajat, K., & Uddin, M. S. (2010). Synthesis of carboxymethyl-β-cyclodextrin conjugated magnetic nano-adsorbent for removal of methylene blue. *Colloids and Surfaces A: Physicochemical and Engineering Aspects, 367*(1–3), 85-95. doi: http://dx.doi.org/10.1016/j.colsurfa.2010.06.018

Badruddoza, A. Z. M., Shawon, Z. B. Z., Tay, W. J. D., Hidajat, K., & Uddin, M. S. (2013). Fe_3O_4/cyclodextrin polymer nanocomposites for selective heavy metals removal from industrial wastewater. *Carbohydrate polymers, 91*(1), 322-332. doi: http://dx.doi.org/10.1016/j.carbpol.2012.08.030

Bagheri, H., Mir, A., & Babanezhad, E. (2005). An electropolymerized aniline-based fiber coating for solid phase microextraction of phenols from water. *Analytica chimica acta, 532*(1), 89-95.

Bagheri, H., & Mohammadi, A. (2003). Pyrrole-based conductive polymer as the solid-phase extraction medium for the preconcentration of environmental pollutants in water samples followed by gas chromatography with flame ionization and mass spectrometry detection. *Journal of Chromatography A, 1015*(1), 23-30.

Bagheri, H., Mohammadi, A., & Salemi, A. (2004). On-line trace enrichment of phenolic compounds from water using a pyrrole-based polymer as the solid-phase extraction sorbent coupled with high-performance liquid chromatography. *Analytica chimica acta, 513*(2), 445-449.

Bagheri, H., & Saraji, M. (2001). New polymeric sorbent for the solid-phase extraction of chlorophenols from water samples followed by gas chromatography–electron-capture detection. *Journal of Chromatography A, 910*(1), 87-93.

Bagheri, H., & Saraji, M. (2003). Conductive polymers as new media for solid-phase extraction: isolation of chlorophenols from water sample. *Journal of Chromatography A, 986*(1), 111-119.

Baltazar, Q. Q., Leininger, S. K., & Anderson, J. L. (2008). Binary ionic liquid mixtures as gas chromatography stationary phases for improving the separation selectivity of alcohols and aromatic compounds. *Journal of Chromatography A, 1182*(1), 119-127.

Bender, M. L., & Komiyama, M. (1978). *Cyclodextrin chemistry* (Vol. 820): Springer-Verlag Berlin.

Berbicz, F., Nogueira, A. C., Neto, A. M., Natali, M. R. M., Baesso, M. L., & Matioli, G. (2011). Use of photoacoustic spectroscopy in the characterization of inclusion complexes of benzophenone-3-hydroxypropyl-β-cyclodextrin an ex vivo evaluation of the percutaneous penetration of sunscreen. *European Journal of Pharmaceutics and Biopharmaceutics, 79*(2), 449-457.

Berthod, A., Ruiz-Angel, M., & Carda-Broch, S. (2008). Ionic liquids in separation techniques. *Journal of Chromatography A, 1184*(1), 6-18.

Bhaskar, M., Aruna, P., Ganesh Jeevan, R. J., & Radhakrishnan, G. (2004). β-Cyclodextrin-polyurethane polymer as solid phase extraction material for the analysis of carcinogenic aromatic amines. *Analytica chimica acta, 509*(1), 39-45.

Bhatnagar, A., & Minocha, A. K. (2009). Adsorptive removal of 2,4-dichlorophenol from water utilizing Punica granatum peel waste and stabilization with cement. *Journal of Hazardous Materials, 168*(2–3), 1111-1117. doi: http://dx.doi.org/10.1016/j.jhazmat.2009.02.151

Bhattarai, B., Muruganandham, M., & Suri, R. P. S. (2014). Development of high efficiency silica coated β-cyclodextrin polymeric adsorbent for the removal of emerging contaminants of concern from water. *Journal of Hazardous Materials, 273*(0), 146-154. doi: http://dx.doi.org/10.1016/j.jhazmat.2014.03.044

Bi, W., & Row, K. H. (2010). Comparison of different silica-based imidazolium stationary phases for LC in separation of alkaloids. *Chromatographia, 71*(1-2), 25-30.

Bi, W., Tian, M., & Row, K. H. (2010a). Solid-phase extraction of liquiritin and glycyrrhizin from licorice using porous alkyl-pyridinium polymer sorbent. *Phytochemical Analysis, 21*(5), 496-501.

Bi, W., Tian, M., & Row, K. H. (2010b). Solid-phase extraction of matrine and oxymatrine from Sophora Flavescens Ait using amino-imidazolium polymer. *Journal of Separation Science, 33*(12), 1739-1745.

Borissova, M., Palk, K., & Koel, M. (2008). Micellar electrophoresis using ionic liquids. *Journal of Chromatography A, 1183*(1), 192-195.

Boyd, E. M., Killham, K., & Meharg, A. A. (2001). Toxicity of mono-, di-and tri-chlorophenols to lux marked terrestrial bacteria,Burkholderia species Rasc c2 and Pseudomonas fluorescens. *Chemosphere, 43*(2), 157-166.

Campuzano, S., Serra, B., Pedrero, M. a., Villena, F., & Pingarrón, J. M. (2003). Amperometric flow-injection determination of phenolic compounds at self-assembled monolayer-based tyrosinase biosensors. *Analytica chimica acta, 494*(1), 187-197.

Carmichael, A. J., & Seddon, K. R. (2000). Polarity study of some 1-alkyl-3-methylimidazolium ambient-temperature ionic liquids with the solvatochromic dye, Nile Red. *Journal of Physical Organic Chemistry, 13*(10), 591-595.

Cassano, A., Tasselli, F., Conidi, C., Drioli, E., Timpone, R., D'Avella, M., . . . Corleone, V. (2013). PAN hollow fibre membranes with triacetyl-β-cyclodextrin for the removal of pesticides from citrus essential oils. *Separation and Purification Technology, 116*(0), 124-130. doi: http://dx.doi.org/10.1016/j.seppur.2013.05.029

Castro López, M. d. M., Perez, C., Dopico García, M. S., López Vilariño, J. M., González Rodríguez, M. V., & Barral Losada, L. F. (2012). Preparation, evaluation and characterization of quercetin-molecularly imprinted polymer for preconcentration and clean-up of catechins. *Analytica chimica acta, 721*, 68-78.

Celebioglu, A., Demirci, S., & Uyar, T. (2014). Cyclodextrin-grafted electrospun cellulose acetate nanofibers via "Click" reaction for removal of phenanthrene. *Applied Surface Science, 305*(0), 581-588. doi: http://dx.doi.org/10.1016/j.apsusc.2014.03.138

Chadha, R., Bala, M., Arora, P., Jain, D., Pissurlenkar, R. R., & Coutinho, E. C. (2014). Valsartan inclusion by methyl-β-cyclodextrin: Thermodynamics, molecular modelling, Tween 80 effect and evaluation. *Carbohydrate polymers, 103*, 300-309.

Chai, K., & Ji, H. (2012). Dual functional adsorption of benzoic acid from wastewater by biological-based chitosan grafted β-cyclodextrin. *Chemical Engineering Journal, 203*, 309-318.

Chen, L., Berry, R. M., & Tam, K. C. (2014). Synthesis of β-Cyclodextrin-Modified Cellulose Nanocrystals (CNCs)@Fe3O4@SiO2 Superparamagnetic Nanorods. *ACS Sustainable Chemistry & Engineering, 2*(4), 951-958. doi: 10.1021/sc400540f

Chen, M.-L., Zhao, Y.-N., Zhang, D.-W., Tian, Y., & Wang, J.-H. (2010). The immobilization of hydrophilic ionic liquid for Cr (VI) retention and chromium speciation. *Journal of Analytical Atomic Spectrometry, 25*(11), 1688-1694.

Chen, M., Diao, G., & Zhang, E. (2006). Study of inclusion complex of β-cyclodextrin and nitrobenzene. *Chemosphere, 63*(3), 522-529.

Chen, Y., Guo, Z., Wang, X., & Qiu, C. (2008). Sample preparation. *Journal of Chromatography A, 1184*(1), 191-219.

Chernykh, E., & Brichkin, S. (2010). Supramolecular complexes based on cyclodextrins. *High Energy Chemistry, 44*(2), 83-100.

Chin, Y. P., Mohamad, S., & Abas, M. R. B. (2010). Removal of Parabens from Aqueous Solution Using β-Cyclodextrin Cross-Linked Polymer. *International Journal of Molecular Sciences, 11*(9), 3459-3471.

Chitta, K., Van Meter, D., & Stalcup, A. (2010). Separation of peptides by HPLC using a surface-confined ionic liquid stationary phase. *Analytical and bioanalytical chemistry, 396*(2), 775-781.

Chou, F.-M., Wang, W.-T., & Wei, G.-T. (2009). Using subcritical/supercritical fluid chromatography to separate acidic, basic, and neutral compounds over an ionic liquid-functionalized stationary phase. *Journal of Chromatography A, 1216*(16), 3594-3599.

Connors, K. A. (1997). The stability of cyclodextrin complexes in solution. *Chemical reviews, 97*(5), 1325-1358.

Crini, G. (2008). Kinetic and equilibrium studies on the removal of cationic dyes from aqueous solution by adsorption onto a cyclodextrin polymer. *Dyes and Pigments, 77*(2), 415-426. doi: http://dx.doi.org/10.1016/j.dyepig.2007.07.001

Crini, G., & Morcellet, M. (2002). Synthesis and applications of adsorbents containing cyclodextrins. *Journal of Separation Science, 25*(13), 789-813. doi: 10.1002/1615-9314(20020901)25:13<789::AID-JSSC789>3.0.CO;2-J

Crini, G., & Peindy, H. N. (2006). Adsorption of C.I. Basic Blue 9 on cyclodextrin-based material containing carboxylic groups. *Dyes and Pigments, 70*(3), 204-211. doi: http://dx.doi.org/10.1016/j.dyepig.2005.05.004

Cwiertnia, B., Hladon, T., & Stobiecki, M. (1999). Stability of Diclofenac Sodium in the Inclusion Complex with β-Cyclodextrin in the Solid State. *Journal of Pharmacy and Pharmacology, 51*(11), 1213-1218. doi: 10.1211/0022357991776930

Dai, S., Burleigh, M., Ju, Y., Gao, H., Lin, J., Pennycook, S., . . . Xue, Z. (2000). Hierarchically imprinted sorbents for the separation of metal ions. *Journal of the American Chemical Society, 122*(5), 992-993.

Denizli, A., Ökan, G., & Uçar, M. (2002). Dye-affinity microbeads for removal of phenols and nitrophenols from aquatic systems. *Journal of Applied Polymer Science, 83*(11), 2411-2418.

Ding, L., He, J., Huang, L., & Lu, R. (2010). Studies on a novel modified β-cyclodextrin inclusion complex. *Journal of Molecular Structure, 979*(1), 122-127.

Du, K.-F., Yan, M., Wang, Q.-Y., & Song, H. (2010). Preparation and characterization of novel macroporous cellulose beads regenerated from ionic liquid for fast chromatography. *Journal of Chromatography A, 1217*(8), 1298-1304.

Dubinin, M., & Radushkevich, L. (1947). Equation of the characteristic curve of activated charcoal. *Chem. Zentr, 1*(1), 875.

Duchet, L., Legeay, J. C., Carrié, D., Paquin, L., Vanden Eynde, J. J., & Bazureau, J. P. (2010). Synthesis of 3, 5-disubstituted 1, 2, 4-oxadiazoles using ionic liquid-phase organic synthesis (IoLiPOS) methodology. *Tetrahedron, 66*(4), 986-994.

Eid, E. E., Abdul, A. B., Suliman, F. E. O., Sukari, M. A., Rasedee, A., & Fatah, S. S. (2011). Characterization of the inclusion complex of zerumbone with hydroxypropyl-β-cyclodextrin. *Carbohydrate polymers, 83*(4), 1707-1714.

El-Sheikh, A. H., Al-Quse, R. W., El-Barghouthi, M. I., & Al-Masri, F. a. S. (2010). Derivatization of 2-chlorophenol with 4-amino-anti-pyrine: A novel method for improving the selectivity of molecularly imprinted solid phase extraction of 2-chlorophenol from water. *Talanta, 83*(2), 667-673.

Elci, L., Kolbe, N., Elci, S. G., & Anderson, J. T. (2011). Solid phase extractive preconcentration coupled to gas chromatography–atomic emission detection for the determination of chlorophenols in water samples. *Talanta, 85*(1), 551-555.

Fan, Y., Feng, Y.-Q., & Da, S.-L. (2003). On-line selective solid-phase extraction of 4-nitrophenol with β-cyclodextrin bonded silica. *Analytica chimica acta, 484*(2), 145-153.

Faraji, H. (2005). β-Cyclodextrin-bonded silica particles as the solid-phase extraction medium for the determination of phenol compounds in water samples followed by gas chromatography with flame ionization and mass spectrometry detection. *Journal of Chromatography A, 1087*(1–2), 283-288. doi: http://dx.doi.org/10.1016/j.chroma.2005.06.009

Febrianto, J., Kosasih, A. N., Sunarso, J., Ju, Y.-H., Indraswati, N., & Ismadji, S. (2009). Equilibrium and kinetic studies in adsorption of heavy metals using biosorbent: A summary of recent studies. *Journal of Hazardous Materials, 162*(2–3), 616-645. doi: http://dx.doi.org/10.1016/j.jhazmat.2008.06.042

Feng, Q.-Z., Zhao, L.-X., Yan, W., Lin, J.-M., & Zheng, Z.-X. (2009). Molecularly imprinted solid-phase extraction combined with high performance liquid chromatography for analysis of phenolic compounds from environmental water samples. *Journal of Hazardous Materials, 167*(1), 282-288.

Fontanals, N., Borrull, F., & Marcé, R. M. (2012). Ionic liquids in solid-phase extraction. *TrAC Trends in Analytical Chemistry, 41*, 15-26.

Fontanals, N., Galià, M., Marcé, R. M., & Borrull, F. (2004a). Solid-phase extraction of polar compounds with a hydrophilic copolymeric sorbent. *Journal of Chromatography A, 1030*(1), 63-68.

Fontanals, N., Puig, P., Galià, M., Marcé, R. M., & Borrull, F. (2004b). New hydrophilic polymeric resin based on 4-vinylpyridine–divinylbenzene for solid-phase extraction of polar compounds from water. *Journal of Chromatography A, 1035*(2), 281-284.

Fontanals, N., Ronka, S., Borrull, F., Trochimczuk, A. W., & Marcé, R. M. (2009). Supported imidazolium ionic liquid phases: a new material for solid-phase extraction. *Talanta, 80*(1), 250-256.

Fritz, J. S. (1999). *Analytical solid-phase extraction*: Wiley-Vch New York.

Gaidamauskas, E., Norkus, E., Butkus, E., Crans, D. C., & Grincien , G. (2009). Deprotonation of -cyclodextrin in alkaline solutions. *Carbohydrate research, 344*(2), 250-254.

Gharibzahedi, S. M. T., Razavi, S. H., & Mousavi, M. (2014). Characterizing the natural canthaxanthin/2-hydroxypropyl-β-cyclodextrin inclusion complex. *Carbohydrate polymers, 101*, 1147-1153.

Ghosh, S., Badruddoza, A. Z. M., Hidajat, K., & Uddin, M. S. (2013). Adsorptive removal of emerging contaminants from water using superparamagnetic Fe3O4 nanoparticles bearing aminated β-cyclodextrin. *Journal of Environmental Chemical Engineering, 1*(3), 122-130. doi: http://dx.doi.org/10.1016/j.jece.2013.04.004

Glisoni, R. J., Cuestas, M. L., Mathet, V. L., Oubiña, J. R., Moglioni, A. G., & Sosnik, A. (2012). Antiviral activity against the hepatitis C virus (HCV) of 1-indanone thiosemicarbazones and their inclusion complexes with hydroxypropyl-β-cyclodextrin. *European Journal of Pharmaceutical Sciences, 47*(3), 596-603.

Gokmen, M. T., & Du Prez, F. E. (2012). Porous polymer particles—A comprehensive guide to synthesis, characterization, functionalization and applications. *Progress in Polymer Science, 37*(3), 365-405.

Gong, A., Ping, W., Wang, J., & Zhu, X. (2014). Cyclodextrin polymer/Fe3O4 nanocomposites as solid phase extraction material coupled with UV–vis spectrometry for the analysis of rutin. *Spectrochimica Acta Part A: Molecular and Biomolecular Spectroscopy, 122*(0), 331-336. doi: http://dx.doi.org/10.1016/j.saa.2013.11.050

Gonil, P., Sajomsang, W., Ruktanonchai, U. R., Pimpha, N., Sramala, I., Nuchuchua, O., . . . Puttipipatkhachorn, S. (2011). Novel quaternized chitosan containing β-cyclodextrin moiety: Synthesis, characterization and antimicrobial activity. *Carbohydrate polymers, 83*(2), 905-913.

Gu, Y., & Zhu, X. (2011). Speciation of Cr (III) and Cr (VI) ions using a β-cyclodextrin-crosslinked polymer micro-column and graphite furnace atomic absorption spectrometry. *Microchimica Acta, 173*(3-4), 433-438.

Guo, X., Wang, Z., & Zhou, S. (2004). The separation and determination of nitrophenol isomers by high-performance capillary zone electrophoresis. *Talanta, 64*(1), 135-139.

Hall, K., Eagleton, L., Acrivos, A., & Vermeulen, T. (1966). Pore-and solid-diffusion kinetics in fixed-bed adsorption under constant-pattern conditions. *Industrial & Engineering Chemistry Fundamentals, 5*(2), 212-223.

Hameed, B. H. (2007). Equilibrium and kinetics studies of 2,4,6-trichlorophenol adsorption onto activated clay. *Colloids and Surfaces A: Physicochemical and Engineering Aspects, 307*(1–3), 45-52. doi: http://dx.doi.org/10.1016/j.colsurfa.2007.05.002

Han, D.-M., Fang, G.-Z., & Yan, X.-P. (2005). Preparation and evaluation of a molecularly imprinted sol–gel material for on-line solid-phase extraction coupled with high performance liquid chromatography for the determination of trace pentachlorophenol in water samples. *Journal of Chromatography A, 1100*(2), 131-136.

Hanna, K., De Brauer, C., & Germain, P. (2003). Solubilization of the neutral and charged forms of 2, 4, 6-trichlorophenol by β-cyclodextrin, methyl-β-cyclodextrin and hydroxypropyl-β-cyclodextrin in water. *Journal of Hazardous Materials, 100*(1), 109-116.

Harada, A. (1997). Construction of supramolecular structures from cyclodextrins, polymers. *Carbohydrate polymers, 34*(3), 183-188.

He, L. J., Zhang, W. Z., Wen, B., Liu, X., & Jiang, S. X. (2003). Separation of ephedrines using 1-butyl-3-methylimidazolium-tetrafluoroborate ionic liquids as eluent in high-performance liquid chromatography (HPLC). *Chinese Chemical Letters, 14*(6), 603-604.

Ho, Y.-S., & McKay, G. (1999). Pseudo-second order model for sorption processes. *Process Biochemistry, 34*(5), 451-465.

Ho, Y., McKay, G., Wase, D., & Forster, C. (2000). Study of the sorption of divalent metal ions on to peat. *Adsorption Science & Technology, 18*(7), 639-650.

Hu, L., Zhang, H., Song, W., Gu, D., & Hu, Q. (2012). Investigation of inclusion complex of cilnidipine with hydroxypropyl-β-cyclodextrin. *Carbohydrate polymers, 90*(4), 1719-1724.

Huang, K., Zhang, X., & Armstrong, D. W. (2010). Ionic cyclodextrins in ionic liquid matrices as chiral stationary phases for gas chromatography. *Journal of Chromatography A, 1217*(32), 5261-5273.

Huang, Z., Wu, Q., Liu, S., Liu, T., & Zhang, B. (2013). A novel biodegradable β-cyclodextrin-based hydrogel for the removal of heavy metal ions. *Carbohydrate polymers, 97*(2), 496-501. doi: http://dx.doi.org/10.1016/j.carbpol.2013.04.047

Huh, K. M., Tomita, H., Ooya, T., Lee, W. K., Sasaki, S., & Yui, N. (2002). pH Dependence of Inclusion Complexation between Cationic Poly(ε-lysine) and α-Cyclodextrin. *Macromolecules, 35*(9), 3775-3777. doi: 10.1021/ma012003h

Iqbal, M. J., & Ashiq, M. N. (2007). Adsorption of dyes from aqueous solutions on activated charcoal. *Journal of Hazardous Materials, 139*(1), 57-66.

Jiang, P., Sun, H.-W., Shen, R.-X., Shi, J., & Lai, C.-M. (2000). Molecular mechanics study of β-cyclodextrin 6-O-monobenzoate inclusion complexes. *Journal of Molecular Structure: Theochem, 528*(1), 211-217.

Jiang, T.-F., Gu, Y.-L., Liang, B., Li, J.-B., Shi, Y.-P., & Ou, Q.-Y. (2003). Dynamically coating the capillary with 1-alkyl-3-methylimidazolium-based ionic liquids for separation of basic proteins by capillary electrophoresis. *Analytica chimica acta, 479*(2), 249-254.

Karathanos, V. T., Mourtzinos, I., Yannakopoulou, K., & Andrikopoulos, N. K. (2007). Study of the solubility, antioxidant activity and structure of inclusion complex of vanillin with β-cyclodextrin. *Food Chemistry, 101*(2), 652-658.

Khan, A. R., Forgo, P., Stine, K. J., & D'Souza, V. T. (1998). Methods for selective modifications of cyclodextrins. *Chemical reviews, 98*(5), 1977-1996.

Kilic, M., Apaydin-Varol, E., & Pütün, A. E. (2011). Adsorptive removal of phenol from aqueous solutions on activated carbon prepared from tobacco residues: Equilibrium, kinetics and thermodynamics. *Journal of Hazardous Materials, 189*(1–2), 397-403. doi: http://dx.doi.org/10.1016/j.jhazmat.2011.02.051

Kono, H., & Nakamura, T. (2013). Polymerization of β-cyclodextrin with 1,2,3,4-butanetetracarboxylic dianhydride: Synthesis, structural characterization, and bisphenol A adsorption capacity. *Reactive and Functional Polymers, 73*(8), 1096-1102. doi: http://dx.doi.org/10.1016/j.reactfunctpolym.2013.04.006

Koumanova, B., & Yaneva, Z. (2006). Low-cost adsorbents for the removal of nitrophenols from waste waters *Management of Intentional and Accidental Water Pollution* (pp. 263-275): Springer.

Krossing, I., Slattery, J. M., Daguenet, C., Dyson, P. J., Oleinikova, A., & Weingärtner, H. (2006). Why are ionic liquids liquid? A simple explanation based on lattice and solvation energies. *Journal of the American Chemical Society, 128*(41), 13427-13434.

Kubisa, P. (2009). Ionic liquids as solvents for polymerization processes—progress and challenges. *Progress in Polymer Science, 34*(12), 1333-1347.

Lagergren, S. (1898). About the theory of so-called adsorption of soluble substances. *Kungliga Svenska Vetenskapsakademiens Handlingar, 24*(4), 1-39.

Larsen, K. L., Aachmann, F. L., Wimmer, R., Stella, V. J., & Kjølner, U. M. (2005). Phase solubility and structure of the inclusion complexes of prednisolone and 6α-methyl prednisolone with various cyclodextrins. *Journal of Pharmaceutical Sciences, 94*(3), 507-515. doi: 10.1002/jps.20192

Leyva, E., Moctezuma, E., Strouse, J., & García-Garibay, M. (2001a). Spectrometric and 2D NMR Studies on the Complexation of Chlorophenols with Cyclodextrins. *Journal of Inclusion Phenomena and Macrocyclic Chemistry, 39*(1-2), 41-46. doi: 10.1023/A:1008150908997

Leyva, E., Moctezuma, E., Strouse, J., & García-Garibay, M. A. (2001b). Spectrometric and 2D NMR studies on the complexation of chlorophenols with cyclodextrins. *Journal of Inclusion Phenomena and Macrocyclic Chemistry, 39*(1-2), 41-46.

Li, J.-F., Wei, Y.-X., Ding, L.-H., & Dong, C. (2003a). Study on the inclusion complexes of cryptotanshinone with β-cyclodextrin and hydroxypropyl-β-cyclodextrin. *Spectrochimica Acta Part A: Molecular and Biomolecular Spectroscopy, 59*(12), 2759-2766.

Li, J., Ni, X., Zhou, Z., & Leong, K. W. (2003b). Preparation and Characterization of Polypseudorotaxanes Based on Block-Selected Inclusion Complexation between Poly(propylene oxide)-Poly(ethylene oxide)-Poly(propylene oxide) Triblock Copolymers and α-Cyclodextrin. *Journal of the American Chemical Society, 125*(7), 1788-1795. doi: 10.1021/ja026623p

Li, N., Mei, Z., & Ding, S. (2010). 2,4-Dichlorophenol sorption on cyclodextrin polymers. *Journal of Inclusion Phenomena and Macrocyclic Chemistry, 68*(1-2), 123-129. doi: 10.1007/s10847-010-9751-2

Li, N., Mei, Z., & Wei, X. (2012a). Study on sorption of chlorophenols from aqueous solutions by an insoluble copolymer containing -cyclodextrin and polyamidoamine units. *Chemical Engineering Journal, 192*, 138-145.

Li, N., Mei, Z., & Wei, X. (2012b). Study on sorption of chlorophenols from aqueous solutions by an insoluble copolymer containing β-cyclodextrin and polyamidoamine units. *Chemical Engineering Journal, 192*, 138-145.

Li, R., Jiang, S., Tan, J., Lu, L.-L., & Jiang, Z.-T. (2011a). Spectrophotometric Determination of Amaranth Colorant Concentration in Foods after Preconcentrating with β-Cyclodextrin Polymer. *Analytical Chemistry Letters, 1*(1), 8-15. doi: 10.1080/22297928.2011.10648200

Li, R., Jiang, Z.-T., & Wang, R.-X. (2009). Solid phase extraction combined direct spectrophotometric determination of brilliant blue in food using β-cyclodextrin polymer. *Food Analytical Methods, 2*(4), 264-270.

Li, X., Zhao, B., Zhu, K., & Hao, X. (2011b). Removal of Nitrophenols by Adsorption Using β-Cyclodextrin Modified Zeolites. *Chinese Journal of Chemical Engineering, 19*(6), 938-943. doi: http://dx.doi.org/10.1016/S1004-9541(11)60075-X

Li, Y., Xie, X., Lee, M. L., & Chen, J. (2011c). Preparation and evaluation of hydrophilic C18 monolithic sorbents for enhanced polar compound retention in liquid chromatography and solid phase extraction. *Journal of Chromatography A, 1218*(48), 8608-8616. doi: http://dx.doi.org/10.1016/j.chroma.2011.09.070

Lin, C.-H., & Tseng, S.-K. (1999). Electrochemically reductive dechlorination of pentachlorophenol using a high overpotential zinc cathode. *Chemosphere, 39*(13), 2375-2389. doi: http://dx.doi.org/10.1016/S0045-6535(99)00153-8

Liu, A., Hidajat, K., Kawi, S., & Zhao, D. (2000). A new class of hybrid mesoporous materials with functionalized organic monolayers for selective adsorption of heavy metal ions. *Chemical Communications*(13), 1145-1146.

Liu, H., Cai, X., Wang, Y., & Chen, J. (2011a). Adsorption mechanism-based screening of cyclodextrin polymers for adsorption and separation of pesticides from water. *Water Research, 45*(11), 3499-3511. doi: http://dx.doi.org/10.1016/j.watres.2011.04.004

Liu, L., & Guo, Q.-X. (2002). The driving forces in the inclusion complexation of cyclodextrins. *Journal of Inclusion Phenomena and Macrocyclic Chemistry, 42*(1-2), 1-14.

Liu, Q.-S., Zheng, T., Wang, P., Jiang, J.-P., & Li, N. (2010). Adsorption isotherm, kinetic and mechanism studies of some substituted phenols on activated carbon fibers. *Chemical Engineering Journal, 157*(2), 348-356.

Liu, Q., Shi, J., Zeng, L., Wang, T., Cai, Y., & Jiang, G. (2011b). Evaluation of graphene as an advantageous adsorbent for solid-phase extraction with chlorophenols as model analytes. *Journal of Chromatography A, 1218*(2), 197-204.

Liu, S. J., Zhou, F., Xiao, X. H., Zhao, L., Liu, X., & Jiang, S. X. (2004). Surface confined ionic liquid-A new stationary phase for the separation of ephedrines in high-performance liquid chromatography. *Chinese Chemical Letters, 15*(9), 1060-1062.

Liu, X., Yin, J., Zhu, L., Zhao, G., & Zhang, H. (2011c). Evaluation of a magnetic polysulfone microcapsule containing organic modified montmorillonite as a novel solid-phase extraction sorbent with chlorophenols as model compounds. *Talanta, 85*(5), 2451-2457.

López-de-Dicastillo, C., Gallur, M., Catalá, R., Gavara, R., & Hernandez-Muñoz, P. (2010). Immobilization of β-cyclodextrin in ethylene-vinyl alcohol copolymer for active food packaging applications. *Journal of Membrane Science, 353*(1–2), 184-191. doi: http://dx.doi.org/10.1016/j.memsci.2010.02.049

López-Vidal, S., & Arce, L. (2005). Optimisation of a headspace solid-phase micro-extraction procedure for the determination of 2, 4, 6-trichloroanisole and various related compounds in cork washing waste water by use of gas chromatography-mass spectrometry. *Chromatographia, 62*(9-10), 527-531.

Mahlambi, M. M., Malefetse, T. J., Mamba, B. B., & Krause, R. W. (2010). β-Cyclodextrin-ionic liquid polyurethanes for the removal of organic pollutants and heavy metals from water: synthesis and characterization. *Journal of polymer research, 17*(4), 589-600.

Manosroi, J., Apriyani, M. G., Foe, K., & Manosroi, A. (2005). Enhancement of the release of azelaic acid through the synthetic membranes by inclusion complex formation with hydroxypropyl-β-cyclodextrin. *International Journal of Pharmaceutics, 293*(1), 235-240.

Martinis, E. M., Berton, P., Monasterio, R. P., & Wuilloud, R. G. (2010). Emerging ionic liquid-based techniques for total-metal and metal-speciation analysis. *TrAC Trends in Analytical Chemistry, 29*(10), 1184-1201.

McEwen, A. B., Ngo, H. L., LeCompte, K., & Goldman, J. L. (1999). Electrochemical properties of imidazolium salt electrolytes for electrochemical capacitor applications. *Journal of the Electrochemical Society, 146*(5), 1687-1695.

McKay, G., Blair, H. S., & Gardner, J. R. (1982). Adsorption of dyes on chitin. I. Equilibrium studies. *Journal of Applied Polymer Science, 27*(8), 3043-3057. doi: 10.1002/app.1982.070270827

Mecerreyes, D. (2011). Polymeric ionic liquids: Broadening the properties and applications of polyelectrolytes. *Progress in Polymer Science, 36*(12), 1629-1648.

Melton, L., & Slessor, K. (1971). Synthesis of monosubstituted cyclohexaamyloses. *Carbohydrate research, 18*(1), 29-37.

Memon, S., Memon, N., Memon, S., & Latif, Y. (2011). An efficient calix [4] arene based silica sorbent for the removal of endosulfan from water. *Journal of Hazardous Materials, 186*(2), 1696-1703.

Mirzajani, R., Pourreza, N., Kiasat, A. R., & Najjar, S. S. (2013). Application of β-cyclodextrin in polymeric solid phase for separation and determination of lead in different environmental matrices. *International Journal of Environmental Analytical Chemistry, 93*(7), 800-810.

Misiuk, W., & Zalewska, M. (2009). Investigation of inclusion complex of trazodone hydrochloride with hydroxypropyl-β-cyclodextrin. *Carbohydrate polymers, 77*(3), 482-488.

Miskam, M., Abu Bakar, N. K., & Mohamad, S. (2014). Determination of polar aromatic amines using newly synthesized sol–gel titanium (IV) butoxide cyanopropyltriethoxysilane as solid phase extraction sorbent. *Talanta, 120*, 450-455.

Mlika, R., Hbaieb, S., Ben Chaabene, R., Chevalier, Y., Kalfat, R., & Ben Ouada, H. (2012). Electrochemical properties of gold electrodes functionalized by new pseudo-polyrotaxanes of polyaniline and chemically modified β-cyclodextrin inclusion complex. *Synthetic Metals, 162*(1), 186-192.

Mohamad, S., Surikumaran, H., Raoov, M., Marimuthu, T., Chandrasekaram, K., & Subramaniam, P. (2011). Conventional Study on Novel Dicationic Ionic Liquid Inclusion with β-Cyclodextrin. *International Journal of Molecular Sciences, 12*(9), 6329-6345.

Mohamad, S., Yusof, N. H. M., & Asman, S. (2013). Effect of bifunctional isocyanate linker on adsorption of chromium (VI) diphenylcarbazide complex onto beta-cyclodextrin. *Asian Journal Of Chemistry, 25*(4), 2213-2220.

Moon, J.-Y., Jung, H.-J., Moon, M. H., Chung, B. C., & Choi, M. H. (2008a). Inclusion complex-based solid-phase extraction of steroidal compounds with entrapped β-cyclodextrin polymer. *Steroids, 73*(11), 1090-1097. doi: http://dx.doi.org/10.1016/j.steroids.2008.04.008

Moon, J.-Y., Kim, J. Y., Moon, M. H., Chung, B. C., In, M. K., & Choi, M. H. (2008b). Validated gas chromatographic–mass spectrometric analysis of urinary cannabinoids purified with a calcium-hardened β-cyclodextrin polymer. *Journal of Chromatography A, 1204*(1), 87-92. doi: http://dx.doi.org/10.1016/j.chroma.2008.07.083

Mussmann, P., Levsen, K., & Radeck, W. (1994). Gas-chromatographic determination of phenols in aqueous samples after solid phase extraction. *Fresenius' journal of analytical chemistry, 348*(10), 654-659.

Ning, L., Zheng, M., & ShengMing, C. (2009). Removal of 4-chlorophenol from aqueous solutions by cyclodextrin polymer. *Fresenius Environmental Bulletin, 18*(11a), 2249-2253.

Nkambule, T. I., Krause, R. W., Mamba, B. B., & Haarhoff, J. (2009). Removal of natural organic matter from water using ion-exchange resins and cyclodextrin polyurethanes. *Physics and Chemistry of the Earth, Parts A/B/C, 34*(13–16), 812-818. doi: http://dx.doi.org/10.1016/j.pce.2009.07.013

Ong, T.-T., Wang, R.-Q., Muderawan, I. W., & Ng, S.-C. (2008). Synthesis and application of mono-6-(3-methylimidazolium)-6-deoxyperphenylcarbamoyl-β-cyclodextrin chloride as chiral stationary phases for high-performance liquid chromatography and supercritical fluid chromatography. *Journal of Chromatography A, 1182*(1), 136-140.

Ong, T. T., Tang, W., Muderawan, W., Ng, S. C., & Chan, H. S. O. (2005). Synthesis and application of single-isomer 6-mono (alkylimidazolium)-β-cyclodextrins as chiral selectors in chiral capillary electrophoresis. *Electrophoresis, 26*(20), 3839-3848.

Ozmen, E. Y., Sezgin, M., Yilmaz, A., & Yilmaz, M. (2008). Synthesis of β-cyclodextrin and starch based polymers for sorption of azo dyes from aqueous solutions. *Bioresource Technology, 99*(3), 526-531. doi: http://dx.doi.org/10.1016/j.biortech.2007.01.023

Padilla-Sánchez, J., Plaza-Bolaños, P., Romero-González, R., Barco-Bonilla, N., Martínez-Vidal, J., & Garrido-Frenich, A. (2011). Simultaneous analysis of chlorophenols, alkylphenols, nitrophenols and cresols in wastewater effluents, using solid phase extraction and further determination by gas chromatography–tandem mass spectrometry. *Talanta, 85*(5), 2397-2404.

Pan, B., Pan, B., Zhang, W., Zhang, Q., Zhang, Q., & Zheng, S. (2008). Adsorptive removal of phenol from aqueous phase by using a porous acrylic ester polymer. *Journal of Hazardous Materials, 157*(2), 293-299.

Pan, B., Zhang, X., Zhang, W., Zheng, J., Pan, B., Chen, J., & Zhang, Q. (2005). Adsorption of phenolic compounds from aqueous solution onto a macroporous polymer and its aminated derivative: isotherm analysis. *Journal of Hazardous Materials, 121*(1), 233-241.

Pan, J., Zou, X., Wang, X., Guan, W., Li, C., Yan, Y., & Wu, X. (2011). Adsorptive removal of 2,4-didichlorophenol and 2,6-didichlorophenol from aqueous solution by β-cyclodextrin/attapulgite composites: Equilibrium, kinetics and thermodynamics. *Chemical Engineering Journal, 166*(1), 40-48. doi: http://dx.doi.org/10.1016/j.cej.2010.09.067

Pavan, F. A., Dias, S. L. P., Lima, E. C., & Benvenutti, E. V. (2008). Removal of Congo red from aqueous solution by anilinepropylsilica xerogel. *Dyes and Pigments, 76*(1), 64-69. doi: http://dx.doi.org/10.1016/j.dyepig.2006.08.027

Petter, R. C., Salek, J. S., Sikorski, C. T., Kumaravel, G., & Lin, F. T. (1990). Cooperative binding by aggregated mono-6-(alkylamino)-. beta.-cyclodextrins. *Journal of the American Chemical Society, 112*(10), 3860-3868.

Pierotti, R., & Rouquerol, J. (1985). Reporting physisorption data for gas/solid systems with special reference to the determination of surface area and porosity. *Pure Appl Chem, 57*(4), 603-619.

Ping, W., Zhu, X., & Wang, B. (2013). An Ionic Liquid Loaded β-Cyclodextrin-Cross-Linked Polymer as the Solid Phase Extraction Material Coupled with High-Performance Liquid Chromatography for the Determination of Rhodamine B in Food. *Analytical Letters, 47*(3), 504-516. doi: 10.1080/00032719.2013.841177

Poole, C. F. (2003). New trends in solid-phase extraction. *TrAC Trends in Analytical Chemistry, 22*(6), 362-373. doi: http://dx.doi.org/10.1016/S0165-9936(03)00605-8

Poole, C. F., Gunatilleka, A. D., & Sethuraman, R. (2000). Contributions of theory to method development in solid-phase extraction. *Journal of Chromatography A, 885*(1–2), 17-39. doi: http://dx.doi.org/10.1016/S0021-9673(00)00224-7

Poole, C. F., & Poole, S. K. (2010). Extraction of organic compounds with room temperature ionic liquids. *Journal of Chromatography A, 1217*(16), 2268-2286.

Portillo, M., Prohibas, N., Salvadó, V., & Simonet, B. (2006). Vial position in the determination of chlorophenols in water by solid phase microextraction. *Journal of Chromatography A, 1103*(1), 29-34.

Qi, P., Wang, J., Jin, J., Su, F., & Chen, J. (2010). 2, 4-Dimethylphenol imprinted polymers as a solid-phase extraction sorbent for class-selective extraction of phenolic compounds from environmental water. *Talanta, 81*(4), 1630-1635.

Qian, L., Guan, Y., & Xiao, H. (2008). Preparation and characterization of inclusion complexes of a cationic β-cyclodextrin polymer with butylparaben or triclosan. *International Journal of Pharmaceutics, 357*(1–2), 244-251. doi: http://dx.doi.org/10.1016/j.ijpharm.2008.01.018

Qiu, H., Jiang, S., Liu, X., & Zhao, L. (2006). Novel imidazolium stationary phase for high-performance liquid chromatography. *Journal of Chromatography A, 1116*(1), 46-50.

Qiu, H., Sawada, T., Jiang, S., & Ihara, H. (2010). Synthesis and characterization of poly (ionic liquid)-grafted silica hybrid materials through surface radical chain-transfer polymerization and aqueous anion-exchange. *Materials Letters, 64*(14), 1653-1655.

Ragonese, C., Tranchida, P. Q., Sciarrone, D., & Mondello, L. (2009). Conventional and fast gas chromatography analysis of biodiesel blends using an ionic liquid stationary phase. *Journal of Chromatography A, 1216*(51), 8992-8997.

Raoov, M., Mohamad, S., & Abas, M. R. (2013). Removal of 2, 4-dichlorophenol using cyclodextrin-ionic liquid polymer as a macroporous material: characterization, adsorption isotherm, kinetic study, thermodynamics. *Journal of Hazardous Materials, 263*, 501-516.

Raoov, M., Mohamad, S., & Abas, M. R. (2014a). Synthesis and characterization of β-cyclodextrin functionalized ionic liquid polymer as a macroporous material for the removal of phenols and As(V). *International Journal of Molecular Sciences, 15*(1), 100-119.

Raoov, M., Mohamad, S., bin Abas, M. R., & Surikumaran, H. (2014b). New macroporous β-Cyclodextrin functionalized Ionic liquid polymer as an adsorbent for solid phase extraction with phenols. *Talanta*, 130, 155-163.

Rodriguez-Mozaz, S., Lopez de Alda, M. J., & Barceló, D. (2007). Advantages and limitations of on-line solid phase extraction coupled to liquid chromatography–mass spectrometry technologies versus biosensors for monitoring of emerging contaminants in water. *Journal of Chromatography A, 1152*(1–2), 97-115. doi: http://dx.doi.org/10.1016/j.chroma.2007.01.046

Rojas, G., Silva, J., Flores, J. A., Rodriguez, A., Ly, M., & Maldonado, H. (2005). Adsorption of chromium onto cross-linked chitosan. *Separation and Purification Technology, 44*(1), 31-36. doi: http://dx.doi.org/10.1016/j.seppur.2004.11.013

Saitoh, T., Nakayama, Y., & Hiraide, M. (2002). Concentration of chlorophenols in water with sodium dodecylsulfate–γ-alumina admicelles for high-performance liquid chromatographic analysis. *Journal of Chromatography A, 972*(2), 205-209.

Salipira, K., Krause, R., Mamba, B., Malefetse, T., Cele, L., & Durbach, S. (2008). Cyclodextrin polyurethanes polymerized with multi-walled carbon nanotubes: Synthesis and characterization. *Materials Chemistry and Physics, 111*(2), 218-224.

Sambasevam, K. P., Mohamad, S., Sarih, N. M., & Ismail, N. A. (2013). Synthesis and Characterization of the Inclusion Complex of β-cyclodextrin and Azomethine. *International Journal of Molecular Sciences, 14*(2), 3671-3682.

Sarafraz-Yazdi, A., Dizavandi, Z. R., & Amiri, A. (2012). Determination of phenolic compounds in water and urine samples using solid-phase microextraction based on sol–gel technique prior to GC-FID. *Analytical Methods, 4*(12), 4316-4325.

Sathishkumar, M., Binupriya, A., Kavitha, D., Selvakumar, R., Jayabalan, R., Choi, J., & Yun, S. (2009). Adsorption potential of maize cob carbon for 2, 4-dichlorophenol removal from aqueous solutions: equilibrium, kinetics and thermodynamics modeling. *Chemical Engineering Journal*, *147*(2), 265-271.

Scalia, S., Villani, S., Scatturin, A., Vandelli, M., & Forni, F. (1998). Complexation of the sunscreen agent, butyl-methoxydibenzoylmethane, with hydroxypropyl-β-cyclodextrin. *International Journal of Pharmaceutics, 175*(2), 205-213.

Schroden, R. C., Al-Daous, M., Sokolov, S., Melde, B. J., Lytle, J. C., Stein, A., . . . Rodríguez, E. E. (2002). Hybrid macroporous materials for heavy metal ion adsorption. *Journal of Materials Chemistry, 12*(11), 3261-3267.

Seddon, K. R. (1997). Ionic liquids for clean technology. *Journal of Chemical Technology and Biotechnology, 68*(4), 351-356.

Shaarani, F., & Hameed, B. (2011). Ammonia-modified activated carbon for the adsorption of 2, 4-dichlorophenol. *Chemical Engineering Journal, 169*(1), 180-185.

Shao, D., Sheng, G., Chen, C., Wang, X., & Nagatsu, M. (2010). Removal of polychlorinated biphenyls from aqueous solutions using β-cyclodextrin grafted multiwalled carbon nanotubes. *Chemosphere, 79*(7), 679-685. doi: http://dx.doi.org/10.1016/j.chemosphere.2010.03.008

Shrivastava, A., & Gupta, V. B. (2011). Methods for the determination of limit of detection and limit of quantitation of the analytical methods. *Chronicles of Young Scientists, 2*(1), 21.

Srinivasan, K., Stalin, T., & Sivakumar, K. (2012). Spectral and electrochemical study of host–guest inclusion complex between 2, 4-dinitrophenol and β-cyclodextrin. *Spectrochimica Acta Part A: Molecular and Biomolecular Spectroscopy, 94*, 89-100.

Srivastava, V. C., Swamy, M. M., Mall, I. D., Prasad, B., & Mishra, I. M. (2006). Adsorptive removal of phenol by bagasse fly ash and activated carbon: Equilibrium, kinetics and thermodynamics. *Colloids and Surfaces A: Physicochemical and Engineering Aspects, 272*(1–2), 89-104. doi: http://dx.doi.org/10.1016/j.colsurfa.2005.07.016

Subramaniam, P., Mohamad, S., & Alias, Y. (2010). Synthesis and Characterization of the Inclusion Complex of Dicationic Ionic Liquid and β-Cyclodextrin. *International Journal of Molecular Sciences, 11*(10), 3675-3685.

Sun, P., & Armstrong, D. W. (2010). Ionic liquids in analytical chemistry. *Analytica chimica acta, 661*(1), 1-16. doi: http://dx.doi.org/10.1016/j.aca.2009.12.007

Sun, P., Liu, P., Upadhyaya, P., Jeong, D., Heo, D., & Mina, E. (2010a, 23-28 May 2010). *Silicon-based PIN SPST RF switches for improved linearity.* Paper presented at the Microwave Symposium Digest (MTT), 2010 IEEE MTT-S International.

Sun, Z.-Y., Shen, M.-X., Cao, G.-P., Deng, J., Liu, Y., Liu, T., . . . Yuan, W.-K. (2010b). Preparation of bimodal porous copolymer containing β-cyclodextrin and its inclusion adsorption behavior. *Journal of Applied Polymer Science, 118*(4), 2176-2185. doi: 10.1002/app.32515

Szabados-Nacsa, Á., Sipos, P., Martinek, T., Mándity, I., Blazsó, G., Balogh, Á., . . . Aigner, Z. (2011). Physico-chemical characterization and in vitro in vivo evaluation of loratadine: dimethyl-β-cyclodextrin inclusion complexes. *Journal of Pharmaceutical and Biomedical Analysis, 55*(2), 294-300.

Szejtli, J. (1998). Introduction and general overview of cyclodextrin chemistry. *Chemical reviews, 98*(5), 1743-1754.

Szejtli, J. (2004). Past, present, and future of cyclodextrin research. *Pure and Applied Chemistry, 76*(10), 1825-1845.

Tang, W., Ong, T.-T., Muderawan, I. W., & Ng, S. C. (2007). Effect of alkylimidazolium substituents on enantioseparation ability of single-isomer alkylimidazolium-β-cyclodextrin derivatives in capillary electrophoresis. *Analytica chimica acta, 585*(2), 227-233. doi: http://dx.doi.org/10.1016/j.aca.2006.12.041

Temkin, M., & Pyzhev, V. (1940). Recent modifications to Langmuir isotherms. *Acta Physiochim. USSR, 12*, 217-222.

Teng, M., Li, F., Zhang, B., & Taha, A. A. (2011). Electrospun cyclodextrin-functionalized mesoporous polyvinyl alcohol/SiO2 nanofiber membranes as a highly efficient adsorbent for indigo carmine dye. *Colloids and Surfaces A: Physicochemical and Engineering Aspects, 385*(1–3), 229-234. doi: http://dx.doi.org/10.1016/j.colsurfa.2011.06.020

Tian, M., Bi, W., & Row, K. H. (2009). Solid-phase extraction of liquiritin and glycyrrhizic acid from licorice using ionic liquid-based silica sorbent. *Journal of Separation Science, 32*(23-24), 4033-4039.

Tian, M., Bi, W., & Row, K. H. (2011). Molecular imprinting in ionic liquid-modified porous polymer for recognitive separation of three tanshinones from Salvia miltiorrhiza Bunge. *Analytical and bioanalytical chemistry, 399*(7), 2495-2502.

Tian, M., Yan, H., & Row, K. H. (2009a). Solid-phase extraction of caffeine and theophylline from green tea by a new ionic liquid-modified functional polymer sorbent. *Analytical Letters, 43*(1), 110-118.

Tian, M., Yan, H., & Row, K. H. (2009b). Solid-phase extraction of tanshinones from Salvia Miltiorrhiza Bunge using ionic liquid-modified silica sorbents. *Journal of Chromatography B, 877*(8), 738-742.

Tongiani, S., Ozeki, T., & Stella, V. J. (2009). Sulfobutyl ether-alkyl ether mixed cyclodextrin derivatives with enhanced inclusion ability. *Journal of Pharmaceutical Sciences, 98*(12), 4769-4780. doi: 10.1002/jps.21791

Tongiani, S., Velde, D. V., Ozeki, T., & Stella, V. J. (2005). Sulfoalkyl ether-alkyl ether cyclodextrin derivatives, their synthesis, NMR characterization, and binding of 6α-methylprednisolone. *Journal of Pharmaceutical Sciences, 94*(11), 2380-2392. doi: 10.1002/jps.20367

Tsujihara, K., Kurita, H., & Kawazu, M. (1977). The highly selective sulfonylation of cycloheptaamylose and syntheses of its pure amino derivatives. *Bull. Chem. Soc. Jpn, 50*, 1567-1571.

Tsukagoshi, K., Kameda, T., Yamamoto, M., & Nakajima, R. (2002). Separation and determination of phenolic compounds by capillary electrophoresis with chemiluminescence detection. *Journal of Chromatography A, 978*(1), 213-220.

Ueno, A., Moriwaki, F., Osa, T., Hamada, F., & Murai, K. (1987). Excimer formation in inclusion complexes of modified cyclodextrins. *Tetrahedron, 43*(7), 1571-1578.

Ventura, C. A., Giannone, I., Paolino, D., Pistarà, V., Corsaro, A., & Puglisi, G. (2005). Preparation of celecoxib-dimethyl-β-cyclodextrin inclusion complex: characterization and in vitro permeation study. *European journal of medicinal chemistry, 40*(7), 624-631.

Villaverde, J., Morillo, E., Pérez-Martínez, J. I., Gines, J. M., & Maqueda, C. (2004). Preparation and characterization of inclusion complex of norflurazon and β-cyclodextrin to improve herbicide formulations. *Journal of agricultural and food chemistry, 52*(4), 864-869.

Vimonses, V., Lei, S., Jin, B., Chow, C. W., & Saint, C. (2009). Kinetic study and equilibrium isotherm analysis of Congo Red adsorption by clay materials. *Chemical Engineering Journal, 148*(2), 354-364.

Wan Ibrahim, W. A., Veloo, K. V., & Sanagi, M. M. (2012). Novel sol–gel hybrid methyltrimethoxysilane–tetraethoxysilane as solid phase extraction sorbent for organophosphorus pesticides. *Journal of Chromatography A, 1229*, 55-62.

Wang, H. Y., Han, J., Feng, X. G., & Pang, Y. L. (2006). Study of inclusion complex formation between tropaeolin OO and β-cyclodextrin by spectrophotometry and Infrared spectroscopy. *Spectrochimica Acta Part A: Molecular and Biomolecular Spectroscopy, 65*(1), 100-105.

Wang, L., Zhang, J., Zhao, R., Zhang, C., Li, C., & Li, Y. (2011). Adsorption of 2,4-dichlorophenol on Mn-modified activated carbon prepared from Polygonum orientale Linn. *Desalination, 266*(1–3), 175-181. doi: http://dx.doi.org/10.1016/j.desal.2010.08.022

Wang, R.-Q., Ong, T.-T., & Ng, S.-C. (2008). Synthesis of cationic β-cyclodextrin derivatives and their applications as chiral stationary phases for high-performance liquid chromatography and supercritical fluid chromatography. *Journal of Chromatography A, 1203*(2), 185-192.

Wang, R.-Q., Ong, T.-T., Tang, W., & Ng, S.-C. (2012). Cationic cyclodextrins chemically-bonded chiral stationary phases for high-performance liquid chromatography. *Analytica chimica acta, 718*, 121-129.

Weber, W., & Morris, J. (1963). Kinetics of adsorption on carbon from solution. *J. Sanit. Eng. Div. Am. Soc. Civ. Eng, 89*(17), 31-60.

Wen, X., Tan, F., Jing, Z., & Liu, Z. (2004). Preparation and study the 1: 2 inclusion complex of carvedilol with β-cyclodextrin. *Journal of Pharmaceutical and Biomedical Analysis, 34*(3), 517-523.

Williams III, R. O., Mahaguna, V., & Sriwongjanya, M. (1998). Characterization of an inclusion complex of cholesterol and hydroxypropyl-β-cyclodextrin. *European Journal of Pharmaceutics and Biopharmaceutics, 46*(3), 355-360.

Xiaohua, X., Liang, Z., Xia, L., & Shengxiang, J. (2004). Ionic liquids as additives in high performance liquid chromatography: Analysis of amines and the interaction mechanism of ionic liquids. *Analytica chimica acta, 519*(2), 207-211.

Xiaoli, C., & Youcai, Z. (2006). Adsorption of phenolic compound by aged-refuse. *Journal of Hazardous Materials, 137*(1), 410-417. doi: http://dx.doi.org/10.1016/j.jhazmat.2006.02.015

Yang, F., Shen, R., Long, Y., Sun, X., Tang, F., Cai, Q., & Yao, S. (2011). Magnetic microsphere confined ionic liquid as a novel sorbent for the determination of chlorophenols in environmental water samples by liquid chromatography. *Journal of Environmental Monitoring, 13*(2), 440-445.

Yao, C., & Anderson, J. L. (2009). Retention characteristics of organic compounds on molten salt and ionic liquid-based gas chromatography stationary phases. *Journal of Chromatography A, 1216*(10), 1658-1712.

Yilmaz, E., Memon, S., & Yilmaz, M. (2010). Removal of direct azo dyes and aromatic amines from aqueous solutions using two β-cyclodextrin-based polymers. *Journal of Hazardous Materials, 174*(1–3), 592-597. doi: http://dx.doi.org/10.1016/j.jhazmat.2009.09.093

Yongfeng, K., Wuping, D., Yan, L., Junxia, K., & Jing, X. (2012). Molecularly imprinted polymers of allyl-β-cyclodextrin and methacrylic acid for the solid-phase extraction of phthalate. *Carbohydrate polymers, 88*(2), 459-464. doi: http://dx.doi.org/10.1016/j.carbpol.2011.12.027

Yoo, K. S., & Lee, S.-H. (2010). Influence of Ionic Liquid as a Template on Preparation of Porous η-Al2O3 to DME Synthesis from Methanol. *Bull. Korean Chem. Soc, 31*(6), 1629.

Zanoni, M. V. B., Rogers, E. I., Hardacre, C., & Compton, R. G. (2010). The electrochemical reduction of the purines guanine and adenine at platinum electrodes in several room temperature ionic liquids. *Analytica chimica acta, 659*(1), 115-121.

Zha, F., Li, S., & Chang, Y. (2008). Preparation and adsorption property of chitosan beads bearing β-cyclodextrin cross-linked by 1, 6-hexamethylene diisocyanate. *Carbohydrate polymers, 72*(3), 456-461.

Zhang, J., Shen, X., & Chen, Q. (2011). Separation Processes in the Presence of Cyclodextrins Using Molecular Imprinting Technology and Ionic Liquid Cooperating Approach. *Current Organic Chemistry, 15*(1), 74-85. doi: 10.2174/138527211793797765

Zhang, X.-J., Ma, T.-Y., & Yuan, Z.-Y. (2008). Titania–phosphonate hybrid porous materials: preparation, photocatalytic activity and heavy metal ion adsorption. *Journal of Materials Chemistry, 18*(17), 2003-2010.

Zhao, F., Meng, Y., & Anderson, J. L. (2008). Polymeric ionic liquids as selective coatings for the extraction of esters using solid-phase microextraction. *Journal of Chromatography A, 1208*(1), 1-9.

Zhao, M.-X., Zhao, M., Zeng, E.-Z., Li, Y., Li, J.-M., Cao, Q., . . . Mao, Z.-W. (2014). Enhanced anti-cancer efficacy to cancer cells by doxorubicin loaded water-soluble amino acids-modified β-cyclodextrin platinum complexes. *Journal of inorganic biochemistry*.

Zhong, N., Byun, H.-S., & Bittman, R. (1998). An improved synthesis of 6-O-monotosyl-6-deoxy-β-cyclodextrin. *Tetrahedron Letters, 39*(19), 2919-2920. doi: http://dx.doi.org/10.1016/S0040-4039(98)00417-1

Zhou, N., Sang, R., & Zhu, X. (2013a). Functionalized β-Cyclodextrin Polymer Solid Phase Extraction Coupled with UV–Visible Spectrophotometry for Analysis of Kaempferol in Food Samples. *Food Analytical Methods*, 7(4), 1256-1262.

Zhou, N., & Zhu, X.-S. (2013). Ionic liquids functionalized β-cyclodextrin polymer for separation/analysis magnolol. *Journal of Pharmaceutical Analysis*, 4(4), 242-249.

Zhou, Z., Li, X., Chen, X., & Hao, X. (2010). Synthesis of ionic liquids functionalized β-cyclodextrin-bonded chiral stationary phases and their applications in high-performance liquid chromatography. *Analytica chimica acta, 678*(2), 208-214.

Zhu, X., Wu, M., & Gu, Y. (2009). β-Cyclodextrin-cross-linked polymer as solid phase extraction material coupled with inductively coupled plasma mass spectrometry for the analysis of trace Co (II). *Talanta, 78*(2), 565-569.

Zhu, X., Wu, M., Sun, J., & Zhang, X. (2008). β-Cyclodextrin-Cross-Linked Polymer as Solid Phase Extraction Material Coupled Graphite Furnace Atomic Absorption Spectrometry for Separation/Analysis of Trace Copper. *Analytical Letters, 41*(12), 2186-2202. doi: 10.1080/00032710802237749

APPENDIX A

LIST OF PUBLICATIONS

1) Raoov, M., Mohamad, S., & Abas, M. R. (2013). Removal of 2, 4-dichlorophenol using cyclodextrin-ionic liquid polymer as a macroporous material: characterization, adsorption isotherm, kinetic study, thermodynamics. Journal of Hazardous Materials, 263, 501-516 (**Q1, 4.331**).

2) Raoov, M., Mohamad, S., Abas, M. R., & Surikumaran, H. (2014). New macroporous β-Cyclodextrin functionalized Ionic liquid polymer as an adsorbent for solid phase extraction with phenols. Talanta. 130, 155–163 (**Q1, 3.511**).

3) Raoov, M., Mohamad, S., & Abas, M. (2013). Synthesis and Characterization of β-Cyclodextrin Functionalized Ionic Liquid Polymer as a Macroporous Material for the Removal of Phenols and As(V). International Journal of Molecular Sciences, 15(1), 100-119 (**Q2, 2.339**).

4) Mohamad, S., Surikumaran, H., Raoov, M., Marimuthu, T., Chandrasekaram, K., & Subramaniam, P. (2011). Conventional study on novel dicationic ionic liquid inclusion with β-cyclodextrin. International Journal of Molecular Sciences, 12(9), 6329-6345 (**Q2, 2.339**).

5) Noorashikin, M., Raoov, M., Mohamad, S., & Abas, M. (2013). Cloud Point Extraction of Parabens Using Non-Ionic Surfactant with Cylodextrin Functionalized Ionic Liquid as a Modifier. International Journal of Molecular Sciences, 14(12), 24531-24548 (**Q2, 2.339**).

6) Noorashikin, M. S., Raoov, M., Mohamad, S., & Abas, M. R. Extraction of Parabens from Water Samples Using Cloud Point Extraction with a Non-Ionic Surfactant with β-Cyclodextrin as Modifier. Journal of Surfactants and Detergents, 1-12 (**Q2, 1.352**).

7) Mohamad, S., N. K. A, Bakar., Ishak, A. R., Surikumaran, H., Pandian, K., Raoov, M., Zain, N.N.M., Chandrasekaram, K. Asian Journal of Chemistry; 26(12) (2014), 3545-3552 (**Q4, 0.404**).

8) Raoov, M., Mohamad, S., Abas, M. R. Comparative studies on adsorptive removal of phenols by macroporous cyclodextrin functionalized ionic liquid polymer: Adsorption Isotherm, Kinetic study, Thermodynamics, Journal of Colloid and Interface Science (**Submitted**).

9) Surikumaran, H. Mohamad, S., Norzilawati, M. S., Raoov, M. β-Cyclodextrin based Molecular Imprinted Solid Phase Extraction for Class Selective Extraction of Priority Phenols in Water Samples, Journal of applied polymer science (**Under review**).

10) Zain, N. N. M., Bakar, N. K. A., Mohamad, S., Raoov, M. β-Cyclodextrin functionalized with ionic liquid as modifier for extraction of para-Nitrophenol in Cloud Point Extraction, Journal of Separation Science (**Submitted**).

APPENDIX B

LIST OF PRESENTATIONS

1) Removal of 2,4-dichlorophenol using new benzylimidazolium based cyclodextrin-ionic liquid polymer. (2013), Muggundha Raoov, Sharifah Mohamad, Mhd Radzi Abas, Asia-Pacific.International Congress on Engineering and Natural Sciences (APICENS 2013). Bangkok, Thailand,16-18 April 2013 (**Oral**).

2) Synthesis and properties of new cyclodextrin ionic liquid polymer for removal of phenol. 17th Malaysian Chemical Congress (17MCC) (2012), Muggundha Raoov, Sharifah Mohamad, Mhd Radzi Abas (International).15-17 October 2012, PWTC, Kuala Lumpur. (**Poster**).

3) Synthesis and characterization of β-cyclodextrin-ionic liquid polymer as a macroporous material for the removal of phenols and As(V). (2013), Muggundha Raoov, Sharifah Mohamad, Mhd Radzi Abas Malaysia Polymer International Conference (MPIC 2013). 25-26 September 2013, Bangi, Putrajaya (**Oral**).

4) Solid phase extraction of chlorophenols using β-Cyclodextrin functionalized ionic liquid polymer (2013). Muggundha Raoov, Sharifah Mohamad, Mhd Radzi Abas. International Conference on Ionic liquids 2013 (ILCIL 2013). 11-13 Dicember 2013, Langkawi Island, Kedah, Malaysia (**Oral**).

5) New macroporous β-cyclodextrin functionalized ionic liquid polymer as an adsorbent for solid phase extraction with phenols. Muggundha Raoov, Sharifah Mohamad, Mhd Radzi Abas. The 6th International Symposium on Nano and Supramolecular Chemistry. 10-14 August 2014, Denpasar, Bali, Indonesia (**Oral**).

6) A comparative study on the adsorptive removal of phenols by macroporous cyclodextrin functionalized ionic liquid polymer. Adsorption Isotherm, Kinetic study, and Thermodynamics. Muggundha Raoov, Sharifah Mohamad, Mhd Radzi Abas.The 6th International conference on postgraduate education (ICPE-6 2014) 17-18 December 2014, UTEM, Melaka, Malaysia (**Poster**).